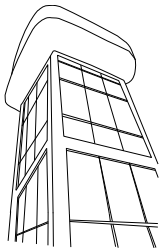

Ven Te Chow
Hydrosystems Laboratory

University of Illinois at
Urbana-Champaign

Bubbly Creek Sediment Oxygen Demand (SOD) Study with the U of I Hydrodynamic SOD Sampler

March 26, 2010

Prepared by:

David Waterman
Andrew Waratuke
Davide Motta
Yovanni Cataño-Lopera
and
Marcelo H. Garcia

Prepared for:

Metropolitan Water Reclamation District of Greater Chicago
100 East Erie Street
Chicago, IL 60611

ABSTRACT

Bubbly Creek in Chicago, Illinois, is a water-quality limited stream, and one of the parameters of impairment is low dissolved oxygen content. The stream is known to have a deep bed of organic, nutrient-rich sediments, the result of former waste discharge by the Union Stock Yards, former municipal raw sewage discharge, and ongoing combined sewer overflow discharge by the Racine Avenue Pumping Station (RAPS) located at the head of the existing alignment of Bubbly Creek. The sediment exerts an oxygen demand on the overlying water column, which is known as the sediment oxygen demand (SOD). The SOD is considered to be a significant contributor to the low dissolved oxygen content observed in Bubbly Creek.

The current study was undertaken to characterize the SOD of Bubbly Creek under a variety of flow conditions using onsite field experiments as the basis of the analysis. Of particular interest was the determination of the dependence of the SOD on stream velocity, including those conditions where bottom sediments are resuspended. The results are intended to be used in future water quality modeling to evaluate various strategies being considered by the Metropolitan Water Reclamation District of Greater Chicago for improving the water quality of Bubbly Creek and downstream receiving waters.

The University of Illinois Ven Te Chow Hydrosystems Laboratory (VTCHL) designed a sampling apparatus (referred to in this report as the U of I Hydrodynamic SOD Sampler) to undertake the field experiments. The primary component of the sampling apparatus was a chamber lowered to the streambed, the base of which was open, exposing a fixed area of the sediment surface to water pumped through the otherwise closed circuit. The chamber and other components were specially designed to accommodate relatively high flow rates for the purpose of characterizing high bed shear stress and sediment resuspension conditions. In addition to the field experiments with the U of I Hydrodynamic SOD Sampler, a number of laboratory analyses were performed to quantify the suspended sediment characteristics.

In order to correlate the results of field and laboratory experiments to oxygen demand that would occur for actual stream flow conditions, the computational fluid dynamics program Flow-3D was utilized to calculate bed shear stresses generated at the exposed sediment surface within the SOD chamber; and a two-dimensional hydrodynamics model (STREMR-HySedWq, previously developed at the University of Illinois) was utilized to simulate bed shear stresses for actual flow events in Bubbly Creek.

The ultimate goal of this study was to find a relationship between the near-bed flow velocity in Bubbly Creek and the resulting sediment oxygen demand (SOD). To achieve this goal, the current study split SOD into two separate components: (1) SOD_{NR} is the sediment oxygen demand associated with non-resuspension conditions and is calculated using traditional methods to yield a value with units ($g/m^2/day$); (2) SOD_R is the oxygen demand associated with resuspension conditions, which is most accurately characterized using non-traditional methods and units that reflect suspension in the water column (mg/L/day). Because the latter component is highly dependent on the dispersion and fate of sediment that is put into suspension, it was not possible to establish an absolute value of SOD_R for a given stream flow rate. The approach chosen to characterize SOD_R was to establish the relationships for the quantity of sediment put into suspension as a function of bed shear stress and to establish a relationship for the resulting oxygen demand as a function of suspended sediment concentration in a fashion similar to first-order BOD kinetics. These relationships will ultimately need to be incorporated into a model containing hydrodynamic, sediment transport, and water quality components in order to yield the oxygen demand associated with sediment resuspension for a Bubbly Creek flow event. Although this final modeling component was beyond the scope of the current study, the relationships have been established in such a manner that incorporation into the 3D hydrodynamic model of Bubbly Creek currently being developed by VTCHL will be relatively straight-forward.

A brief summary of important values relating to the above paragraph include the following:

- SOD_{NR} values at 20°C varied from 6.7 to 12.1 $g/m^2/day$. Using the average depth in Bubbly Creek of 2.2 m, the result would be water column oxygen drawdown rate of 3.0 to 5.5 mg/L/day. (The field experiments represent well-mixed, oxygenated conditions near the bed, and actual SOD_{NR} can be expected to be lower when near bed conditions are less mixed or dissolved oxygen levels are very low.)
- The initial, instantaneous oxygen demand associated with resuspension (a surrogate for SOD_R) at 20°C and ambient dissolved oxygen concentration 2.0 mg/L varied from 12.1 to 33.4 $g/m^2/day$ for scenarios when the thin organic film on the sediment surface was resuspended; and from 83.6 to 195.6 $g/m^2/day$ for full resuspension. Using the 2.2 m average depth of Bubbly Creek, the resulting initial, instantaneous water column drawdown rate would be 5.5 to 88.9 mg/L/day. (This surrogate for SOD_R is simply intended to provide a sense of the magnitude of SOD_R relative to SOD_{NR}. Actual water column oxygen drawdown is dependent on dispersal and fate of suspended sediment and is best characterized using the dynamic oxygen sink term developed.)

- Critical shear velocity values varied from 0.17 cm/sec to resuspend the thin organic film on the sediment surface through 2.54 cm/sec to resuspend a fine to medium grained sand characteristic of upper Bubbly Creek.

The results of this study illustrate the strong influence of flow velocity on oxygen demand and the need to account for these effects in any stream purification scenarios considered to improve water quality in Bubbly Creek.

ACKNOWLEDGEMENTS

The staff at the University of Illinois Ven Te Chow Hydrosystems Laboratory (VTCHL) would like to recognize and thank the USGS Illinois Water Science Center, particularly Jim Duncker and Ryan Jackson, for their efforts on this project. The study could not have taken place without their extensive collaboration during design, testing, and field implementation. Field work performed by Greg Goodwin and Ryan Beaulin of the USGS is also appreciated.

Collaboration with Dr. Heng Zhang of the Metropolitan Water Reclamation District of Greater Chicago is gratefully acknowledged. In addition to collaboration regarding methods used in this study, Dr. Zhang also coordinated the analytical testing of sediment and water samples by the District's research and development laboratories at the Stickney Water Reclamation Plant. The work of laboratory staff at the Stickney plant for their analysis of the large quantity of samples generated in this study is also acknowledged.

The following faculty, staff, and students of the Ven Te Chow Hydrosystems Laboratory provided invaluable assistance during various phases of this project. Dr. Xiaofeng Liu provided additional simulations of bed shear stresses using a 3-dimensional model of Bubbly Creek for comparison with the STREMR-HySedWq results utilized in this report. Dr. Gary Parker, Jose Mier and Blake Landry provided valuable collaboration regarding the sediment transport aspects of the project. Tatiana Garcia provided valuable assistance regarding the water quality aspects of the project. The assistance of all these individuals is gratefully acknowledged. We also acknowledge the staff at the UIUC Civil and Environmental Engineering Shop who constructed the SOD chamber in accordance with the precise design specifications provided.

Table of Contents

LIST OF FIGURES

LIST OF TABLES

Chapter 1: INTRODUCTION

1.1 Objectives

The University of Illinois Hydrosystems Laboratory was commissioned by the Metropolitan Water Reclamation District of Greater Chicago (the District) to characterize sediment oxygen demand (SOD) in Bubbly Creek, a tributary of the South Branch of the Chicago River. Bubbly Creek is known to have a deep bed of organic, nutrient-rich sediments, the result of former waste discharge by the Union Stock Yards, former municipal raw sewage discharge, and ongoing combined sewer overflow discharge by the Racine Avenue Pumping Station (RAPS) located at the head of the existing alignment of Bubbly Creek. The sediment exerts an oxygen demand on the overlying water column. Bubbly Creek is 303(d)-listed by the US Environmental Protection Agency as impaired due to low dissolved oxygen (among other parameters), and the SOD is considered to be a significant contributor to the impairment.

Previous studies have characterized the SOD of various waterways in the Chicago area. Of particular significance are those studies performed by Thomas Butts of the Illinois State Water Survey (1974); and Irwin Polls and Charles Spielman of the Metropolitan Sanitary District of Greater Chicago (1977). While extensive data was gathered, their efforts did not focus on Bubbly Creek; and their sampling protocol characterized SOD under a relatively static water condition. Research performed in the intervening years has indicated that for non-resuspension conditions SOD tends to increase with increasing flow velocity up to a certain velocity threshold (Mackenthun and Stefan, 1998); and therefore SOD sampling performed using traditional methods under relatively static water conditions may significantly underestimate the actual SOD. It is also known that once the stream velocity and the resultant bed shear stress reaches a high enough value, sediment resuspension will occur, which can greatly increase the oxygen demand when the organic content of the sediment is high, although the magnitude of that increase is not well known. Neither velocity-dependence nor resuspension effects on oxygen demand were characterized in the previous studies by Butts (1974) and Polls (1977). The primary areas of focus in the current study have been to characterize SOD as a function of water velocity / bed shear stress; to characterize the bed shear stress threshold at which sediment resuspension is initiated; to characterize the magnitude of resuspension as bed shear stress increases; and to characterize the oxygen demand that is exerted under the various scenarios. The results of this study are intended to be used in future water quality modeling to evaluate various strategies being considered by the District for improving the water quality of Bubbly Creek and downstream receiving waters.

1.2 A Brief Physical Description of Bubbly Creek

A large scale plan view of the current configuration of Bubbly Creek is shown on Figure 1-1 on page 4, which identifies landmarks along the stream that are referenced throughout this report. An overview showing the location of Bubbly Creek in the context of a larger view of the Chicago River system is included as Figure A1 in Appendix A. More detailed figures at smaller scale showing bathymetry and stream profiles are also included in Appendix A.

The following descriptive information was extracted from Motta (2008), which summarizes the physical characteristics of the stream.

> Bubbly Creek is the South Fork of the South Branch of the Chicago River, having a length of approximately 2000 meters (without considering the turning basin), a mean width of approximately 44 meters (between about 23 and 61 m), a mean depth of 2.2 m (from 1.2 to 3.6 m) and a fairly straight channel alignment.
>
> Following is a description of the flow regimes in Bubbly Creek:
>
> 1. During dry periods, the water in the creek is basically stagnant;
> 2. With light rainfall events there are no noticeable changes, since the combined sewage conveyed from the 36 square miles service area (463400 people and 169900 households served) to the Racine Avenue Pumping Station (RAPS) is pumped to the Stickney Water Reclamation Plant of the Metropolitan Water Reclamation District of Greater Chicago and not discharged into the creek;
> 3. During heavy storms, the RAPS discharges combined sewer overflow (CSO) into the creek, so that there is a northward flow in Bubbly Creek which finally discharges into the South Branch of the Chicago River;
> 4. For excessively heavy storms, several CSO outfalls located along the channel may discharge to the creek depending on the intensity of the rainfall event. There are 9 such outfalls along the banks of the creek.

In addition to stream dimensions and flow characteristics described above, the nature of the sediment and streambed is key information to include in a general discussion of the physical characteristics of Bubbly Creek. A deep bed of organic sediments is present resulting from decades of discharge of "large quantities of blood, offal, hair, and other animal wastes" from the Union Stock Yards (USACE, 2007); along with raw sewage from the municipal sewer system. (A more detailed history of Bubbly Creek is provided in Section 1.4 of this report.) Some information regarding the depth and characteristics of the waste-derived sediment is known from previous studies. A substantial set of sediment data was obtained by the USACE (CDM, 2005), and the data from that study is summarized in greater detail in Section 1.3 of this report. For the purposes of providing a brief physical description, the information that is of particular significance is that sediment depth varied between 1.68 and 5.12 meters thick - a

substantial amount of sediment. A profile view of the stream showing the location of the top of sediment and the base of the sediment (in other words, the top of the native subsoil) is included as Figures A13 and A14 in Appendix A. The data reveals that the top of native subsoil varies between an elevation of -4.95 and -7.87 meters relative to the Chicago City Datum (CCD). It is unlikely that these top of subsoil elevations represent the natural streambed prior to human settlement and consequent waste deposition. According to the USACE (2007), in the past "the channel was systematically deepened and widened to allow for drainage and disposal of wastes from the nearby meatpacking industries." This is a viable explanation for the depth to native subsoil, which has allowed for such a substantial accumulation of sediment.

The bathymetry provided on Figures A4 through A12 in Appendix A represents the top of sediment for the entire plan view of the stream. To derive an approximate depth of the waste-derived sediment at any particular location, the bathymetric elevation of the top of sediment can be compared to the mean elevation of the base of sediment, which is approximately -6.4 meters (CCD).

Figure 1-1: Plan View of Bubbly Creek

1.3 Summary of Previously Collected Data for SOD and Sediment in Bubbly Creek

Sediment oxygen demand (SOD) sampling along Bubbly Creek, the Chicago Area Waterway System, and the upper Illinois River has been performed by various organizations in the past. A brief summary of previous findings is provided for reference.

- Thomas A. Butts (1974) of the Illinois State Water Survey
  - Sampling was performed on the upper Illinois River in the Peoria pool, Starved Rock pool, and Dresden Island pool; the closest to Chicago being the latter, which extends from 5 to 15 miles downstream of the Lockport dam.
  - The SOD values progressively decreased in the downstream direction from pool to pool.
  - For the Dresden Island pool (closest to Chicago), 12 experimental stations were sampled with SOD_{20} that varied between 1.25 and 8.08; the mean value was 3.86 $g/m^2/day$.
- Irwin Polls and Charles Spielman (1977) of the Metropolitan Sanitary District of Greater Chicago
  - Sampling was performed throughout the Chicago Area Waterway System, including a sampling station at Bubbly Creek.
  - An SOD_{20} of 3.42 $g/m^2/day$ was measured on 09/27/76 at the Archer Avenue bridge.
  - An SOD_{20} of 4.42 $g/m^2/day$ was measured on 12/06/76 at the Archer Avenue bridge.
  - Both results were obtained in a laboratory from sediment sampled in the field; laboratory analysis was required due to the low dissolved oxygen level in Bubbly Creek.
  - Throughout the Chicago Area Waterway System, SOD_{20} measurements varied between 1.23 to 23.32 $g/m^2/day$; and the mean value was 6.98 $g/m^2/day$.
- Metropolitan Water Reclamation District of Greater Chicago (2007)
  - An SOD_{20} of 3.26 $g/m^2/day$ was measured near the east bank at 33rd Street.
  - An SOD_{20} of 1.38 $g/m^2/day$ was measured near the west bank in the turning basin.
  - Throughout the Chicago Area Waterway System, SOD_{20} measurements varied between 0.23 to 4.81 $g/m^2/day$; and the mean value was 2.01 $g/m^2/day$.

Note 1: SOD_{20} refers to SOD normalized to a temperature of 20°C using a standard equation that takes into account the exponential increase of oxygen demand with temperature.

Note 2: The methods used to measure SOD in these previous studies are briefly outlined in Section 2.2.2 of this report.

In addition to past SOD data, previous data has been collected regarding sediment characteristics in Bubbly Creek. The USACE obtained the most comprehensive set of sediment data (CDM, 2005), which included sample cores from thirteen locations; and five surface grab samples obtained with a Ponar dredge. For each of these samples, various chemical and physical properties were analyzed. In the current study, we utilized the grain-size distribution and specific-gravity determinations from the USACE report in the sediment transport calculations presented later in this document. A copy of the data used is included in Appendix D for reference. The following information was extracted from Motta (2008), which summarizes the most relevant sediment data from the USACE report and various other studies.

- Sediment depth: according to the analysis by USACE (April 2004) along the whole length of Bubbly Creek (cores and grab samples, USACE, 2005), sediment depths ranged between 1.68 to 5.12 m. At the turning basin, the average sediment depth measured by UIC (Yin *et al.*, 2007) was 5.38 m in October - November 2005 (maximum 7.07 m, minimum 3.71 m);
- Porosity: at the turning basin, according to the 2005 analysis by UIC (Yin *et al.*, 2007), the sediment porosity was on average 76.51% for the cores and 87.09% for the surface grabs;
- Particle density: UIC (Yin *et al.*, 2007) found a value of 2392 kg/m^3 for the cores and 2423 kg/m^3 for the surface grabs at the turning basin. According to the analysis by USACE along the whole length of Bubbly Creek in April 2004 (cores and grab samples, USACE, 2005), the specific gravity of the particles was on average 2.10, with maximum and minimum values respectively of 2.57 and 1.37;
- Particle size: from the 2004 study by USACE (cores and grab samples, USACE, 2005), the particle size of the particles, expressed as median size D_{50}, was on average 82 µm (fine sand-coarse silt size), with maximum and minimum values respectively of 258 µm and 20 µm. A "mean" granulometric curve was characterized by 5.43% gravel, 49.15% sand, 26.74% silt and 18.68% clay. Results by the District (2008) at Archer Avenue confirmed these ranges;
- Organic matter (OM) content of the bed sediments: UIC in 2005 measured a value of 152.66 mg/g for the cores and 132.70 mg/g for the surface grabs at the turning basin (Yin *et al.*, 2007). For USACE (2005), the mean value for the Total Organic Carbon (TOC) along the whole length of Bubbly Creek in 2004 was 97.205 mg/g, with a maximum value of 170 mg/g and a minimum value of 5.9 mg/g. USEPA (Collier and Cieniawski, 2003) and the District (2008) confirmed, for several locations in the creek, the order of magnitude reported by UIC and USACE;
- Chemical oxygen demand (COD): while all agencies' data substantially agree about the organic content of the sediments, relevant discrepancies are observed in terms of quantification of COD. For USACE (2005) the mean value for COD along the whole length of Bubbly Creek in April 2004 (cores and grab samples) was 2.221 mg/g, with a maximum value of 6.6 mg/g and a minimum value of 0.38 mg/g. UIC (Yin *et al.*, 2006) reports data by CDM for COD at the turning basin and along Bubbly Creek (average) which are both around 1.2 mg/g. On the other hand, according to the measurements by USEPA (Collier and Cieniawski, 2003) downstream from the I-55 crossing in October 2000, the COD was on average 363.25 mg/g, with maximum and minimum values of 682 mg/g and 193 mg/g.

1.4 A Brief History of Bubbly Creek

With the intent of providing some insight into the nature of current conditions within Bubbly Creek, a brief historical background is provided in this section.

Before being given the name Bubbly Creek, the stream was originally the South Fork of the South Branch of the Chicago River. The South Fork flowed west and north, joining with the West Fork to form the South Branch of the Chicago River. The South Branch flowed in a general easterly direction to eventually join with the North Branch to form the Main Stem of the Chicago River, which discharged to Lake Michigan. An illustration of the pre-settlement alignment of the upper South Branch system is provided on Figure 1-2 at the end of this section. (Some present-day features are also included on the figure for spatial reference.) Figures 1-3 and 1-4 illustrate some of the alterations described in the following chronology.

This chronology was condensed from the book, *The Chicago River: a Natural and Unnatural History* (Hill, 2000), unless otherwise indicated:

1848: Construction of the Illinois & Michigan Canal was completed. Approach channels to the upper canal were located at the junction of the South Fork and the West Fork of the South Branch, altering the configuration of the lower South Fork. (See Figure 1-3).

Mid-1800s to 1865: Slaughterhouses and meatpacking plants were distributed in an unconsolidated fashion along the South Branch and South Fork. These industries discharged waste directly to the streams, contributing to the poor water quality throughout the Chicago River system.

1865: The stock yards were consolidated into a single region known as the Union Stock Yards south of the current head of Bubbly Creek.

~1866: A ditch known as the Stock Yards Slip was constructed that connected to the South Fork. (See Figure 1-3). Waste from the stock yards was discharged to the ditch. Foul conditions in the South Fork resulted in it earning the colloquial name "Bubbly Creek". Ed Lace, co-author of the above-referenced book, relays the following anecdote of conditions in the early 20th century, resulting primarily from the waste discharge by the Stock Yards:

> *"Nothing yet devised by the city regarding sewage control could help the South Fork, as most of its flow was not water. As the offal settled to the bottom it began to rot. Grease separated and rose to the surface. Bubbles of methane formed on the bed of the river and rose to the surface, which was coated with grease. Some of these bubbles were quite large and when they burst a stink arose. There were many local names for this part of the river, most unprintable. The one that stuck was Bubbly Creek."*

The creation of the Stock Yards Slip formed a fork in Bubbly Creek. As a result, the Stock Yards Slip was also referred to as the "East Arm" of the South Fork; and the natural west-to-east alignment of the upper South Fork was also referred to as the "West Arm".

Late 1800s to 1916: Raw sewage from sewer mains along Damen Avenue and Ashland Avenue discharged directly to the "West Arm" of Bubbly Creek.

Late 1800s to 1926: Raw sewage from sewer mains on Halsted Street discharged to the Stock Yards Slip.

1900: The Sanitary and Ship Canal was completed, thereby reversing the flow direction of the South Branch (the receiving waterway), such that flow at the terminus of Bubbly Creek was conveyed west instead of east during normal flow conditions.

1904-1907: The turning basin was constructed at the junction of the South Fork and West Fork, altering the configuration of lower Bubbly Creek.

1916: The Sanitary District of Chicago completed the Stockyards Intercepting Sewer, which provided a new outlet for city sewers along Damen and Ashland Avenue. (It is presumed that the new outlet was further downstream along Bubbly Creek at Racine Avenue.) After the completion of the new sewer, the upper West Arm was filled down to Ashland Avenue.

1923: Congress declared the remainder of the West Arm downstream to 39th Street non-navigable, and that reach was consequently filled.

1921-1926: An intercepting sewer was constructed by the City of Chicago that provided for sewage to bypass the Stock Yards Slip and discharge directly into Bubbly Creek at Racine Avenue.

1933: The Illinois & Michigan Canal was officially closed. The approach channels at the turning basin were filled.

1939: Racine Avenue Pumping Station was constructed. Raw sewage continued to be discharged to Bubbly Creek while the Stickney Water Reclamation Plant became fully operational.

~1940: The Stock Yards Slip was filled; exact date uncertain.

1942: The Stickney Water Reclamation Plant was opened, and Racine Avenue Pumping Station began pumping sewage to Stickney for treatment rather than discharging raw sewage directly to Bubbly Creek during normal flow conditions.

1942-1985: Bubbly Creek continued to receive raw sewage, but only during combined sewer overflow (CSO) events, which occurred approximately 50 times per year.

1971: The Union Stock Yards closed.

1985: The first segment of the Tunnel and Reservoir Plan (TARP) was completed and operational.

1985-Present: More segments of the Tunnel and Reservoir Plan went into operation. CSO events from the Racine Avenue Pumping Station were gradually reduced down to approximately 17 per year, reducing the waste load received by Bubbly Creek.

Figure 1-2: Historical Condition of the Upper South Branch System

Figure 1-3: Modifications to the Upper South Branch System through 1939

Figure 1-4: Current Configuration of the Upper South Branch System

Chapter 2: METHODOLOGY

2.1 Rationale / Overview of Methodology

The ultimate goal of this study was to form a relationship between the flow velocity in Bubbly Creek and the resulting sediment oxygen demand (SOD). In mathematical terms, the goal can be stated as follows:

SOD = f(Flow Velocity)

The simplest way to interpret the results of the field experiments would be to consider experimental conditions in the SOD chamber to be equivalent to actual stream flow conditions. For example, if the velocity in the SOD chamber = **X** cm/sec and the resulting SOD = **Y** g/m^2/day; then one could draw the conclusion that if the stream velocity = **X** cm/sec, then the resulting SOD will = **Y** g/m^2/day. While this would be the simplest way to interpret the data, a more refined approach will yield more realistic results. The direct relationship described in the example above is not valid for a number of reasons. For resuspension conditions, the SOD dependence on velocity is actually a dependence on the bed shear stress produced by that velocity; and the bed shear stress produced by a given velocity profile within the chamber will necessarily be different than the bed shear stress produced by a natural velocity profile through the entire cross section of the stream, even though the magnitude of the mean velocities may be the same. Furthermore, when considering a full sediment resuspension scenario (not just bedload at lower bed shear stress), the oxygen demand will depend on the total amount of sediment that is put into suspension. However the dynamics of the development of a sediment concentration profile will be entirely different in a stream as compared to a confined SOD chamber. In a stream, sediment put into suspension disperses through turbulent advection from near the bed into the remainder of the water column. But in the SOD chamber, the suspended sediment is constrained, not being allowed to disperse throughout the water column, and the resulting oxygen demand in the chamber could be quite different than that of the stream when subjected to the same bed shear stress.

There are numerous scenarios that could be described that illustrate that the conditions in the SOD chamber cannot be directly related to conditions in the natural stream channel. The above cases were provided to illustrate that a number of transformations are required to reach our ultimate goal of forming a valid relationship between SOD and Flow Velocity that can be used to estimate SOD in Bubbly Creek.

The transformations that formed the basis of our methodology are outlined as follows:

(1) $V_{in\ SOD\ chamber} = f(Q_{SOD\ chamber})$

(2) $\tau_{b\ in\ SOD\ chamber} = f(V_{in\ SOD\ chamber})$

(3) $SOD_{NR} = f(\tau_b, \text{Sediment Texture})$

(4) $TSS = f(\tau_b, \text{Sediment Texture})$

(5) $SOD_R = f(TSS)$

The above establish experimentally determined relations that can be input into a model of Bubbly Creek to output the desired results of oxygen demand for a given flow rate.

(6) $V_{in\ Bubbly\ Creek} = f(Q_{Bubbly\ Creek})$

(7) $\tau_{b\ for\ Bubbly\ Creek\ Flow} = f(V_{Bubbly\ Creek})$

(8) $TSS = f(\tau_b, \text{Sediment Texture})$

(9) $\text{Oxygen Demand}_{SED} = SOD_{NR} + SOD_R$

where:

- V is the flow velocity (m/sec)
- Q is the flow rate (m^3/sec)
- τ_b is the bed shear stress (N/m^2)
- TSS is total suspended sediment concentration (mg/L)
- SOD_R is the oxygen demand exerted in the water column by resuspended sediment (g/m^3/day)
- SOD_{NR} is the oxygen demand exerted by the sediment under a condition of no resuspension (g/m^2/day)
- $\text{Oxygen Demand}_{SED}$ is the total oxygen sink associated with sediment, including both resuspension and nonresuspension conditions, to be incorporated in a water quality model. Note that the SOD_{NR} term must be multiplied by sediment area and divided by volume of overlying water to yield a depth-averaged oxygen sink term.

The logic in this subsection will become more apparent when the field experimental methods are described in the following section. However it was appropriate to include this statement at the beginning of the section, so the reader has a clear understanding of the rationale behind each step of the methodology described.

2.2 Field Experimental Methods and Procedures

2.2.1 The U of I Hydrodynamic SOD Sampler

The following figures illustrate the sampling apparatus utilized in the current study. A more narrative description is provided in Section 2.2.2.

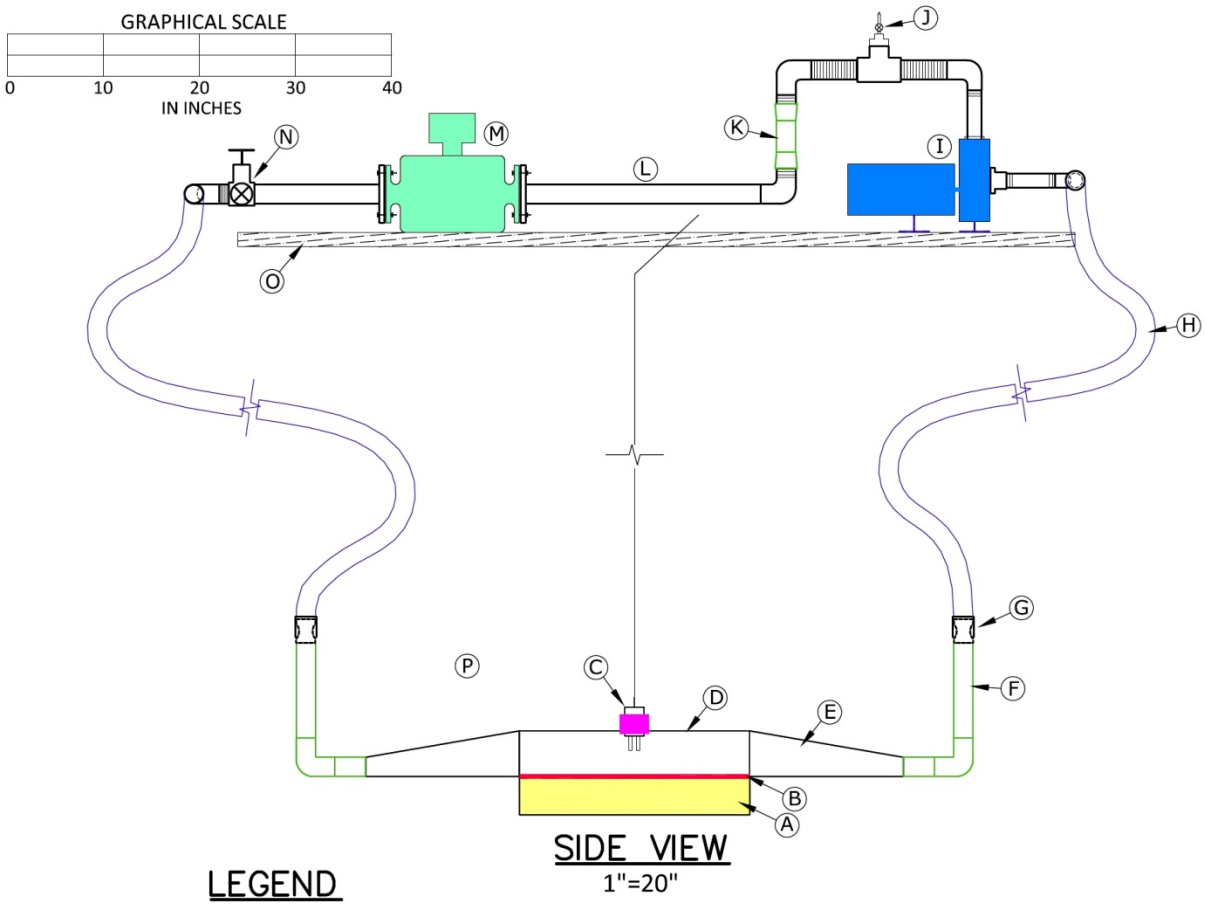

LEGEND

- (A) 4" Stainless steel skirt to penetrate sediment; Bounds all 4 sides of the chamber; Establishes 24" x 9.5" limit of sediment area exposed within chamber
- (B) 2" Stainless steel flange for bearing; Bounds all 4 sides of the chamber
- (C) YSI Professional Plus water quality sensor; Equipped with two probes: (1) Dissolved Oxygen; and (2) ph/ORP; Sensor fits in rubber gasket.
- (D) 9.5" inside diameter half-section of Plexiglas; forms top shell of SOD chamber
- (E) Flow convergence / expansion sections; half-conical; closed on bottom
- (F) 2" diameter PVC sections
- (G) Quick-connect firehose fitting
- (H) 2" diameter rubber firehose; 15' length (each)
- (I) AMT centrifugal pump rated at 80 gpm at 10 ft head; with 0.75 HP electric motor
- (J) Check valve for priming; vaccuum pump connected here
- (K) Clear plastic pipe segment for viewing turbidity characteristics
- (L) 2" diameter Steel pipe segments
- (M) Flow-meter
- (N) Adjustable gate valve for controlling flow rate
- (O) 2x10 treated lumber used to mount the above-surface portion of the system
- (P) (Aluminum frame with 4-point connection that is attached to the on-boat hoist is not shown for clarity purposes)

Figure 2-1: U of I Hydrodynamic SOD Sampler (Schematic)

Figure 2-2: Photograph of the SOD Chamber

This photograph shows the SOD chamber with Plexiglas shell, stainless steel flange and stainless steel skirt that penetrates the sediment. The contraction / expansion sections are shown prior to the PVC pipes being attached. (This photograph shows parts A through E of the diagram on Figure 2-1). The aluminum frame (part P) not shown on Fig 2-1 for clarity, is also evident in this photo.

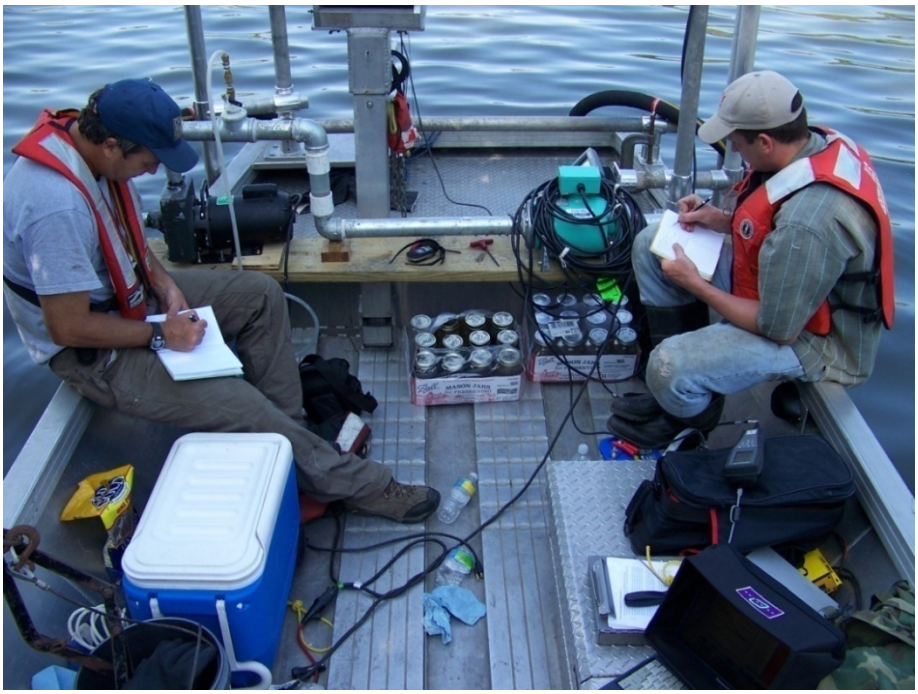

Figure 2-3: Photograph of board-mounted portion of sampler

Figure 2-3 shows the board-mounted portion of the sampler while deployed in the field; parts I through M of the diagram on Figure 2-1 are evident; along with the 2-inch diameter rubber fire hose (part H) hanging over the front of the boat.

Figure 2-4: Photograph of board-mounted portion of sampler (close-up)

A close-up showing the clear plastic pipe segment (part K) containing turbid water during operation at Bubbly Creek. The electric motor and centrifugal pump (part I) are also shown.

Figure 2-5: Photograph showing a large-scale view of the boat with SOD sampler deployed

A photograph of the field operations taken by USGS staff from the 35th Street bridge while the SOD sampler was deployed at Sample Station #4. The rubber hoses hanging over the front of the boat are evident. The vertical aluminum piping seen on both sides of the boat were driven into the sediment as anchors.

2.2.2 Design and Evolution of the SOD Sampler

The U of I Hydrodynamic SOD Sampler shown in Figures 2-1 through 2-5 was based largely on the SOD sampler originally designed by Thomas Butts (1974) and utilized in the Chicago Area Waterway System by Irwin Polls (1977). Significant modifications were made to the Butts / Polls sampler to allow characterization of velocity-dependence and resuspension effects. We feel it is important to describe the modifications of the U of I Hydrodynamic SOD sampler relative to the Butts / Polls sampler, along with the rationale for these modifications. Figure 2-6 illustrates the Butts / Polls sampler for reference in the following discussion.

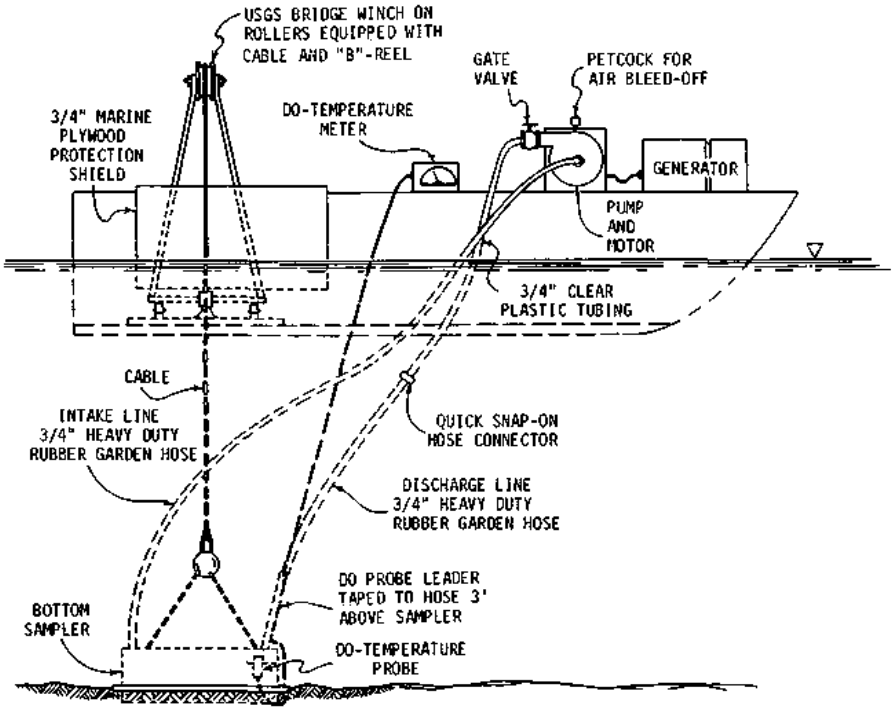

Figure 2-6: The Butts / Polls SOD Sampler (schematic)

The key elements of both systems are as follows: (1) a chamber that is lowered to the streambed, the base of which is open, exposing a fixed area of the sediment surface to the water that is pumped through the otherwise closed circuit; (2) A dissolved oxygen and temperature probe within the chamber; (3) A pump; and (4) Hoses to connect the pumping apparatus on the surface to the chamber on the streambed. The procedures of operation of both systems are also very similar. Both systems are primed such that all free air is evacuated, and then the enclosed water is pumped in a closed loop, allowing the dissolved oxygen concentration to draw down as the water flows past the exposed sediment surface at the base of the chamber. Both systems assume that the

biochemical oxygen demand (BOD) of the enclosed water is exerted at a much lower rate than the SOD, such that any dissolved oxygen drawdown represents primarily SOD. And both systems require that once the system is primed and evacuated of free air, no additional air is allowed to enter into the closed system – this achieves the condition of a control volume on which the SOD calculations are based.

While the above paragraph describes the similarities of the two different systems, the differences are significant. As indicated in Section 1.1 of this report, the Butts / Polls sampler characterized SOD in a relatively static water condition. The ¾-inch garden hoses connecting the pump to the chamber had limited conveyance capacity, and the velocity through the chamber was intended solely as a means to ensure proper functioning of the DO (dissolved oxygen) probe and to maintain well-mixed conditions within the chamber. (Note that the DO probe that Butts and Polls utilized was a Clark-type polarographic electrode probe, a stirring-dependent probe; the specifications for those probes in use at the time required a velocity of 1 foot per second to prevent downward drift of the readings due to oxygen usage by the probe.) According to Butts (1974), the mean velocity through the SOD chamber at full pumping capacity was 0.05 feet per second, although at the outlet of the ¾-inch garden hose where the probe was placed, the velocity exceeded the 1 foot per second specification. The hoses that connected to the chamber were near vertical. Under the low flow operating conditions, the risk of jetting water into the chamber vertically and disturbing the exposed sediment surface was determined to be minimal.

The U of I Hydrodynamic SOD Sampler was required to flow at higher velocities than the Butts / Polls sampler in order to achieve the design goals of characterizing velocity-dependence and resuspension effects. The higher velocities necessitated the major modifications. A key design consideration was to establish a smooth hydrodynamic longitudinal flow condition through the chamber, so that secondary flows would not develop that would generate bed shear stresses whose effects would be difficult to characterize. This design consideration necessitated that the inflow to the chamber be horizontal to approximate natural stream velocity conditions, which would not generally be directed downward, jetting perpendicular into to the streambed. Due to the same hydrodynamic considerations, the SOD chamber was designed with a gradual flow expansion at the inflow side of the chamber and a gradual contraction at the outflow side of the chamber to maintain as smooth a flow condition as possible. (Also note that the expansion / contraction features were

closed at the bottom which provided additional bearing to support the chamber on the soft sediment surface.) The chamber itself has a smaller volume than the Butts / Polls system, being constructed of a half-section of 9.5-inch inside diameter Plexiglas; whereas the Butts / Polls chamber was constructed of a half-section of 14-inch diameter steel pipe. The smaller diameter allowed for higher velocities through the chamber. The remainder of the system consisted of larger elements to accommodate the higher flow rates; for example, 2-inch diameter hoses and pipes, higher capacity pump, etc. The U of I Hydrodynamic SOD sampler also utilized a stirring-dependent Clark-type polarographic DO probe, although the membrane materials have changed in the intervening years such that the specified minimum velocity is 0.5 ft/sec to prevent downward drift of the DO readings.

2.2.3 Sampling Procedures and Required Field Modifications

The initial phase of SOD field sampling on Bubbly Creek was performed during the period of August 10-12, 2009. The second phase of SOD testing was performed on September 8-9, 2009.

1. Pre-Deployment Preparation

   Before deploying to the field, the SOD sampling stations were decided upon; the decision was made that the most useful data could be obtained from the locations of the previous sediment borings sampled by the USACE (CDM, 2005). Core samples through the loose sediment down to the native subsoil were obtained at thirteen stations. In addition five grab samples with a Ponar dredge were collected at stations that were typically at or near the core sample locations. (The data regarding the grain-size and specific gravity analyses are included in Appendix D of this report.) The rationale for using these locations in the current SOD characterization study was that many characteristics of the sediment profile are known, which gave us the opportunity to evaluate our results under the context of the specific sediment conditions at the sampling station.

   The latitude-longitude values for each USACE sampling station were provided in the above-referenced document. We imported those coordinates into the GPS software being used for the field work to allow us to navigate to the specific points with a high degree of accuracy.

Prior to leaving the boat ramp on each day of sampling, the YSI Professional Plus sensor was calibrated for the DO parameter using a 1-point saturated air calibration technique.

2. Setting up on a Sample Station / Priming and Setting the SOD Sampler

Upon navigating to the sampling station using the on-boat Trimble AG132 GPS, the boat was anchored onto the station using two 2-inch diameter, 20-foot length aluminum pipes driven vertically by hand into the sediment until sufficient resistance was met to ensure the pipes would not dislodge during sampling. These pipes were attached to the boat via speed rail fittings attached to the outside of the boat. (The aluminum pipes are shown on Figure 2-5.)

Once the boat was anchored in place, some background water quality measurements were taken with the YSI sensor to determine the ambient DO levels near the surface and at the streambed. The water depth was measured by a Lowrance LCX-15 MT Echo Sounder attached to the front of the boat. The YSI sensor was then clamped into the gasket on top of the SOD chamber, and the chamber was placed in the water. The system was primed by lowering the chamber to just below the water surface (with top submerged); a small vacuum pump was connected to the hose barb (part J of Figure 2-1); the check valve was opened; and the vacuum pump was powered on, drawing in ambient water from Bubbly Creek through the base of the chamber to fill the entire volume of the sampling apparatus. Most of the air was evacuated during this process. However, typically there were still some small pockets of air that remained trapped in the piping and hoses at this stage, so additional air evacuation was performed by running the centrifugal pump at the maximum flow rate with the SOD chamber still near the surface. Because flow through the SOD chamber was always at a lower velocity than anywhere else in the system due to the larger cross-sectional area, any air bubbles tended to accumulate in the high point of the chamber. Therefore, while still running the pump, the chamber was manually rocked back and forth and inverted to evacuate air bubbles that collected. When in the inverted position, small air bubbles skimmed over the topmost edge of the opening until all air was evacuated. When bubbles no longer emerged from the chamber, we ensured the lack of air bubble entrainment by carefully examining the water pumping through the clear plastic pipe segment (part K of Figure 2-1). The SOD chamber was then turned into its normal upright position, and the centrifugal pump was turned off to create as calm a condition in the chamber as possible for the process of setting the chamber on the streambed.

The stream depth recorded from the Echo Sounder was used as a guide while lowering the chamber using the boat-mounted hoist. A graduated reel connected to the hoist line was calibrated to indicate the instantaneous depth of the bottom flange of the chamber; and graduation marks set at 1-foot intervals along the fire hoses were used to guide the hoses down at an even rate. This lowering process was performed in an extremely gentle manner once the reel and hose graduations indicated the chamber was nearing the bed of the stream. Typically when the streambed was first contacted and a small amount of pressure applied by the chamber cutting edge, bubbles from the bed were released, which became evident at the surface. Additional slack was given on the hoist line to allow the chamber to seat into the sediment and to ensure that any small movements of the boat during sampling would not cause the hoist line to drag the chamber out of its seated position. No sampling stations were encountered where the sediment was so loose / soft that once the hoist line was given slack, the chamber continued to sink deep into the sediment. (This was a concern during the design of the sampler.) Once the field staff was convinced that the chamber was fully seated, the SOD test was then ready to be initiated.

3. Running the SOD test

First, a brief description is provided of how the sampling was intended to be implemented. This will be referred to as the "optimum sampling procedure":

(a) Prepare and seat the chamber into the streambed per the protocol above.

(b) Tighten the flow control valve (part N of Figure 2-1) to almost entirely closed. Turn on the centrifugal pump. Very gently open the gate valve until the desired flow rate for the first trial is achieved.

(c) On a given station, the first trial is the lowest flow rate to be tested. Run the test until the dissolved oxygen (DO) drawdown curve has established a steady, equilibrium slope. (A graph of the readings is viewed in real-time using the YSI data management software on the laptop computer, which connects to the YSI sensor via a USB connection.) Any sediment resuspension that occurs during this process is noted, as indicated by the color and opacity of the water passing through the clear plastic pipe segment (part K of Figure 2-1). Establishment of the equilibrium DO drawdown slope dictates the end of the trial.

(d) The next trial is run by simply increasing the flow rate to the next flow rate to be tested. (In other words, the chamber is not picked up and reset, the system is not reprimed, etc.) The trial runs exactly as described in step (c) for the new flow rate.

(e) Additional trials are run until the pump flow rate is at the maximum value.

As expected, actual conditions in the field necessitated changes to the above sampling procedure. The optimum sampling procedure could be most closely followed when the ambient dissolved oxygen (DO) level in Bubbly Creek was relatively high. Under those circumstances, each trial could draw down the DO by a fraction of the total concentration, and numerous trials could be run successively. However, it was very common for the ambient DO to be very low (<2 mg/L), particularly in the morning hours. (This situation is discussed in greater detail in Chapter 3.) Under those circumstances, a single trial could draw down the DO to 0 mg/L, and no further trials could be run successively without unseating the chamber from the streambed, evacuating the low-DO water, re-priming the system, and resetting the chamber in a different location. This was a time-consuming procedure that would take the majority of the day to run a relatively small number of trials. Therefore a modified sampling procedure was established for the morning hours; and a procedure closer to the optimum procedure was performed in the afternoon, where ambient DO conditions were found to be much more favorable.

Revised morning sampling procedures:

(a2) Prepare and seat the chamber into the streambed per item 2 above.

(b2) Run a single trial per items 3(b) and 3(c) above, drawing the DO all the way down to near 0 mg/L.

(c2) Initiate a “scour test” where DO is not recorded.

- (i) Increase the flow rate and run for approximately 5 minutes, noting any change in turbidity.
- (ii) Continue the procedure until the onset of the major resuspension phase. (This situation is discussed in greater detail in Chapter 3.) Once the major resuspension phase is reached, pull a water sample by connecting a ½” diameter hose to the top hose barb (part J of Figure 2-1); open the top check valve, allowing a small volume of water to jet through the hose into a sample container.
- (iii) Continue the above steps until the flow rate is maximized.

(d2) Unseat the chamber from the sediment, evacuate the turbid water, re-prime the system, and reset the chamber on the bed in a different location.

(e2) Run a single trial per items 3(b) and 3(c) of the optimum sampling procedure at the desired flow rate.

Revised afternoon sampling procedures:

(a3) Run exactly per the optimum sampling procedure until DO draws down to 0.

(b3) If the major resuspension phase has not yet occurred, run the “scour test” and additional setup per (c2) through (e2) above.

2.2.4 SOD_{NR} Calculations

1. Basic Equations

Mass balance for a constituent within a control volume is expressed by the following differential equation:

$$\left[\frac{dC}{dt} + \nabla F_{C,D} - \sum S_i\right] = 0 \quad (1)$$

where C = the concentration of the constituent of concern (g/L)

t = time (day)

ΣS = Net change resulting from Sources / Sinks (g/L/day)

$\nabla F_{C,D}$ = Net convective and diffusive flux of the constituent across the boundary of the control volume (g/L/day)

In the context of the current study, the constituent of concern is oxygen. The principle utilized by Butts and Polls was that the control volume was considered to be the volume of the entire sampling apparatus, which was a closed circuit of fixed volume, which eliminates convective or diffusive flux (ie, $\nabla F_{C,D} = 0$). They also presumed that the only Source / Sink component in the sampling apparatus was the oxygen demand exerted by the sediment; (ie, $\Sigma S_i = SOD_{NR}$). This sink term can be expressed in terms of oxygen drawdown rate per unit volume as:

$$S_1 = \frac{\mathrm{SOD_{NR}} * \mathrm{A}}{\mathrm{V}} \quad (2)$$

where SOD_{NR} = sediment oxygen demand under non-resuspension condition ($g/m^2/day$)

A = area of exposed sediment (m^2)

V = Volume of Water enclosed in the system (Liters)

Therefore the mass balance equation can be reformulated as:

$$\frac{dC}{dt} = \frac{\mathrm{SOD_{NR}} * \mathrm{A}}{\mathrm{V}} \quad (3)$$

(*Note that the SOD_{NR} could also be represented as a diffusive flux out of the system rather than an internal sink term, but the result would yield the same equation*.)

Butts (1974) formulated the above mass balance relationship as follows:

$$\mathrm{SOD_{NR}} = \frac{V}{A} * \mathrm{S_{DO}} * \mathrm{CF} \quad (4)$$

where S_{DO} = dC/dt = Slope of the DO drawdown curve ((mg/L)/minute)

CF = Conversion Factor to convert the resulting ((mg/min)/m^2) to (g/m^2/day)

Since V and A are constant, based solely on the construction of the sampling apparatus, the only variable is S_{DO}. Therefore the equation can be written as a simple linear equation in the form of:

$$\mathrm{SOD_{NR}} = \beta * \mathrm{S_{DO}} \quad (5)$$

where β = a constant taking into account the volume, area, and unit conversion factors

For the U of I Hydrodynamic SOD sampler, the following values were measured or calculated:

Volume (V) = 51.2 Liters

Area (A) = 0.147 m^2

$$\mathrm{CF} = 1.44 \left(\frac{1\ \mathrm{mg}}{\mathrm{min} * \mathrm{m}^2} * \frac{1\ \mathrm{g}}{1000\ \mathrm{mg}} * \frac{1440\ \mathrm{min}}{\mathrm{day}} \right)$$

These values yield the following SOD_{NR} equation:

$$\mathrm{SOD_{NR}} = 501.6\ \mathrm{S_{DO}} \quad (6)$$

For comparison, the linear equations from Butts' and Polls' systems were as follows:

Butts: SOD_{NR} = 206.6 S_{DO}

Polls: SOD_{NR} = 274.96 S_{DO}

The variation in the constant β reveals the fact that the U of I Hydrodynamic SOD Sampler had greater total volume and lesser exposed area of sediment in the chamber, which would result in a slower DO drawdown than in the other two systems if operated under the same environmental conditions and pumping rates.

2. Modified Basic Equation to Account for BOD of ambient water

The basic SOD_{NR} equation shown above assumes that the only oxygen source / sink in the closed system is oxygen demand exerted by exposure to the sediment. However in reality, any oxidizable material in the ambient water will also exert an oxygen demand that would occur whether or not the water was exposed to the sediment. In general, the ambient water biochemical oxygen demand (BOD) would be exerted at a much lower rate than SOD_{NR}; and if the BOD was relatively low compared to the SOD_{NR}, then this effect could be neglected without introducing significant error.

Mackenthun and Stefan (1998) measured the BOD of the ambient water separately in their experiments, calculating the drawdown in the units of [mg/L/min]. When evaluating the oxygen drawdown curve from their experiments, they isolated the BOD contribution from the SOD_{NR} contribution. The standard operating procedures of the US Environmental Protection Agency (Parsons, 2007) also account for the BOD as a separate sink term in their SOD_{NR} measurements.

The first sink term was shown in Eq. (2), and the additional sink term can be represented as follows:

$$S_2 = S_{BOD} \tag{7}$$

where S_{BOD} = Rate of drawdown associated with Biochemical Oxygen Demand present in ambient water (mg/L/day)

Unlike the SOD_{NR} sink, the BOD sink term on a per volume basis is independent of the total volume of the system.

Modifying the mass balance Eq. (3) to include the additional sink term for BOD yields the following:

$$\frac{dC}{dt} = \left(\frac{SOD_{NR} * A}{V}\right) + S_{BOD} \tag{8}$$

Using the nomenclature of Butts and Polls per Eq. (4), where S_{DO} is the slope of the oxygen drawdown curve (dC/dt), the following is a modification of Eq. (4) to account for BOD:

$$SOD_{NR} = \frac{V}{A} * (S_{DO} - S_{BOD}) * CF \tag{9}$$

Therefore, the controlling equation for determining sediment oxygen demand becomes:

$$SOD_{NR} = 501.6\ (S_{DO} - S_{BOD}) \quad (10)$$

3. Temperature Correction Equation

It is known that SOD is temperature-dependent, and in order to normalize field data from various stations sampled at different temperatures, Polls (1977) used the following temperature correction factor:

$$SOD_{NR\ 20} = SOD_{NR\ T} * 1.047^{(20-T)} \quad (11)$$

where $SOD_{NR\ 20}$ = SOD_{NR} normalized to 20°C

$SOD_{NR\ T}$ = Measured SOD_{NR} at any temperature

T = Temperature in °C

(1.047 is a temperature coefficient commonly denoted by the variable, Θ)

The coefficient 1.047 used above is a standard for BOD temperature corrections. Research performed in the intervening years has suggested a different coefficient for the above equation when applied to SOD_{NR} measurements. The value of 1.065 was the average of calculated values from individual SOD_{NR} experimental studies derived from a literature review performed by Thomann and Mueller (1987), which was referenced in Mackenthun and Stefan (1998). Therefore the temperature correction equation used in this analysis for sediment oxygen demand in a non-resuspension condition is as follows:

$$SOD_{NR\ 20} = SOD_{NR\ T} * 1.065^{(20-T)} \quad (12)$$

In those experimental trials where sediment was put into suspension, resulting in oxidation occurring in a fashion more similar to BOD oxidation, the standard coefficient of 1.047 was used per Equation (11).

2.2.5 S_{BOD} Calculations for use in the SOD_{NR} Calculation

Optimally, S_{BOD} would have been field-measured on ambient water at the same time that each SOD sampling trial was being performed. However, performing S_{BOD} measurements requires a sealed system and a means of stirring the water, and we were not equipped with this field-experimental setup before the SOD testing was initiated.

Therefore on October 1, 2009 (during the same field work as the Ponar dredge sampling described in the following Section 2.2.6), we collected samples of water for laboratory analysis of BOD oxygen uptake rate. At various locations along the length of the stream, one-gallon plastic containers were submerged into Bubbly Creek such that the top of the container was 16 to 18 inches below the water surface. (Note that when priming the SOD sampler, water was brought into the system from near the surface due to the higher oxygen content and to facilitate the evacuation of air as described in the priming procedure; the intent was to gather water for laboratory analysis that was representative of the water used in the field experiments.) The one-gallon plastic containers were submerged with the lid on to prevent surface debris from being included in the samples. Once the container was submerged, the lid was opened, and all air was purged from the container as it filled with water. The samples were labeled and placed in a cooler.

The laboratory methods for measuring the S_{BOD} are included in Section 2.3.

Because we were not able to measure S_{BOD} during the field-sampling, some corrections had to be applied to account for the differences in temperature and dissolved oxygen content between the laboratory conditions and field conditions during SOD sampling. These corrections are described as follows:

1. Temperature Correction

   The same equation described earlier for temperature corrections of SOD_{NR} is also commonly used for S_{BOD}:

   $$S_{BOD\ 20} = S_{BOD\ T} * 1.047^{(20-T)} \quad (13)$$

2. Oxygen Concentration Correction

   Past research suggests that SOD_{NR} is independent of oxygen concentration when oxygen is in the range of 3-8 mg/L. However the same is not true for S_{BOD}. Standard equations used to describe

BOD oxidation kinetics are based on the rate of BOD oxidation being dependent on the amount of oxygen available. Because the laboratory analysis was conducted in such a manner that the water was saturated with oxygen prior to sampling, it was not valid to assume that S_{BOD} would be exerted at the same rate in situ under low dissolved oxygen conditions as in the laboratory. Therefore a correction was necessary.

The following equation is the oxidation sink term due to BOD from dissolved oxygen kinetics utilized by Motta (2008).

$$S_{BOD} = -K_D \Theta_D^{(T-20)} * \left(\frac{C_{DO}}{K_{BOD} + C_{DO}} \right) * C_{BOD} \quad (14)$$

Where: S_{BOD} = Rate of drawdown associated with Biochemical Oxygen Demand present in ambient water (mg/L/day)

K_D is the deoxygenation (oxidation) rate coefficient at 20 °C (1/day)

$\Theta_D^{(T-20)}$ is the temperature correction factor described in the subsection above, whose standard value is 1.047

C_{DO} is the concentration of dissolved oxygen (mg/L)

C_{BOD} is the concentration of oxidizable material remaining in terms of how much oxygen it will require to oxidize it (mg/L); C_{BOD} is synonymous with the commonly measured "ultimate BOD".

K_{BOD} is a half-saturation constant for BOD oxidation (mg/L); Motta (2008) used the value 0.5, derived from a review of previous studies

This equation is used in the numerical model to iterate through time where:

$$C_{DO}(t + 1) = C_{DO}(t) + S_{O2} + \text{any other source/sink terms.}$$

At each successive time interval the values of C_{DO} and C_{BOD} are modified by oxidation that occurred in the previous time interval.

The current problem to be solved is not to define the evolution of dissolved oxygen concentration through time, but rather to find a relation between S_{O2} for in situ conditions where dissolved oxygen may be low; to S_{O2} in the laboratory where the dissolved oxygen was effectively unlimited. In order to simplify the explanation, the temperature correction factor is calculated independently and only the oxygen-limiting factor is considered. The key relation is:

$$X = \frac{\left(\frac{C_{DO\ in\ situ}}{K_{BOD} + C_{DO\ in\ situ}} \right) * C_{BOD\ in\ situ}}{\left(\frac{C_{DO\ lab}}{K_{BOD} + C_{DO\ lab}} \right) * C_{BOD\ lab}} \quad (15)$$

If the water samples collected were truly representative of C_{BOD} for the field experiments, then at time = 0, $C_{BOD\ in\ situ} = C_{BOD\ lab}$. If we next assume that the water quality is such that C_{BOD} was present in sufficient quantity that it did not limit the reaction – in other words, only a very small percentage of the C_{BOD} was eliminated during the course of the tests (which we feel is a reasonable assumption) – then at any time throughout the experiments,

$C_{BOD\ in\ situ} \approx C_{BOD\ lab}$. As such, the C_{BOD} term cancels out of the equation, leaving the correction factor as:

$$X = \frac{\left(\frac{C_{DO\ in\ situ}}{K_{BOD} + C_{DO\ in\ situ}} \right)}{\left(\frac{C_{DO\ lab}}{K_{BOD} + C_{DO\ lab}} \right)} \tag{16}$$

where X is simply a dimensionless multiplication factor that represents the relative percentage at which BOD is exerted for differing experimental conditions as a function of the amount of dissolved oxygen present. The BOD sink for each field experiment with its unique DO concentration was calculated using this factor multiplied by the laboratory determined value of S_{BOD}.

2.2.6 Ponar Dredge Surface Sediment Sampling

The Ponar dredge is a relatively simple device that functions like a clamshell dredge. The clamshell is lowered using a rope, and tension on the rope keeps a lever mechanism engaged that maintains the clamshell in the open position. Upon settling on the bed, tension is taken off of the rope, and the lever disengages, allowing the clamshell to close under its own weight as the rope is retrieved. The closing of the clamshell scoops sediment from the surface of the streambed. It collects a sample from the sediment surface to a depth of less than 6 inches.

For the current field experiments, the Ponar dredge was lowered off the side of the boat by hand using a nylon rope. Upon raising the dredge up to the water surface, the dredge was placed in a 5-gallon bucket, and the clamshell opened, releasing into the bucket the sediment and any water that was captured while the dredge was raised. A representative sample of the mixture was collected in a 1-quart container, which was then placed in a cooler containing ice.

A Ponar grab sample was collected at each SOD sampling station. We noted any relevant features regarding sediment texture, color, odor, etc. These samples were submitted to the District lab for analysis of percentage volatile solids. In addition to the samples collected during the SOD experiments, we performed additional investigation on October 1, 2009, for the primary purpose of collecting fresh sediment for use in laboratory oxygen uptake experiments. The secondary purpose of the sampling was to characterize the spatial variability of sediment types in a more comprehensive sampling pattern than the limited number of SOD stations. Those grab samples were collected as described previously, except that before placing the sample in the 1-quart container, the sediment texture was determined using the field method, where a small portion of the soil is kneaded between thumb and forefinger to form a ribbon. The soil was generally too saturated to form a ribbon even for the fine-grained samples. However it was possible to note the relative percentage and size of the sand component; and to estimate relative amounts of organic material characterized by a greasy texture. (Note that this was a rather unappealing task.) Below are photographs taken during Ponar dredge sampling at Bubbly Creek.

Figure 2-7: Photograph showing the Ponar dredge

The clamshell dredge in the open position as it is lowered to the streambed.

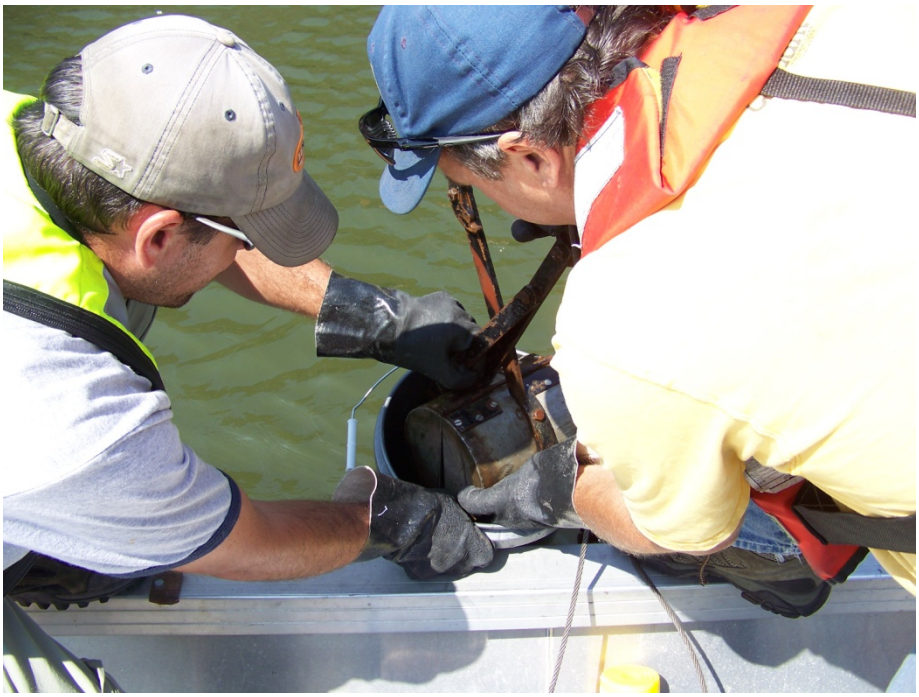

Figure 2-8: Photograph showing the Ponar dredge being retrieved from the streambed

Jim Duncker and Ryan Jackson of the USGS capture the dredge in a 5-gallon bucket; after the photo was taken the dredge was opened to spill its contents into the bucket.

2.3 Laboratory Methods and Procedures

2.3.1 Analytic Testing by MWRD Laboratory

The District made available the staff and resources of the analytic laboratory section of the Stickney Water Reclamation Plant to analyze solids and liquids collected in the field as part of this study.

All laboratory analyses were performed in accordance with Section 2540 of the *Standard Methods for the Examination of Water & Wastewater* (AWWA, 2005). A very brief description of the methods detailed in the manual is provided below.

Liquid Samples:

Liquid samples were analyzed for total suspended solids (TSS) and volatile suspended solids (VSS). The TSS analysis was performed by mixing the suspended sediment solution and obtaining a representative sample using a pipette; the sample volume was chosen with the intent to obtain 2.5 to 200 mg of dried residue. This sample was filtered through a glass-fiber filter disk, and the captured residue placed in a crucible and dried at 105°C for one hour. The residue was then weighed and the weight of the filter and crucible subtracted to yield a TSS concentration.

The VSS represents the fraction of the solids captured in the above analysis that volatilized in an oven at 550°C.

Solids Samples:

Sediment samples collected with the Ponar dredge were analyzed for total solids by percent weight and volatile solids by percent weight. The analysis for total solids by percent weight was performed by placing a representative sample of the sediment mixture totaling 25 to 50 grams on an evaporating dish, which was then weighed. The dish with sediment was then dried at 105°C for one hour. The remainder was again weighed, and the procedure repeated until the weight change was less than 4%. After subtracting the weight of the dish, the total solids by percent weight was calculated as the initial weight divided by the final weight.

The volatile solids by percent weight represents the fraction of the dried solid from the above analysis that volatilized at 550°C.

2.3.2 Oxygen Demand Laboratory Analysis

Collection of sediment samples and ambient water from Bubbly Creek on October 1, 2009 was described in Section 2.2.5 and 2.2.6. The water and sediment samples were kept in coolers with ice until the laboratory analysis was performed, which occurred on October 2, 2009 and October 6, 2009.

Laboratory analysis was performed by Ven Te Chow Hydrosystems Laboratory (VTCHL) staff utilizing the research and development laboratory at the Stickney Water Reclamation Plant.

The intention of the analysis was to obtain a relationship between total suspended solids concentration and oxygen uptake rates for various types of sediment at various concentrations of solution. Ambient water from the stream was used as the medium of the suspended sediment mixtures to ensure the presence of the type of microbial populations from the water column that would contribute to oxygen uptake in Bubbly Creek during an actual sediment resuspension event. A secondary goal of the analysis was to determine the S_{BOD} of ambient water for use in the SOD calculations.

The specific procedures used in the analysis are described as follows:

1. Three hours prior to the initiation of the experiments, the water and sediment samples to be tested were selected, removed from the cooler, and set in an area of 20 to 25°C where they could reach an equilibrium temperature similar to laboratory conditions.

2. A YSI 5100 dissolved oxygen / temperature sensor was powered on and calibrated. (The probe end of the YSI 5100 contains a rubber sleeve that fits tightly into the top of a standard 300 ml BOD bottle to seal the system from exposure to air during an oxygen uptake test. The probe also contains a stirring attachment.) The YSI 5100 uses a Clark-type polarographic electrode probe, which is stirring dependent; the self-stirrer incorporated into the model ensures that adequate stirring is provided.

3. The ambient water tests were the first trials initiated on each day of sampling. The tests involved pouring approximately 400 to 500 ml of the Bubbly Creek water sample into a clean 1-quart plastic container; placing the lid on the container; and then shaking vigorously to saturate the water with oxygen. The water was then poured into a clean BOD bottle to the point of overflow. The YSI 5100 probe was then inserted, causing some minor overflow and ensuring no

excess air in the system. The self-stirrer was turned on and dissolved oxygen readings were recorded manually periodically throughout the test.

4. The tests on sediment solution involved a more complicated procedure. A representative portion of the sediment sample was obtained by gently stirring the sediment in its 1-quart sample container using a stainless steel stirring rod, which distributed the liquid portion that typically had settled at the top of the container. After the gentle stirring, a fraction of the sediment was removed from the sampling container to prevent spillage and to facilitate stirring during the next step. What remained in the sample container was then stirred vigorously with the stirring rod. A stainless steel spoon was then used to dig into the container and extract a portion of the sediment from the center to bottom of the container for use in establishing the suspended sediment mixture for analysis.

   For those sediments that were predominantly fine-grained, the initial trial involved mixing the maximum concentration at a volume in excess of what was needed for an individual oxygen uptake test. This allowed for a simple dilution of the excess in following steps to establish the lower concentration mixes. (Note that the sediment mixtures were so rich in organic material that there was no concern of the organics in the excess solution being depleted during the time period between mixing and later testing to such an extent that the experiments would become rate-limited.) Mixing the initial high concentration solution was performed by placing the representative sediment in a 1000 ml glass beaker to reach approximately the 150 ml graduation line. (Volumes were noted, but were by nature not precise, because TSS concentrations would be obtained separately following the experiments through analysis by the District's analytical lab.) Then the beaker was filled with Bubbly Creek water up to the 600 ml graduation. The solution was stirred to fully-mixed and then approximately 400 ml of the mixture was poured into a 1-quart plastic container. The container was closed and then shaken vigorously to saturate the solution with oxygen. The mixture was quickly poured into a BOD bottle and the YSI 5100 probe was inserted and self-stirrer engaged. Dissolved oxygen readings were recorded manually periodically throughout the test. The tests were run until a well-defined drawdown curve was established, or until the DO was reduced to near 0 mg/L. Once the test was completed, the 300 ml mixture was poured into a new 1-quart sample container

and labeled for analysis. At the end of the day all samples were transferred to the analytical lab for TSS and VSS analysis.

Following the initial high concentration test, the excess solution that was mixed previously and kept in the beaker was utilized for the next test. The mixture was diluted with additional Bubbly Creek water, typically adding 2 to 3 times the volume of the remaining mixture in the beaker. Once the diluted solution was well mixed, the same procedure as described above was performed, with excess solution being kept in the beaker for the next dilution.

For those sediments that were predominantly coarse-grained (fine sand and coarser), the same procedure as above was attempted, but the rapid settling of the sand in both the beaker and the 1-quart shaking container made obtaining a uniform mixture of the desired consistency while pouring into the BOD bottle nearly impossible. Therefore the modified procedure for the sandy sediment involved simply adding scoops of material directly to the BOD bottle, then aerating the water sample separately in the 1-quart container and pouring into the BOD bottle to approximately half-full. The BOD bottle was then hand-swirled to ensure that the sediment was not sticking to the bottom and could be entrained; then the BOD bottle was filled to the top, and the test proceeded as described above.

2.3.3 LISST-ST

The LISST-ST was utilized in this study primarily to characterize settling velocity of various sediment samples. Secondarily it was used for analysis of particle size distribution of the samples. The particle size distribution provided in the previously described USACE (CDM, 2005) study was used as the more comprehensive analysis of particle size distributions. The following description of the LISST-ST was extracted from the study by Briskin and Garcia (2002).

> The LISST-ST, or Laser In-Situ Scattering Transmissometer with Settling Tube, is manufactured by Sequoia Scientific. It consists of a Plexiglas settling tube with sliding doors that seal it and a canister that contains a laser, data logger, and batteries. It measures size distribution, concentration, and settling velocity distribution. Two vertical sheets of Plexiglas inside the 5-cm settling tube create a rectangular settling volume that is 5 x 1 x 30 cm. This feature is incorporated for faster suppression of turbulence at fill-up (Sequoia). Settling velocity is measured for 8 log-spaced size classes between 1.25 and 250 µm. Using the LISST-ST instead of a standard settling tube has some advantages. Measurements are taken automatically at log-spaced intervals, meaning settling data can be obtained for the larger and heavier particles that settle out first. Using a standard settling tube requires withdrawing and sometimes dewatering samples in order to obtain concentration data. This added handling may break up aggregates that naturally form as the particles fall and collide. In contrast, the LISST-ST takes data inside the settling tube.
>
> According to the Fraunhofer approximation, the scattering by a spherical particle of diameter d is identical to the diffraction of light by an aperture of equal diameter. This diffraction is independent of particle composition. The small-angle scattering field of an ensemble of particles is the sum of the diffraction from all the apertures, and the scattered intensities simply add, since the apertures do not interact (Pottsmith and Bhogal). In the LISST-ST, a collimated laser beam illuminates suspended particles near the bottom of the settling tube. Scattering at multiple angles is measured by a specially made silicon detector, stored in a computer, and later inverted mathematically on a PC to obtain size distribution (Sequoia). A detailed explanation of laser diffraction size analysis can be found in Agrawal et. al. (1991).
>
> In an idealized experiment, the settling column contains a fully mixed water sample in which all the particles in each size class have the same density. The solids concentration measured by the laser beam at the beginning of the test is constant and equal to the fill-up concentration. Over time, the particles that were initially at the top of the settling column reach the laser. The concentration for any size class of particles goes from the initial value to zero over a duration corresponding to the time for these particles to fall through the 6-mm laser beam (Sequoia). The settling velocity for each size class is computed by dividing the height of the settling column by the total time required by the particles to settle out of

solution. Of course in reality, the solids in a water sample will seldom have a homogeneous composition. This variation in particle density smears the concentration profile. In addition, residual turbulence generated while filling up the tube may affect settling. The LISST-ST finds a settling time that minimizes the mean-square difference between the idealized and normalized history of any size class.

In the current study, the laboratory methods used with the LISST-ST involved the following steps:

(1) Calibrate the LISST-ST at the beginning of each day of sampling by running a background scatter test using tap water.
(2) Add a small representative sample of the sediment to a partially filled gallon container of tap water. Shake vigorously to break up flocculated material that would naturally break apart during turbulent flow conditions.
(3) Add 500 ml of tap water to a glass beaker. Pipette 5-10 ml of the solution from the 1-gallon container into the beaker until the solution was just turbid enough to remain visibility through the beaker. Swirl the beaker to mix.
(4) Gently pour the solution into the settling tube on the LISST-ST. Run a 1-minute analysis for particle size distribution.
(5) Decant the settling-tube. Mix another 500 ml of solution in the same manner as described in step (3). Gently pour into the LISST-ST settling tube and run a 22-hour test for settling velocity distribution.

2.4 CFD and Numerical Modeling

2.4.1 Computational Fluid Dynamics (CFD) model of the SOD Chamber

The three-dimensional flow simulations were performed with a commercial nonhydrostatic finite-difference model, FLOW-3D (Flow Science Inc.). This model has previously been used to resolve the flow around numerous structures including bridge piers (Richardson and Panchang, 1998), submarine pipelines (Smith and Foster, 2005, Hatton et al., 2007), bendway weirs (Abad et al., 2008), SEPA stations (Abad et al. 2004), and tunnel intakes in dams (Groeneveld et al., 2007). The model resolves fluid–fluid and fluid–air interfaces with a non-boundary fitted rectangular grid and a volume of fluid (VOF) approach which resolves the grid cells into separate fractional fluid components containing the fraction of water and fraction of solid in the cell. Similarly, a fractional area-volume obstacle representation (FAVOR) approach is used to parameterize the flow within cells which contain fluid-obstacle boundaries (Hatton et al., 2007). The model solves the 3D Reynolds averaged Navier–Stokes (RANS) equations for incompressible flow simultaneously with the continuity equation. Both equations are given, respectively, by

$$\frac{\partial u_i}{\partial t} + \frac{1}{V_F}\left\{ u_j A_{[j]} \frac{\partial u_i}{\partial x_j} \right\} = -\frac{1}{\rho}\frac{\partial p}{\partial x_i} + G_i + f_i \tag{17}$$

$$V_F \frac{\partial \rho}{\partial t} + \frac{\partial}{\partial x_i}\left(\rho u_i A_{[i]}\right) = 0.0 \tag{18}$$

where *i,j* =1,2,3 stand for the *x*, *y* and *z* components in the Cartesian coordinate system respectively, V_F is the fractional volume open to flow, ρ is the fluid density, *t* is time, x_i is the positional coordinates, u_i is the velocity coordinates, A_i is the fractional areas open to flow, G_i is the body accelerations, and f_i is the viscous terms.

Besides the mass and momentum equations, it is necessary to use a turbulence closure. The RNG turbulence model described by Eqs. (19) and (20) is implemented in a very similar manner to the standard *K-ε* closure for the turbulent kinetic energy and dissipation of turbulent kinetic energy equations respectively. The RNG-based models rely less on empirical constants while setting a framework for the derivation of a range of models at different scales (Flow Science Inc., 2008).

$$\frac{\partial k}{\partial t}+\frac{1}{V_F}\left\{u_j A_{[j]}\frac{\partial k}{\partial x_j}\right\}=P+Diff-\varepsilon \tag{19}$$

$$\frac{\partial \varepsilon}{\partial t}+\frac{1}{V_F}\left\{u_j A_{[j]}\frac{\partial \varepsilon}{\partial x_j}\right\}=\frac{C_{\varepsilon 1}.\varepsilon}{k}P+DDif-C_{\varepsilon 2}.\frac{\varepsilon^2}{k} \tag{20}$$

where *P* is the shear production, *Diff* and *DDif* are the diffusive terms, $C_{\varepsilon 1}$= 1.42 and $C_{\varepsilon 2}$ is a function of the shear rate (not a constant as in the standard *K-ε* model).

A 3D representation of the chamber of the U of I Hydrodynamic SOD Sampler is shown in Fig. 2-9. The mesh block distribution used in FLOW-3D model is presented in Fig. 2-10. In addition a 3D rendering image of the system of structures using Flow-3D's FAVOR is presented in Fig. 2-11.

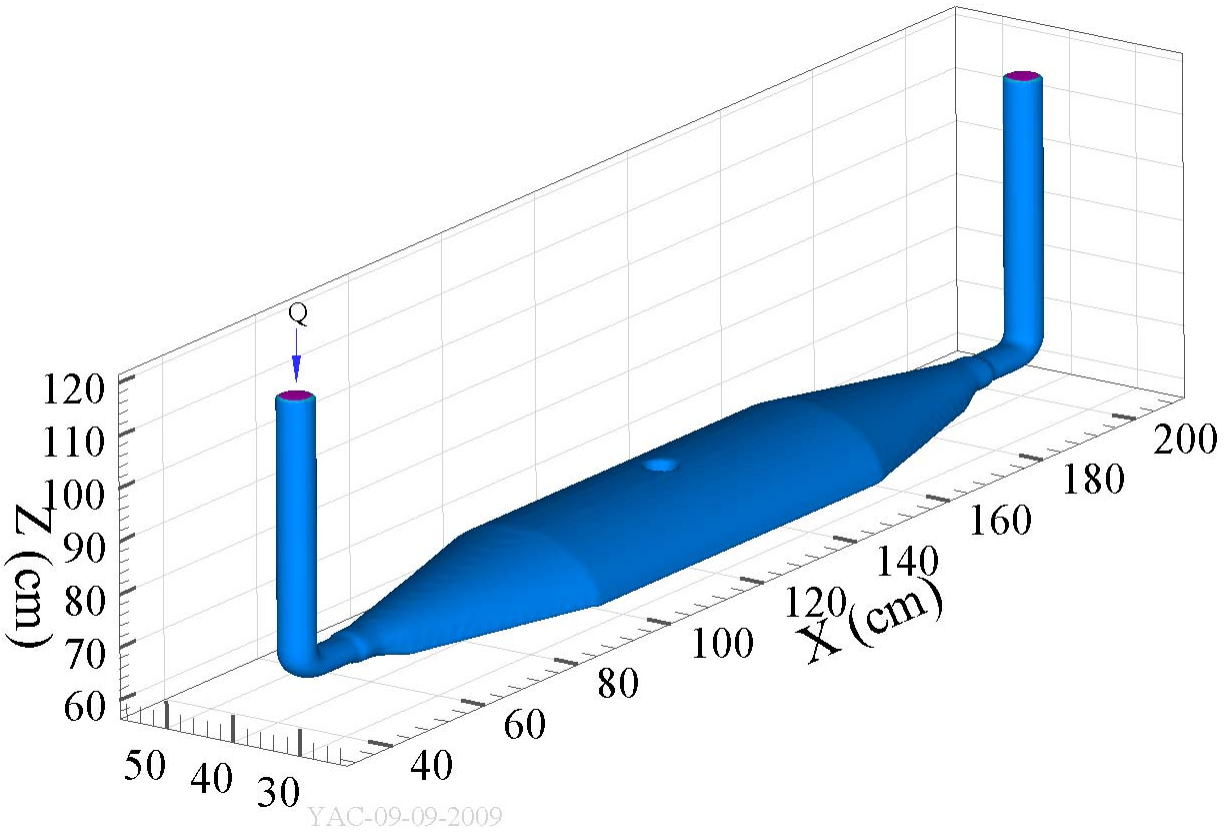

Figure 2-9: Schematic diagram of SOD chamber used in CFD model

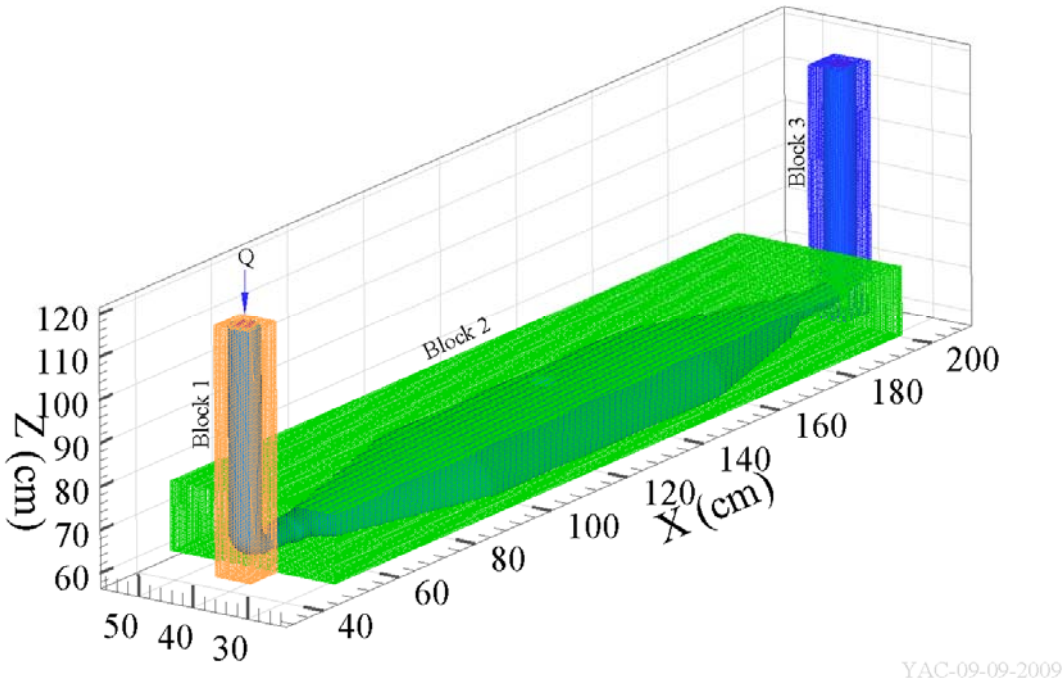

Figure 2-10: Mesh block of SOD chamber used in CFD model

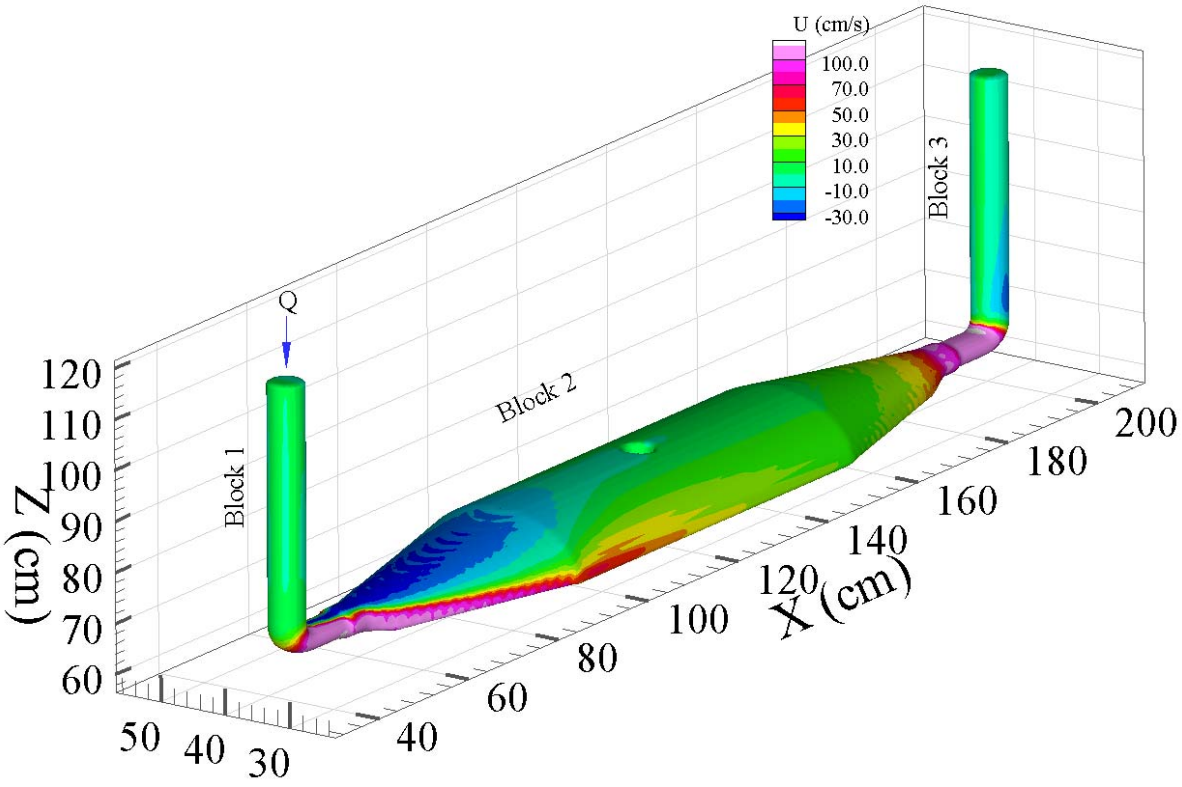

Figure 2-11: 3-D rendering of the Horizontal Velocity u (cm/s) using Flow-3D's FAVOR

A compromise between block-mesh-cell size and computational time was needed in order to attain representative hydraulic results. If very precise results are desired then cell size should be small enough to resolve the most important hydraulic variables influencing the flow dynamics inside the SOD chamber. Resolving both the main flow and turbulent characteristics adequately would require using small computational cells and this requires an enormous amount of computational time mainly due to the size of the structures (Fig. 2-9).

An initial simulation was run with cubic cells of Δx=2.0 cm, ΔY=2.0 cm, and ΔZ=2.0 cm (for all mesh blocks in Fig. 2-10) during a sufficient time to reach steadiness in the flow discharge and associated statistic quantities such as mean kinetic energy and average turbulent energy. A second run was conducted with a smaller cell size of Δx=0.5 cm, ΔY=0.5 cm, and ΔZ=0.5 cm. It was determined that the flow discharges through the SOD chamber in Fig. 2-9 for the two cell sizes differed by small quantities. The finer mesh was chosen for the simulations since it provided adequate resolution of mean flow characteristics such as flow velocity, turbulent kinetic energy (TKE), rate of dissipation of TKE, and bed shear stresses.

2.4.2 Numerical Modeling of Hydrodynamics

All field experiments in this study were analyzed in terms of the bed shear stresses generated by flow through the SOD chamber. In order to relate these bed shear stresses to actual bed shear stresses that would result for real flow events in Bubbly Creek, a model of the hydrodynamics of Bubbly Creek was required. For this study the model STREMR-HySedWq was utilized. The following information on the hydrodynamic portion of the model was extracted from Motta (2008):

> STREMR-HySedWq is a two-dimensional depth-averaged hydrodynamic, sediment transport and water quality model. Bernard (1993) developed the hydrodynamic model, Abad et al. (2007) the sediment transport and Motta (2008), the water quality.
>
> The two-dimensional depth-averaged hydrodynamic model STREMR includes a *k*-ε two-equation turbulence model and a correction for the mean flow due to secondary flow. The model was developed by Robert S. Bernard at the Waterways Experiment Station (WES) of the USACE (Bernard, 1993). It is a numerical model that generates discrete solutions of the incompressible Navier-Stokes equations for depth-averaged 2-D flow. The discretization of the equations is based on the Finite Volume (FV) method, in which a stair-stepped (piecewise constant) discretization of the flow depth is adopted.
>
> A limitation of STREMR is that it imposes a rigid-lid approximation for the free surface which requires the specification of the water surface elevation. However, STREMR accounts for the free surface influence by means of a correction to the pressure equation. The assumption of rigid lid implies that only steady flow and sub-critical flow conditions can be modeled. The assumption of rigid lid was proved to work fairly well for the kind of events analyzed later in this study for Bubbly Creek (Motta et al., 2007).

As described by Motta (2008), the Bubbly Creek model was setup for simulation of the majority of the stream, but excluded the rapid expansion / contraction reaches which include the sedimentation basin north of Racine Avenue Pumping Station and the turning basin at the lower end of the stream. The modeled segment of stream comprises STA 1+50 to 21+80 in accordance with the stationing used in the figures in the current study. The following information on the setup of the model for application to Bubbly Creek was extracted from Motta (2008):

> Based on the most recent bathymetric survey of Bubbly Creek provided by the U.S Geological Service (USGS), a bathymetric grid 0.5 m x 0.5 m was extracted. The shoreline was determined using an aerial image.

A structured mesh was created using the grid generator MESH92 (Bernard, 1992). The elevation of each node of the mesh was assigned as weighted average of the elevations of the four closest surrounding points in the bathymetric grid (Shepard, 1968). The bottom elevation of each cell (I,J) of the domain was then calculated from the elevation of its four vertices.

The computational mesh is structured and made up of 6780 irregular rectangles, 339 in the longitudinal direction and 20 in the transverse direction.

Vertical banks were assumed to complete the cross sections. This assumption is considered reasonable in light of previous hydrodynamic analyses of the creek and not far from the reality, considering that in several locations along the creek the cross sections end up with vertical walls.

The turning basin area was not modeled, since STREMR-HySedWq is constrained by the use of one “block” structured meshes, which are not suitable for a dramatic widening like the one occurring at the turning basin.

Chapter 3: FINDINGS AND OBSERVATIONS

3.1 SOD Sample Stations

The following figures show the locations of the SOD sample stations for reference in the discussion that follows. A table with the latitude-longitude values of each station follows the figures.

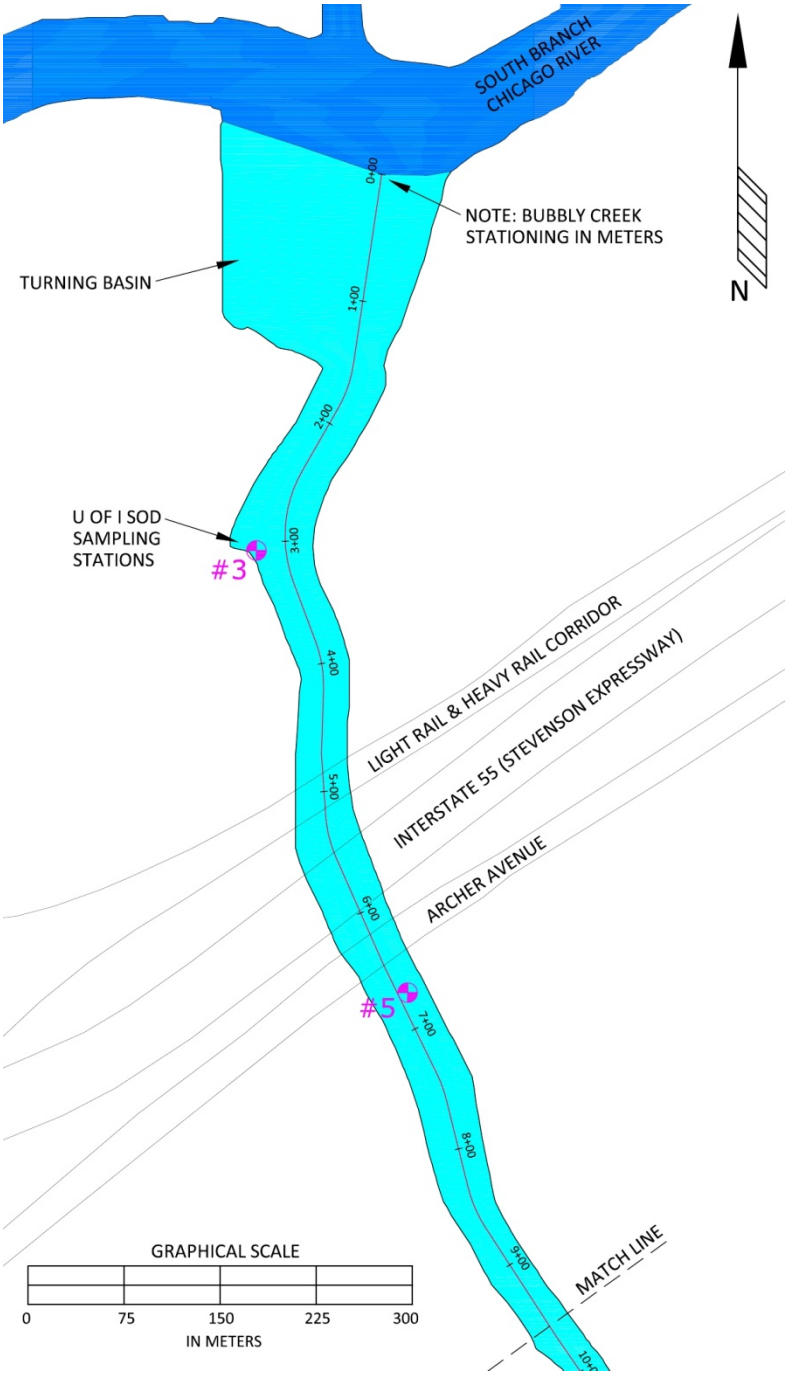

Figure 3-1: SOD Sample Stations (Lower)

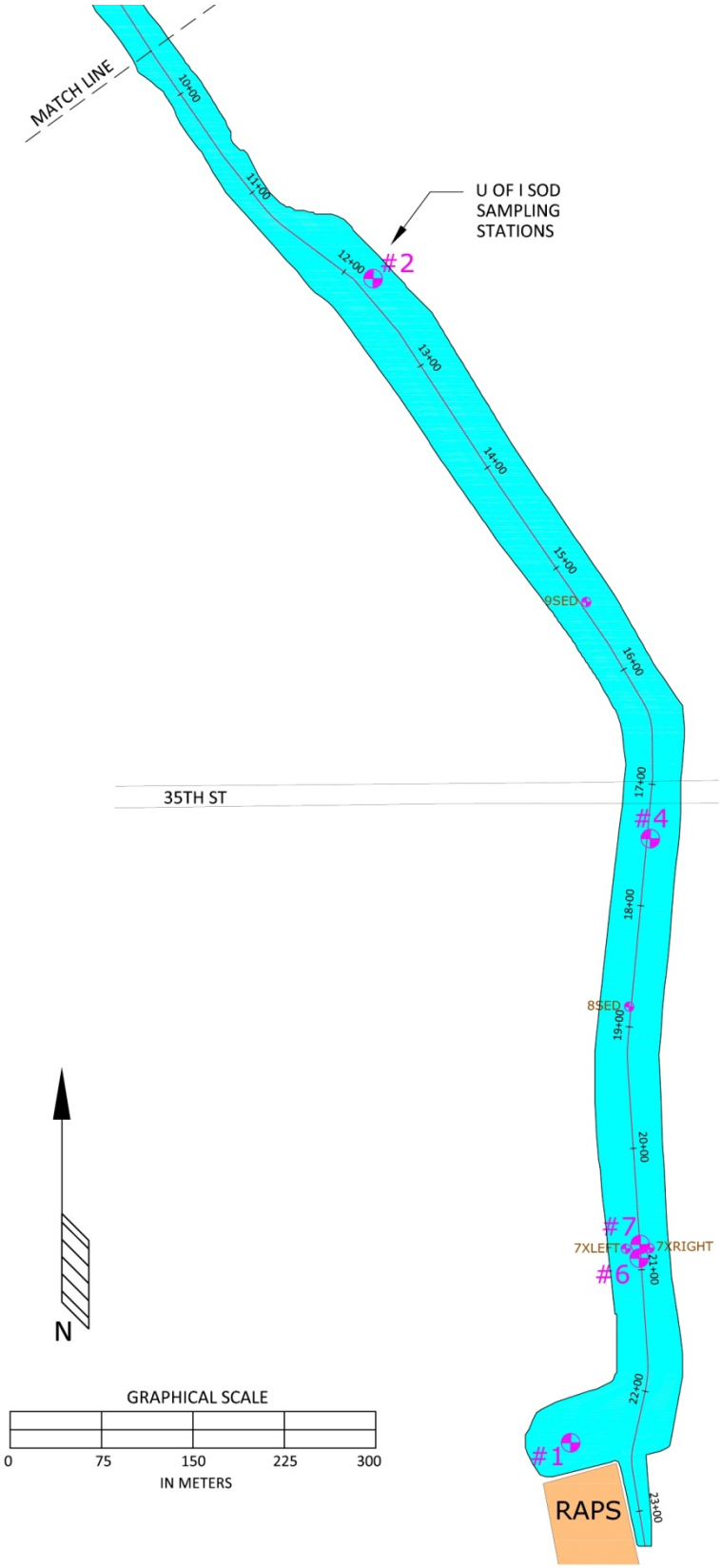

Figure 3-2: SOD Sample Stations (Upper)

Sample Station ID	Latitude	Longitude
1	41.825775306252	-87.658164072243
2	41.834386499234	-87.660157924587
3	41.841494691139	-87.665187896068
4	41.830240980754	-87.657365864283
5	41.838379208304	-87.663757780676
6	41.827143516655	-87.657484333317
7	41.827245149988	-87.657475349984

Table 3-1: SOD Sample Station Locations (Lat-Long)

3.2 General Field Observations

Finding #1: There were 3 (and possibly 4) phases of resuspension

a. "No resuspension" phase: The water was basically clear with the only suspended solids being the amount present in the ambient water.

b. "Flaking" phase - Small to moderate-sized flakes of organic material were scoured off the sediment surface, but had little influence on water color or opacity until the flakes were eventually ground up in the pump impeller after a few passes. It was observed that flakes generally were put into suspension at the beginning of the trial, and then no more were seen for the remainder of the trial while the flow rate remained constant; when the flow rate was increased to the next level, new flakes scoured off.

   In this phase of resuspension, each increase in flow rate was accompanied by an increase in water opacity. The specific change from the "flaking" phase to the following "slurry" phase was sometimes difficult to distinguish when the organic material in suspension reached such a high concentration that the water was too opaque to see through the clear plastic pipe segment.

c. "Slurry" or Full Suspension phase - This was the major resuspension phase, described earlier in the document. In this phase the water would turn dark and almost entirely opaque; the oxygen drawdown would increase substantially above that recorded during the "flaking" phase; and the samples we collected were commonly very thick with suspended sediment. (The most telling sign was the sharp increase in oxygen drawdown.)

d. Intermediate or Bedload phase - As described above, the distinction between the "flaking" phase and the "slurry" phase was sometimes indistinct. For example, at Sample Station #4, during sampling we thought we had passed into the slurry phase at the maximum flow rate

when the water became very opaque. However the total suspended solids concentration and oxygen drawdown did not reach typical magnitudes observed elsewhere for the slurry phase. We postulate that there is an intermediate phase that occurs in those sediments with a substantial sand component. Once all or most of the organic debris lying on the sediment surface is put into suspension ("flaking"), as the bed shear stress is increased, eventually the main part of the sediment begins to be mobilized as bedload. At this stage, we expect the mobilized portion of the sediment will be partitioned into the sandy fraction that saltates along the bed, and the fine-grained and organic fraction that tends to diffuse into suspension. The lower concentrations of suspended sediment and oxygen demand we observed during the intermediate phase may have been due to this phenomena – that only a fraction of the sediment was actually put into suspension. It is also important to note that as the bed shear stress is increased to even higher values, the sandy material would eventually be expected to transition to Full Suspension as well.

An example of the different phases of resuspension observed in the field is shown on Figure 3-3.

Figure 3-3: A photograph showing the different phases of resuspension observed

This photograph was taken in the field which illustrates changing water conditions in the sampling system during the course of a set of trials. These samples were collected from Sample Station #4, where the sediment was coarse and found to be relatively resistant to resuspension. Sample 4AI was collected during the priming process which represents

ambient water conditions (no resuspension) observed during the low flow rate trial. Upon increasing the flow rate, flakes of organic material were first seen at a flow rate of 50 L/min. Increasing the flow rate at approximately 15 L/min intervals through a number of trials, the water opacity changed very little until 140 L/min, at which point the flaking became much heavier and the water turned noticeably more opaque. Sample 4A2 was taken at the end of the 140 L/min trial, which appeared to be a threshold between light flaking and heavy flaking. (The TSS of this sample was 148 mg/L.) The flow rate was again increased at approximately 15 L/min intervals, and at each stage the water became progressively more opaque. Sample 4A3 was pulled at the end of the trial where the maximum flow rate was 190 L/min. During sampling, we thought we had passed into the "slurry" phase, but later analysis of the oxygen demand and TSS concentrations revealed that the major resuspension phase had not yet been reached. Sample 4A3 appears fairly dark, but the TSS was only 386 mg/L. Other sample stations had TSS as high as 10,500 mg/L.

After trials were run at several stations and this classification system was found to be generally applicable regardless of conditions at a specific station, the classification into phases was used to guide the sampling efforts. (For example, the flow rate or length of the trial could be modified based on the phase.)

Finding #2: Algae had a significant influence on the dissolved oxygen concentrations in the water column.

During sampling performed during the morning hours in August, we observed DO concentrations of approximately 2.0 mg/L with little variation between the water surface and near the streambed (<0.5 mg/L). Over the course of the day, the DO steadily rose, reaching a concentration as high as 6.6 mg/L near the surface. The afternoon DO concentrations typically showed a substantial variation between the surface and the streambed - approximately 1.5 to 2.0 mg/L. During the September sampling, this phenomenon was also pronounced, but with starting DO concentrations at a higher value, approximately 4.5 mg/L; and with concentrations rising to approximately 9.0 mg/L at the surface in the afternoon.

Further proof of this algae influence was obtained on the morning of 8/12/09 at 8:45 am (CDT). We performed a longitudinal boat run along the approximate centerline of Bubbly Creek with the DO probe strapped onto the Echo Sounder mount 15.25" beneath the water surface. Although the DO was low due to the morning hour, whenever we crossed a shady location (a bridge, a building on the

east bank, etc.) the DO would drop substantially; and upon returning to the sun, the DO would rise by >1 mg/L.

Finding #3: Bubbly Creek has variable surface sediment textures; and the onset of the major resuspension phase was dependent on the sediment texture at the sample station.

At Sample Stations 4, 6, and 7 the sediment was basically indistinguishable from sewer grit. These stations were also the most difficult to drive the aluminum stakes into while anchoring the boat. There was a general trend of the sediment becoming increasingly fine-grained in the downstream direction.

Finding #4: When comparing two SOD sample stations with fine-grained sediment texture, the sediment that is under deeper water was more resistant to resuspension than the sediment under shallow water.

Sample Station #5 was characteristic of this phenomenon. The sediment was a highly organic muck, similar to that observed elsewhere along lower Bubbly Creek; but the major phase of resuspension was not initiated until the flow rate in the SOD sampler was increased to 172 L/min. In the shallower areas of muck, the major phase of resuspension was reached at flow rates less than 120 L/min.

Finding #5: Resuspended sediment oxygen demand (SOD_R) is entirely different in oxygen drawdown characteristic relative to the "no resuspension" phase which represents the traditional concept of SOD.

The DO drawdown curves for the "no resuspension" phase were generally linear for DO concentrations above 2.0 mg/L, very similar to the previous findings of Butts and Polls. However, the DO drawdown curves observed for the "slurry" phase were exclusively exponential in shape, similar to a standard BOD drawdown curve, although much exaggerated with respect to time.

Finding #6: Acceptable results from the DO probe were obtained even when velocity in the experimental chamber was less than 0.5 ft/sec.

As indicated in Section 2.2.2, the Clark-type DO probe utilized in this study (YSI Professional Plus) specified a minimum velocity of 0.5 ft/sec to prevent downward drift of DO readings. The reason for this specification is that the probe uses oxygen as part of its measurement procedure; and as a result a local zone of low DO can be produced around the probe yielding a non-representative DO

measurement. During field measurements, caution was taken to not lower velocities excessively. For the trials involving lower flow rates, downward drift was observed, which yielded oscillations of the DO drawdown curves due to the following mechanism: the probe utilized oxygen, drawing down oxygen levels near the probe, as new water then entered the near-probe area due to advection, bringing the oxygen levels back up, with the process then repeating. Oscillations were almost unnoticeably small for the high flow rates, but reached amplitudes of approximately 0.5 mg/L for the lowest flow rates (Trials 3A, 4A, 5A, 6A). The oscillations would introduce unacceptable error if the recording interval was sparse and/or the net DO drawdown over the course of the entire trial was low (less than the magnitude of the oscillations), because readings taken at random intervals along the oscillations would yield a noisy result that may not have a discernible drawdown pattern. However, in the current study measurements were recorded at 1 second intervals, which allowed capture of the full oscillatory pattern and the net oxygen drawdown in the control volume. The decision was made to not lower flow rates below 25 L/min due to the concern that the amplitude of the oscillations might overwhelm the total oxygen drawdown over the course of the test.

The full range of flow rates measured during field trials was 25 L/min (0.0147 ft^3/sec) to 224 L/min (0.1318 ft^3/sec). The cross-sectional area of the chamber was 0.0229 m^2 (0.246 ft^2). This yields a mean velocity in the longitudinal direction of the chamber that varies linearly between 0.060 ft/sec to 0.536 ft/sec for the full range of flow rates sampled.

3.3 Surface Sediment Characterization

As briefly described in the previous subsection, sediment samples collected with the Ponar dredge at each SOD sample station revealed that materials were coarse (sand) at the upper end of Bubbly Creek and became increasingly fine-grained (silt/clay) with increasing organic content in the downstream direction. This indicated that the stream behaves similar to a primary settling tank in depositing the sediment load that is discharged during combined sewer overflow (CSO) events from the Racine Avenue Pumping Station. However, with the relatively few number of SOD sample stations, we decided that additional characterization of the spatial variability of sediment was warranted. This was particularly important given the findings that the SOD appeared to be strongly dependent on the sediment type (especially for the resuspension scenarios).

On October 1, 2009, sediment sampling in a more expansive pattern was undertaken in accordance with the methodology outlined in Section 2.2.6. Based on this analysis, we were able to develop a conceptual map of general surface sediment conditions along the length of Bubbly Creek. Figures 3.4 and 3.5 on the following pages show the map of sediment conditions, along with all the data locations on which the conceptual map was derived. In the case of the fine-grained organic muck sediment, a distinction was also made between those located in “shallow” water and those located in “deep” water, as the resuspension characteristics appeared to differ based on the depth of the overlying water. The criterion used for the distinction was the bathymetric elevation -2.5 meters relative to the City of Chicago Datum. (This corresponds to a normal water depth of approximately 1.75 meters.)

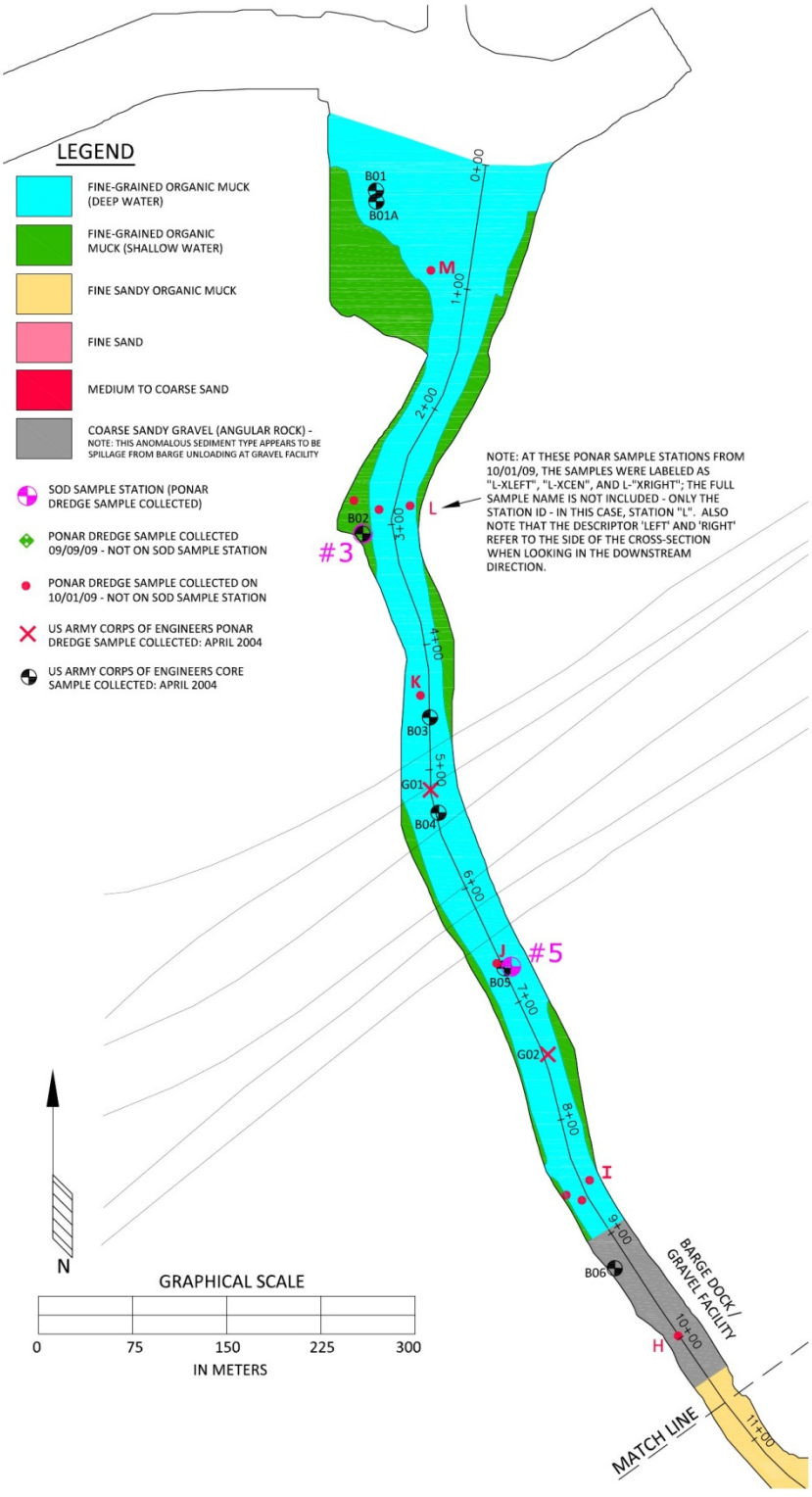

Figure 3-4: Surface Sediment Characterization Map (Lower)

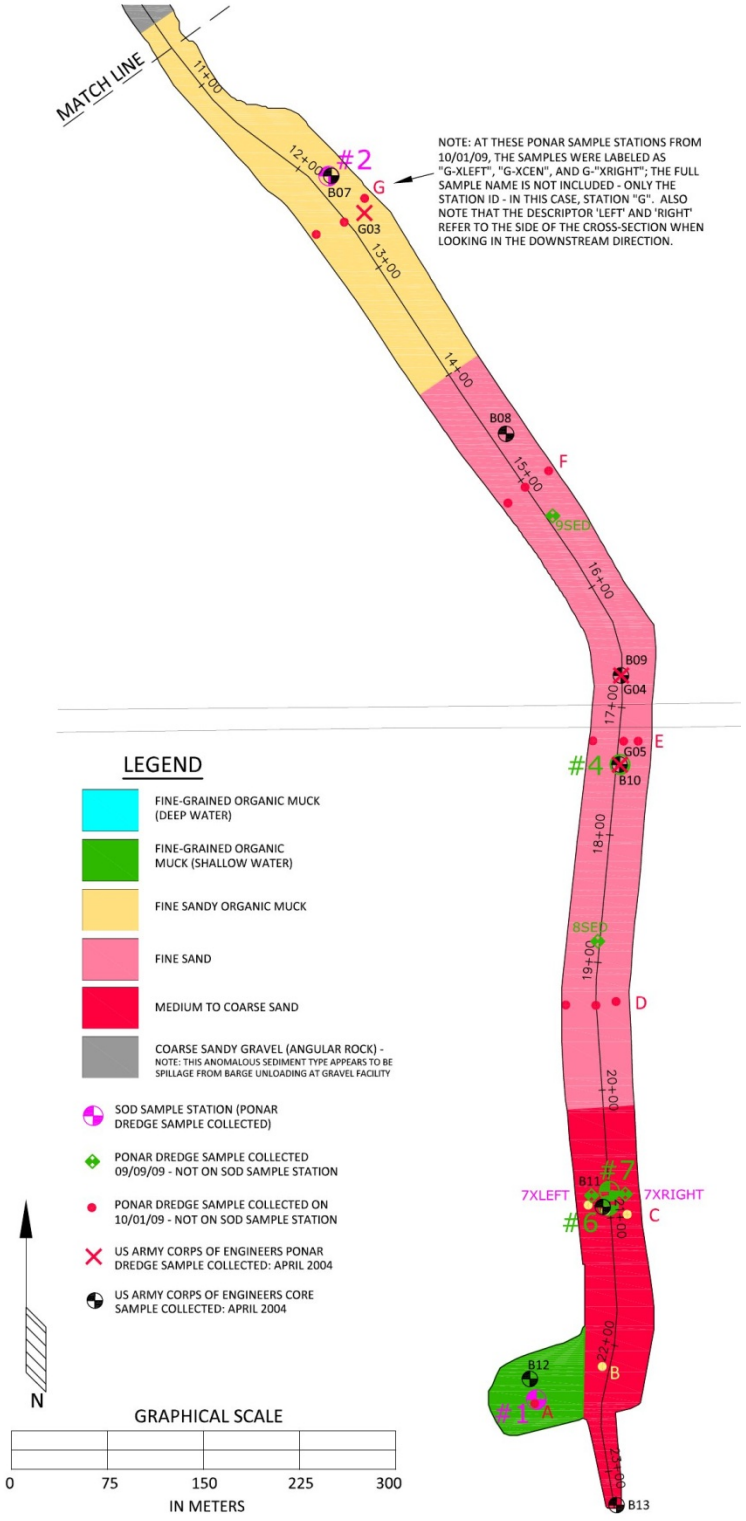

Figure 3-5: Surface Sediment Characterization Map (Upper)

The above figures were based primarily on the findings of the Ponar dredge sampling. The figures have been described as conceptual for a number of reasons. First, this study was not intended as a detailed delineation of sediment types; and a detailed delineation would obviously not consist of areas bounded by straight lines. Secondly, all samples did not match exactly with the mapped classification; this is particularly true near the banks where the sediment composition was much more random than the neat conceptual figure would suggest. Thirdly, all surface sediment data identified conditions at a particular instant of time; and conditions are likely to change on a CSO event-by-event basis. The conceptual map is simply intended to illustrate the general trend of sediment characteristics observed. The trend described generally matches the findings from the core samples and Ponar grab samples in the USACE sediment study (CDM, 2005). Table 3-2 provides laboratory analysis of the nine sediment stations sampled with the Ponar dredge during SOD sampling; Table 3-3 summarizes the findings from all the data sets analyzed.

Description	Total Solid by Weight (%)	Volatile Total Solid by Weight (%)
Sediment STA 1	52.91	11.05
Sediment STA 2	43.43	10.09
Sediment STA 3	22.09	19.80
Sediment STA 4	71.47	1.61
Sediment STA 5	32.05	18.71
Sediment STA 6	72.46	3.36
Sediment STA 7	69.83	3.17
Sediment STA 7-XLEFT	63.17	5.58
Sediment STA 7-XRIGHT	73.49	0.62
Sediment STA 8	74.65	0.64
Sediment STA 9	69.12	1.97

Table 3-2: Laboratory Analysis of Organic Fraction of Ponar Dredge Samples

Note: Volatile Total Solid by Weight represents the percentage of the dried solid that volatilized in an oven at 550°C.

Sample ID *	Field Notes (Texture)	Nearest Corps sample	D50 (µm)	% Sand	% Organic (%VTSW)
A	Muck with various household debris	B12	45	33.7	11.0 [1SED]
B	Sand; moderate to coarse grit	B13	1250	79.6	5.4
C-XCEN	Coarse sand	B11	250	88.6	3.4 [6SED]/ 3.2 [7SED]
C-XLEFT	Sand; moderate to coarse grit				
C-XRIGHT	Fine sand; prominent muck component relative to C-XCEN and C-XLEFT				
D-XCEN	Fine sand; homogeneous grain-size	B11	250	88.6	0.6 [8SED]
D-XLEFT	Fine sand; prominent muck component				
D-XRIGHT	Fine sand; moderate muck; less organic than D-XLEFT				
E-XCEN	Fine sand; homogeneous; light to moderate muck component	G05/ B10	205/ 98	95.3/ 59.8	1.6 [4SED]
E-XLEFT	Fine to moderate-grained sand with some fine gravel				
E-XRIGHT	Muck; completely unconsolidated; slurry				
F-XCEN	Mucky fine sand; sand component homogeneous	B08	90	54.4	2.0 [9SED]
F-XLEFT	Muck; minimal fine sand component				
F-XRIGHT	Mucky coarse sand; lots of fine gravel 3-8mm diam.				
G-XCEN	Mucky fine sand; sand component homogeneous; very fine-grained	G03/ B07	105/ 30	86.0/ 25.5	10.1 [2SED]
G-XLEFT	Muck; cohesive; minimal fine sand component				
G-XRIGHT	Fine sandy muck; cohesive				
H	Coarse sandy gravel; angular rock up to 10 cm diam; very little organic	B06	2800	43.2	11
I-XCEN	Muck; cohesive; minimal sand	G02/ B05	100/ 40	67.2/ 23.3	14/ 12
I-XLEFT	Muck; cohesive; minimal sand				
I-XRIGHT	Mucky coarse sand; non-cohesive; with fine gravel 3mm diam				
J-XCEN	Muck; much undecomposed organic debris (twigs, leaves, etc.); light to moderate amount of coarse sand and fine gravel	G02/ B05	100/ 40	67.2/ 23.3	18.7 [5SED]
K-XCEN	Fine sandy muck	G01/ B03	125/ 21	19.9	10/ 26
L-XCEN	Muck; loose, greasy, non-cohesive; no discernible sand component	B02	28	16.7	19.8 [3SED]
L-XLEFT	Muck; cohesive				
L-XRIGHT	Muck; loose, greasy, non-cohesive				
M-XCEN	Muck; loose, greasy, non-cohesive	B01A	26	32.5	22

Table 3-3: Textures of Ponar sediment samples per field method

Notes regarding Table 3-3:

Note 1: All cells with gray shading are results from the sediment analysis performed in the USACE study (CDM, 2005). The D50 is the sediment diameter from the particle size distribution where 50% of the material is finer than the given diameter. The % Organic (% Volatile Total Solid by Weight) column is the percent of the dried sample that volatilized after being heated per the methods outlined in the above-referenced document. The % Sand column represents the percent of the total weight of the sample after the organics were volatilized. The samples labeled Gxx were grab samples from the surface collected with a Ponar dredge. The samples labeled Bxx were core samples. The portion of the sediment core analyzed was typically a meter or more below the sediment surface. The Corps data used in this table is included in Appendix D.

Note 2: The orange cells show the % Volatile Total Solid by Weight from samples collected by U of I and analyzed by the District's analytical lab as part of the current study. These values were used rather than the results from the USACE study when near a Ponar sample location due to their more recent origin.

Note *: The sample identification number given in the field was "PDS-" followed by the ID shown in the table. The qualifying terms "XCEN", "XLEFT", and "XRIGHT" refer to the position on the stream cross section where the sample was taken at a given sample station. Left and right refer to the position as looking downstream; and XCEN refers to the center of the cross section.

Figure 3-6 shows a profile along the length of Bubbly Creek with the various sediment properties included in the table. Stationing is per the previous plan view figures.

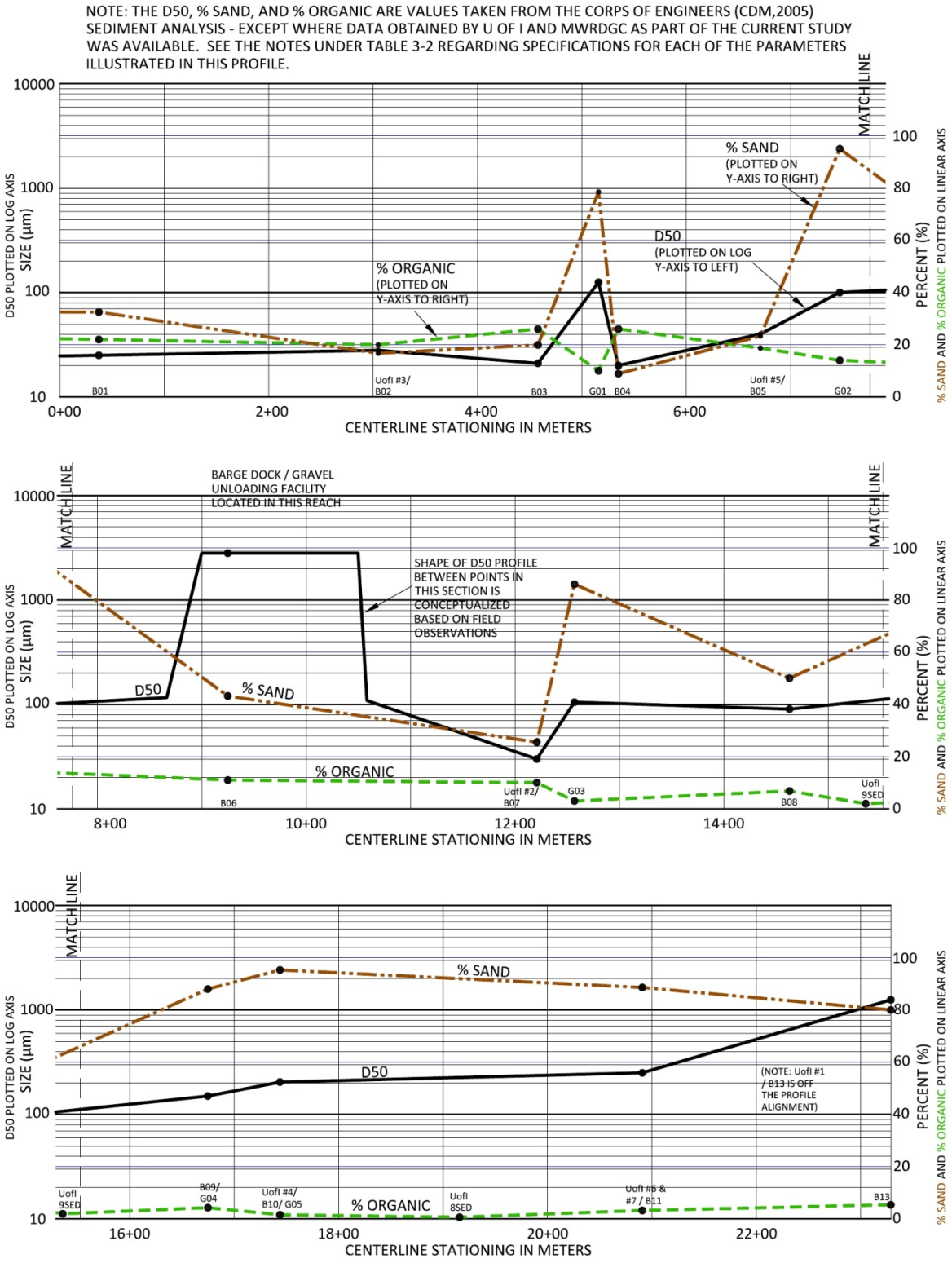

Figure 3-6: Profile along centerline of Bubbly Creek showing various physical parameters of sediment

Table 3-2 and Figure 3-6 illustrate the general trends in sediment transitions described previously. Sediment diameter typically is coarse at the upper end of the stream (D_{50} >100 µm above 35th Street) and becomes finer in the downstream direction (D_{50} <30 µm below Archer Avenue). Associated with the general decrease in D_{50} in the downstream direction is a decrease in the percentage sand that comprises the sediment volume. There is also a general increase in the percent organic composition of the sediment in the downstream direction, with values well under 10% in the upper portion of the stream downstream to the barge dock; and values exceeding 20% below Archer Avenue.

There are also some anomalies evident in the above Figure 3-6. The most evident is in the vicinity of Station 10+00 at the gravel loading / unloading facility (barge dock). The Ponar sample we collected at sample station H revealed angular rock up to 10 cm in diameter, along with high percentages of coarse sand. Sample B06 from the USACE study showed similar results; for that sample, gravel comprised approximately 40% of the sediment volume; with a D_{50} of 2800 µm. It is evident that this is the result of spillage associated with the gravel operation on the east bank.

It is also evident from Figure 3-6 that at each location where the USACE collected and analyzed a Ponar grab sample, the sediment had considerably higher D_{50} and percentage sand, and generally had lower percentage organic material, relative to the sediment deeper below the surface sampled by coring. It is possible that this is an anomaly due to a specific flow event preceding the sampling; or the result of unrepresentative sample locations or the inherent difficulty in getting a representative sample from a Ponar dredge. Regardless of the nature of this anomaly, it highlights the fact that Ponar sediment samples represent only a small area of the sediment surface at a particular instant in time.

3.4 Laboratory Observations

Finding #1: During the oxygen uptake tests on sediment / water mixtures, there was a brief initial stage of rapid oxygen drawdown followed by a more steady oxygen drawdown at a reduced rate.

The initial rapid drawdown typically lasted from 30 to 120 seconds after the probe was inserted into the BOD bottle. This is evident from the drawdown curves for the laboratory experiments included in Appendix C. We speculate that this may be the result of dissolved components from the liquid fraction of the sediment put into the BOD bottle being rapidly oxidized. (It is possible that in the process of sediment being entrained into suspension during actual resuspension conditions in Bubbly Creek, the rapid oxidation of constituents within the liquid fraction in the sediment may also occur.)

Finding #2: The oxygen uptake tests on sediment / water mixtures using a standard dissolved oxygen (DO) probe have an upper limit on the concentration of sediment that can be mixed.

For the highly organic sediments, mixtures in excess of 100,000 mg/L resulted in the oxygen drawing down so rapidly in the BOD bottle that an accurate measurement of DO versus time could not be achieved. Within one minute of saturating the mixture with oxygen, the DO was completely expended. (It took approximately 30 to 45 seconds to pour the mixture into the BOD bottle, insert the probe, and begin taking readings.) In order to take accurate measurements of oxygen uptake for the high concentration mixtures, a more sophisticated system that pumps oxygen into the system over time (such as a respirometer) would be required.

Chapter 4: RESULTS AND DISCUSSION

The following three tables summarize the SOD data collected. Notes regarding the various columns of data are included after the third table.

Trial ID	Flow Rate (L/min)	Resuspension Phase	Time	Ave Water Temp (°C)	($S_{DO} - S_{BOD}$) at 20°C (mg/L/sec)	$SOD_{NR\ 20}$ ($g/m^2/day$)	
1A	45	Flaking (Heavy)	1:20PM	26.6	-0.0008283		
1B	215	Slurry	2:24PM	26.5	-0.0060250		
1C	95	Flaking (Heavy)	3:05PM	28.2	-0.0015997		
2A	59	Flaking (Light)	9:30AM	26.7	-0.0002238	6.7	*2
2B	82.5	Flaking	10:32AM				
2C	100	Flaking	11:30AM				
2D	123	Flaking	12:03PM				
2E	143	Flaking (Heavy)	12:49PM				
2F	224	Slurry	1:40PM	27.5	-0.0040038		
3A	25	None	2:50PM	27.8	-0.0004012	12.1	
3B	60	Flaking	3:27PM	28.1	-0.0007600		
3C	120	Slurry	4:00PM	28.2	-0.0050886		*1
3D	199	Slurry	4:15PM				
4A	26	None	9:00AM	25.9	-0.0002253	6.8	*1
4Ai	38	None	9:50AM				
4Aii	51	Flaking	9:56AM				
4Aiii	60	Flaking	10:01AM				
4Aiv	72	Flaking	10:07AM				
4Av	86	Flaking	10:14AM				
4Avi	109	Flaking	10:19AM				
4Avii	128	Flaking	10:24AM				
4Aviii	140	Flaking (Heavy)	10:29AM				
4Aix	155	Flaking (Heavy)	10:37AM				
4Ax	171	Flaking (Heavy)	10:42AM				
4Axi	190	Flaking (Heavy)	10:46AM				
4B	188	Flaking (Heavy)	11:10AM	26.2	-0.0009824		
5A	30	Flaking	12:29PM	23.6	-0.0011090		
5B	62	Flaking	12:50PM	25.0	-0.0004363		
5C	101	Flaking	1:20pm	25.3	-0.0006383		
5D	135	Flaking	1:48pm	25.4	-0.0005397		
5E	175	Slurry	2:10pm	25.1	-0.0064999		*1
5F	200	Slurry	2:25pm				
6A	30	None	9:30am	24.4	-0.0003040	9.2	
6B	76	Flaking (Light)	10:05am				*3
6C	207	Flaking	10:37am	23.9	-0.0009472		
7A	140	Flaking	11:47am	24.8	-0.0007168		
7B	202.5	Flaking	12:20pm	24.5	-0.0009149		

Table 4-1: SOD Field Data

Trial ID	Flow Rate (L/min)	Sediment Class	Shear (u_*) (cm/s)	Resuspension Phase	TSS (mg/L)	VSS (mg/L)	% Organic	($S_{DO} - S_{BOD}$) at 20°C (mg/L/sec)	
1A	45	2	0.198	Flaking (Heavy)				-0.0008283	
1B	215	2	0.831	Slurry	2984	984	33.0	-0.0060250	
1C	95	2	0.381	Flaking (Heavy)	582	218	37.5	-0.0015997	
2A	59	3	0.255	Flaking (Light)				-0.0002238	*2
2B	82.5	3	0.348	Flaking					
2C	100	3	0.417	Flaking					
2D	123	3	0.509	Flaking					
2E	143	3	0.589	Flaking (Heavy)	434	152	35.0		
2F	224	3	0.930	Slurry	3152	1004	31.8	-0.0040038	
3A	25	2	0.128	None	90	28	31.1	-0.0004012	
3B	60	2	0.253	Flaking	236	76	32.2	-0.0007600	
3C	120	2	0.475	Slurry	3440	940	27.3	-0.0050886	*1
3D	199	2	0.774	Slurry	10528	2692	25.6		
4A	26	4	0.139	None				-0.0002253	*1
4Ai	38	4	0.186	None					
4Aii	51	4	0.237	Flaking					
4Aiii	60	4	0.273	Flaking					
4Aiv	72	4	0.321	Flaking					
4Av	86	4	0.377	Flaking					
4Avi	109	4	0.469	Flaking					
4Avii	128	4	0.548	Flaking					
4Aviii	140	4	0.603	Flaking (Heavy)	148	58	39.2		
4Aix	155	4	0.671	Flaking (Heavy)					
4Ax	171	4	0.744	Flaking (Heavy)					
4Axi	190	4	0.828	Flaking (Heavy)	386	148	38.3		
4B	188	4	0.820	Flaking (Heavy)	***386***	***148***	38.3	-0.0009824	
5A	30	2	0.145	Flaking				-0.0011090	
5B	62	2	0.258	Flaking	110	40	36.4	-0.0004363	
5C	101	2	0.404	Flaking	420	148	35.2	-0.0006383	
5D	135	2	0.532	Flaking	776	224	28.9	-0.0005397	
5E	175	2	0.686	Slurry	5392	1420	26.3	-0.0064999	*1
5F	200	2	0.777	Slurry	5412	1436	26.5		
6A	30	4	0.155	None				-0.0003040	
6B	76	4	0.337	Flaking (Light)					*3
6C	207	4	0.900	Flaking	252	140	55.5	-0.0009472	
7A	140	4	0.603	Flaking	79	46	58.2	-0.0007168	
7B	202.5	4	0.881	Flaking	166	88	53.0	-0.0009149	

Table 4-2: SOD Data with Shear Velocity and Suspended Sediment

Trial ID	Flow Rate (L/min)	Resuspension Phase	Ave Water Temp (°C)	Raw slope of DO Drawdown curve at Field Temp: S_{DO} (mg/L/sec)	($S_{DO} - S_{BOD}$) at Field Temp (mg/L/sec)	($S_{DO} - S_{BOD}$) at 20°C (mg/L/sec)	
1A	45	Flaking (Heavy)	26.6	-0.0012036	-0.0011215	-0.0008283	
1B	215	Slurry	26.5	-0.0082096	-0.0081210	-0.0060250	
1C	95	Flaking (Heavy)	28.2	-0.0024268	-0.0023313	-0.0015997	
2A	59	Flaking (Light)	26.7	-0.0004192	-0.0003413	-0.0002238	*2
2B	82.5	Flaking					
2C	100	Flaking					
2D	123	Flaking					
2E	143	Flaking (Heavy)					
2F	224	Slurry	27.5	-0.0057423	-0.0056503	-0.0040038	
3A	25	None	27.8	-0.0007474	-0.0006556	-0.0004012	
3B	60	Flaking	28.1	-0.0011923	-0.0011026	-0.0007600	
3C	120	Slurry	28.2	-0.0074959	-0.0074159	-0.0050886	*1
3D	199	Slurry					
4A	26	None	25.9	-0.0003931	-0.0003267	-0.0002253	*1
4Ai	38	None					
4Aii	51	Flaking					
4Aiii	60	Flaking					
4Aiv	72	Flaking					
4Av	86	Flaking					
4Avi	109	Flaking					
4Avii	128	Flaking					
4Aviii	140	Flaking (Heavy)					
4Aix	155	Flaking (Heavy)					
4Ax	171	Flaking (Heavy)					
4Axi	190	Flaking (Heavy)					
4B	188	Flaking (Heavy)	26.2	-0.0013808	-0.0013061	-0.0009824	
5A	30	Flaking	23.6	-0.0013856	-0.0013084	-0.0011090	
5B	62	Flaking	25.0	-0.0006293	-0.0005489	-0.0004363	
5C	101	Flaking	25.3	-0.0008936	-0.0008142	-0.0006383	
5D	135	Flaking	25.4	-0.0007690	-0.0006916	-0.0005397	
5E	175	Slurry	25.1	-0.0082865	-0.0082155	-0.0064999	*1
5F	200	Slurry					
6A	30	None	24.4	-0.0004762	-0.0004011	-0.0003040	
6B	76	Flaking (Light)					*3
6C	207	Flaking	23.9	-0.0011995	-0.0011330	-0.0009472	
7A	140	Flaking	24.8	-0.0009737	-0.0008935	-0.0007168	
7B	202.5	Flaking	24.5	-0.0011982	-0.0011249	-0.0009149	

Table 4-3: SOD Calculations / Temperature Normalization

General Note A: Tables 4-1 through 4-3 each include the same sample trials, and some of the same information (Flow Rate, Resuspension Phase). The data was split into three separate tables simply to fit the page; key data columns were carried from one table to the next to facilitate reading.

General Note B: Unless otherwise noted, the gray cells represent those trials during which oxygen drawdown was not measured because the oxygen level was at or near 0 mg/L. These trials were carried out in order to observe transitions in sediment resuspension characteristics.

Note *1: The oxygen drawdown curve for the trials demarcated with *1 was measured during low Dissolved Oxygen (DO) conditions – defined to be a DO during the linear portion of the drawdown curve having a starting value less than 2.5 mg/L. For low dissolved oxygen levels, past research has suggested that the SOD_{NR} is DO-dependent. Therefore these values may underestimate oxygen demand that would be experienced during high DO conditions.

Note *2: For this trial, it was noted in the field notes that a single flake of material passed through the system during testing. The effect of this single flake on oxygen demand appeared to be negligible when compared to other samples with uniform concentrations of suspended materials. Therefore this sample has been treated as a "no resuspension" condition despite the observation of a flake.

Note *3: For this trial, the dissolved oxygen levels actually increased slightly during testing. In the field, we concluded that the chamber must have unseated from the streambed, causing interchange with ambient water outside the sampling system. The chamber was pressed down into the bed using poles, and the sampling commenced. Since an increase in DO yields a negative oxygen demand (which has no physical meaning in the context of the present study), the results of this test have not been included.

Note C: The DO drawdown curves including the linear regressions on which the calculations are based are included in Appendix B.

Note D: $SOD_{NR\ 20}$ refers to the normalized nonresuspension SOD rate at a temperature of 20°C.

Note E: The "Sediment Class" and Shear velocity (u_*) included in Table 4-2 are described immediately afterwards in Section 4.1 of this report.

Note F: TSS (Total Suspended Solids) and VSS (Volatile Suspended Solids) were obtained from samples collected during field-testing and analyzed by the District's analytical lab.

Note G: The "Raw slope of DO Drawdown Curve (S_{DO})" shown on Table 4-3 is the linear regression of the raw field data, shown on the curves in Appendix B. "S_{DO} - S_{BOD}" is the drawdown associated with exposure to sediment isolated from the S_{BOD} of the ambient water as described in Sections 2.2.4 and 2.2.5. As is evident, the S_{BOD} is generally a small fraction of the total oxygen demand. Also note that both values are negative, meaning that S_{BOD} decreases the magnitude.

Note H: "S_{DO} – S_{BOD} at 20°C" is the normalized oxygen drawdown per equations (11) and (12) in Section 2.2.4.

4.1 Bed Shear Stress / Shear Velocity Calculations

As indicated in section 2.1 of this report, the first step required to correlate experimental conditions in the SOD sampling apparatus with actual stream conditions was to establish a relationship:

$$\tau_{b \text{ in SOD chamber}} = f(Q_{\text{SOD chamber}})$$

A relationship between τ_b and Q has been established using CFD (computation fluid dynamics) modeling with the program Flow-3D, although the variable of bed shear stress τ_b (N/m^2) has been replaced with the surrogate parameter of shear velocity, u_* (cm/sec). The mathematical relationship between τ_b and u_* is described later in this section.

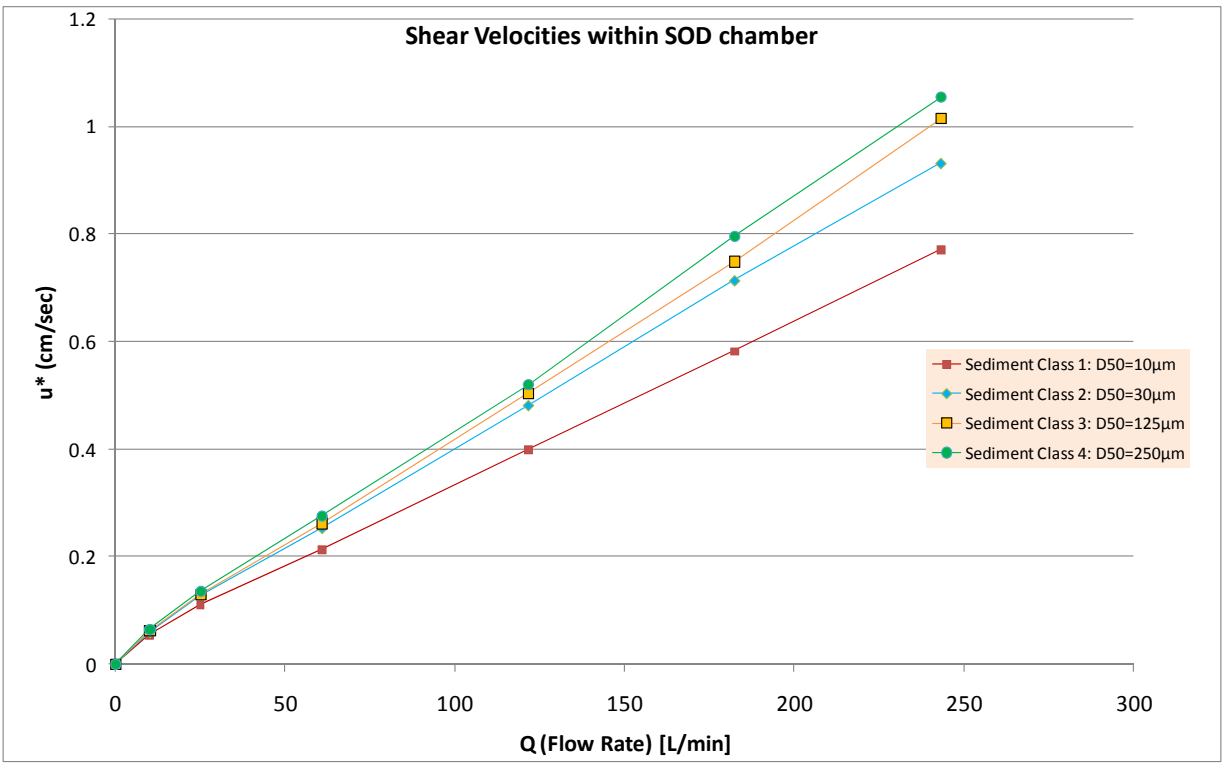

Figure 4-1: Shear Velocities in SOD Chamber

Figure 4-1 was generated through CFD simulations of the SOD sampling system for the various sediment types encountered in the field. Each curve on the graph represents a different sediment type. The D_{50} is based on the particle size distribution, where D_{50} is the particle diameter of which 50% of the material comprising the sediment is finer. The characteristics of the sediment surface influence the magnitude of bed shear stress generated by a given flow condition due to differing roughness; this is the reason that separate curves were established for a number of different sediment types.

The values for u_* included in Table 4-2 were obtained from Figure 4-1 by selecting the most representative sediment type, using the value of Q (flow rate) from the experiment, and performing a linear interpolation between the two points on the curve that bounded the Q of concern.

A brief explanation of the relationship between τ_B and u_* follows. The shear velocity u_* is a surrogate for the bed shear stress generated by the flow of water. The shear velocity (u_*) is defined according to the following equation:

$$u_* = \left(\frac{\tau_B}{\rho}\right)^{0.5} \quad (21)$$

Where: u_* is the shear velocity [m/sec]

τ_B is the bed shear stress [N/m^2]

ρ is the density of water [kg/m^3]

The bed shear stress (or shear velocity) is the critical variable in this analysis because it dictates when bed material is mobilized and ultimately resuspended. Most of the graphical analysis that follows uses u_* as the controlling variable.

4.2 SOD under Non-Resuspension Conditions (SOD_{NR})

As described in Section 2.1, the next step in the analysis is the establishment of the parameter SOD_{NR}, which has been defined as SOD under conditions when material from the bed is not resuspended. (This is the traditional concept of SOD.)

We intended to establish the following relationship:

$SOD_{NR} = f(\tau_b$, Sediment Texture)

Under non-resuspension conditions we were not able to obtain the necessary data to establish the relationship between SOD_{NR} and τ_b (or velocity). As illustrated in Table 4-1, only four values of SOD under non-resuspension conditions were obtained during field experiments. The following limitations hindered us from obtaining the necessary data:

1. The onset of resuspension (flaking phase) always occurred at very low flow rates.
2. Using the Clark-type DO probe, we were limited regarding the minimum flow rate we could set and still obtain viable oxygen drawdown data.
3. Dissolved oxygen in the stream was generally low, which limited the number of experimental trials we could perform at each setup.

To adequately establish the relationship between SOD_{NR} and τ_b, at each station we would have set the chamber on the bed, and run at very low flow rates; and then increased the flow rate in a multitude of small increments. This would have allowed us to determine the oxygen drawdown under a whole range of bed shear stresses before reaching resuspension. However, under the circumstances, we had to decide whether to obtain a large amount of data at low flow rates, and consequently sacrifice the amount of data we could obtain for higher values of flow associated with resuspension scenarios. We made the decision to characterize conditions over a larger range of flow values.

Therefore the relationship we established was limited to: SOD_{NR} = f (Sediment Texture), the results of which are shown on Table 4-4.

Sediment Type	$SOD_{NR\ 20}$ ($g/m^2/day$)	Associated Water Column O_2 Drawdown (mg/L/day) *
Fine-grained organic muck	12.1	5.5
Fine sandy organic muck	6.7	3.0
Fine sand	6.8	3.1
Medium to coarse sand	9.2	4.2

Table 4-4: Non-Resuspension SOD values by sediment type

* The water column oxygen drawdown associated with SOD_{NR20} is an approximation, calculated using the average depth of Bubbly Creek (2.2 m) and assuming well-mixed conditions throughout the water column.

The areal extent of each of the sediment types was shown previously on Figures 3-4 and 3-5. The area of gravel and angular rock at the barge dock was not represented by any of our sample stations. We will use the conservative assumption that the SOD_{NR} in this area is equal to the minimum value, 6.7 $g/m^2/day$.

Comparing the values of SOD_{NR} obtained during this study with previous experiments outlined in Section 1.3, the 2007 study by the District obtained values of 1.38 $g/m^2/day$ in the turning basin and 3.26 $g/m^2/day$ along the east bank near 33rd Street (very near our Sample Station #2). Polls (1977) obtained measurements of 3.42 and 4.42 $g/m^2/day$ at the Archer Avenue bridge. Our values are uniformly higher than these previous measurements.

There are a number of possible explanations for the differences:

(1) It is possible that the previous measurements were performed using sampling techniques with lower flow velocities; and that the difference between the SOD_{NR} values may represent the velocity-dependent effects that we had originally intended to establish.

(2) SOD_{NR} in this type of system is variable in time. The SOD_{NR} is dependent on the recentness of the previous combined sewer overflow (CSO) events; the depositional or erosional characteristic of the recent events; and the amount and type of material deposited. We know that the most recent event before our August 10-12, 2009 sampling was on July 11, 2009; and that the most recent event before our September 8-9, 2009 sampling was on August 28, 2009. We do not know what type of events occurred prior to past sampling performed by the other agencies.

(3) Our SOD measurements were taken under very warm water conditions that approached 30°C in some cases. The values were then normalized to a temperature of 20°C using standard

temperature relationships established in previous research. Polls' measurements were taken at 20°C and 10°C, respectively; and it was not evident in the District's study when their measurements were taken or at what temperature. It is possible that special conditions exist in Bubbly Creek that would warrant modifying the standard temperature relationship.

(4) For both the current and previous studies, the number of measurements has been limited. It is possible that if large numbers of measurements had been taken, statistical analysis would have resolved some of the variability in the data.

S_{BOD} Results for the SOD_{NR} calculations

S_{BOD} values for ambient water were measured in the lab in order to calculate SOD_{NR} values, as described in Section 2.2.4 (Eq. 10). The drawdown curves are included in Appendix C (Tests #1 and #10). As expected, the oxygen drawdown associated with the ambient water was of much lower magnitude than the raw oxygen drawdown curves from the SOD field trials. The laboratory analysis was performed at much higher DO concentrations than generally experienced in the field (>8 mg/L). The measurement at lab temperature and high DO values was 6.3 mg/L/day. The values of S_{BOD} normalized to 20°C and the specific field DO levels varied from 4.4 to 5.7 mg/L/day.

Additional Analysis of SOD_{NR} for Low Velocity Conditions:

As indicated previously in Section 1.1, since the studies of Butts (1974) and Polls (1977) were performed, research performed by Mackenthun and Stefan (1998) has shown that for non-resuspension conditions SOD tends to increase with increasing flow velocity up to a certain velocity threshold. They suggest that for very low velocity conditions, SOD_{NR} is limited by a diffusive boundary layer of very low oxygen content at the sediment/water interface. Diffusion limits the oxygen transported into and across the diffusive boundary layer. Once velocity exceeds the threshold, sufficient mixing is provided such that oxygen content at the sediment/water interface is no longer controlled by diffusive processes. Under this condition, the biological and chemical oxygen consumption in the sediment along with ambient water dissolved oxygen content are the only limitations to SOD_{NR}, and SOD_{NR} does not further increase with additional increases in velocity.

In the context of the above analysis, it is important to note that in the current study, field measurements were taken with well-mixed conditions in the chamber and where ample oxygen (generally >2 mg/L) was present such that it did not significantly limit the sediment oxygen uptake

processes. As a result, it can be expected that if conditions were very stagnant in Bubbly Creek or if ambient water DO content was very low, then SOD_{NR} would be less than the field measured values. (Lower SOD_{NR} values have been recorded in previous studies.)

One way to illustrate this assertion is through an analysis described by Motta (2008), for a hypothetical steady state condition in which the SOD_{NR} is balanced by reaeration at the water surface.

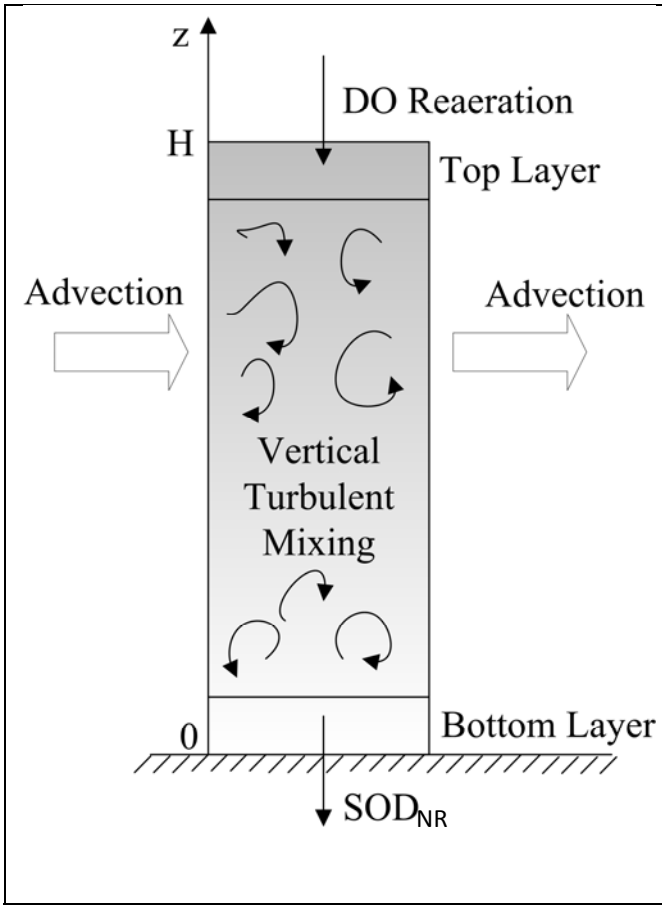

Assumptions for the water column:

- steady state
- BOD has settled or been oxidized
- net advection effect is zero: $(\partial/\partial x = \partial/\partial y = 0)$
- Diffusion into the bottom boundary layer does not limit the SOD_{NR}.
- Balance between reaeration on the top and SOD_{NR} on the bottom

Figure 4-2: Balance Between Surface Reaeration and SOD_{NR}

In the hypothetical scenario illustrated in Figure 4-2, if the surface reaeration rate was less than the field-measured SOD_{NR} (whose rate is limited only by the biochemical processes in the sediment), then SOD_{NR} would drive the DO concentration in the water column to 0 mg/L at steady state; and the actual SOD_{NR} will be oxygen-limited. In this scenario, the actual SOD_{NR} would be a function of surface reaeration, which is a function of velocity. The surface reaeration rate is quantified using the following equation:

$$\left(\frac{dC_{DO}}{dt}\right) = K_A \Theta^{T-20}(C_S - C_{DO}) \quad (22)$$

Where: K_A is the reaeration rate coefficient [day^{-1}]

Θ is the temperature correction factor [dimensionless]

C_S is the saturation dissolved oxygen concentration [mg/L]

C_{DO} is the ambient water dissolved oxygen concentration [mg/L]

The reaeration rate coefficient in this scenario is dictated solely by flow velocity and depth of the water column per the following equation:

$$K_A = \frac{3.93(U^{\frac{1}{2}})}{H^{\frac{3}{2}}} \quad (23)$$

Where: U is the mean velocity [m/s]

H is the water depth [m]

The SOD_{NR} component of oxygen drawdown in the water column is as follows:

$$\left(\frac{dC_{DO}}{dt}\right) = \frac{SOD_{NR}}{H}\Theta^{T-20} \quad (24)$$

The balance between reaeration and SOD can be expressed by setting the right side of Eq. 22 equal to the right side of Eq. 24. The following parameters can be used for this example scenario: T=20°C, which sets C_S=9.23 mg/L; H=2.2 m, the average depth of Bubbly Creek; and C_{DO}≈0.0 at steady state for the low velocity scenario analyzed. Substituting for K_A, the balance between reaeration and SOD can then be reduced to:

$$\left(\frac{3.93(U^{\frac{1}{2}})}{H^{\frac{3}{2}}}\right) C_S = \frac{SOD_{NR}}{H} \quad (25)$$

Using Eq. 25, the actual SOD_{NR} is a function of U up to the point of the field-measured SOD_{NR}. This relation is illustrated in Fig. 4-3:

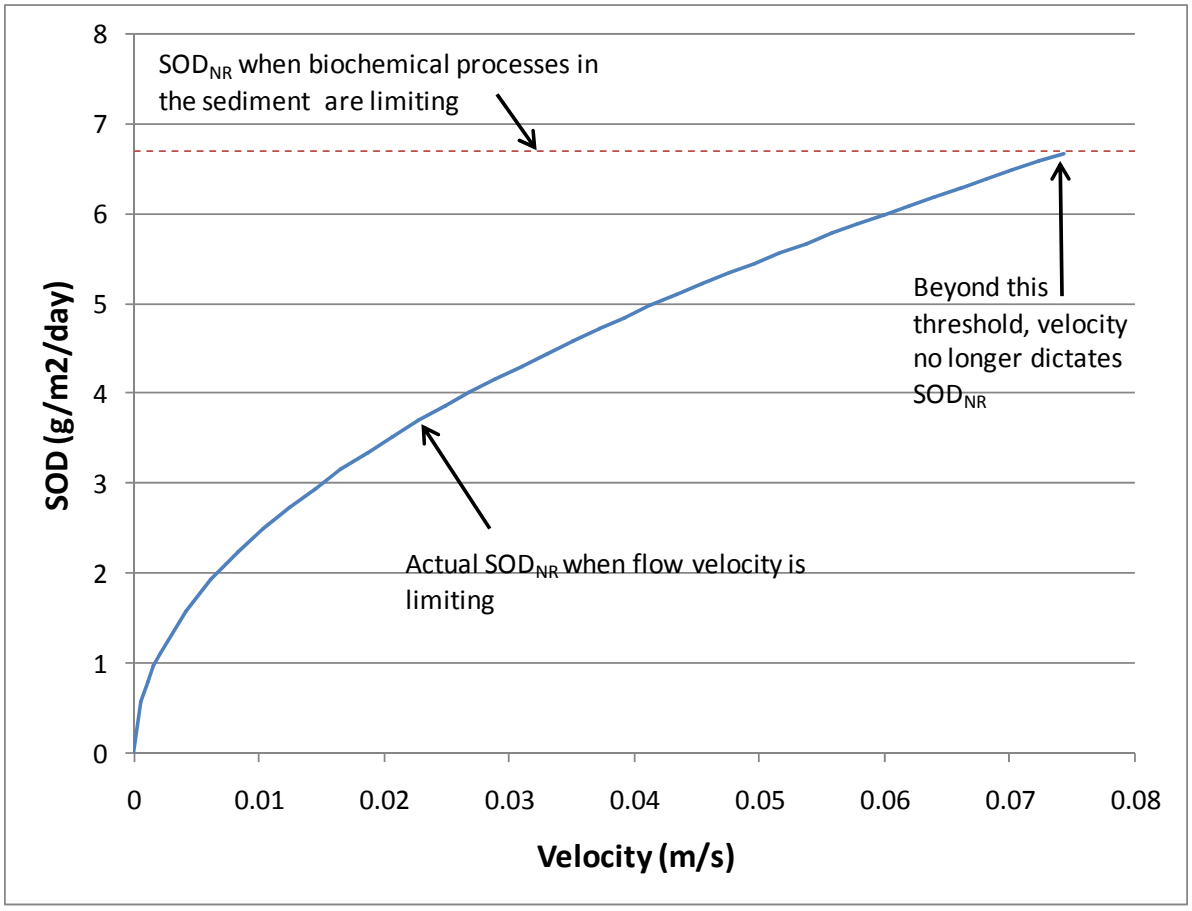

Figure 4-3: Simulation of SOD$_{NR}$ when limited by Flow Velocity

It is important to note that this analysis is hypothetical and solely intended to illustrate how SOD$_{NR}$ may be limited to values less than the field-measured values under stagnant water conditions. In reality, the inputs and outputs to the control volume and behavior within the control volume are more complex (due to algae influence, wind effects at the surface, oxygen gradient due to diffusion effects and diffusive boundary layer influence, inhibition of biological activity in the sediment at very low DO concentrations, etc.).

4.3 The Initiation of Resuspension (Flaking Phase)

As described in Section 2.1, the next step in the analysis is the establishment of a relationship for total suspended solids (TSS) dependent on the bed shear stress and sediment type:

TSS = f (τ_b, Sediment Texture)

The intention was to establish a graphical relationship between TSS and τ_b (or u_*) for each sediment type. Upon analyzing the data, it became evident that the threshold for the "flaking" phase of resuspension was similar regardless of sediment type or location in the channel. This is likely explained by the flakes consisting of a shallow layer of organic debris (dead algae, detritus, biofilm growing on the sediment surface, recent unconsolidated deposition of CSO organics, etc.), whose resuspension behavior does not depend strongly on the texture of the sediment on which it overlies.

The methods used in our field experiments did not allow us to identify a specific shear velocity under which resuspension occurred at each sample station; rather, we identified a range, with the lower boundary being where no resuspension occurred and the upper bound being where we first identified resuspension. The critical shear velocity identified for the onset of resuspension was estimated to be **0.17 cm/sec**, as shown on Figure 4-2.

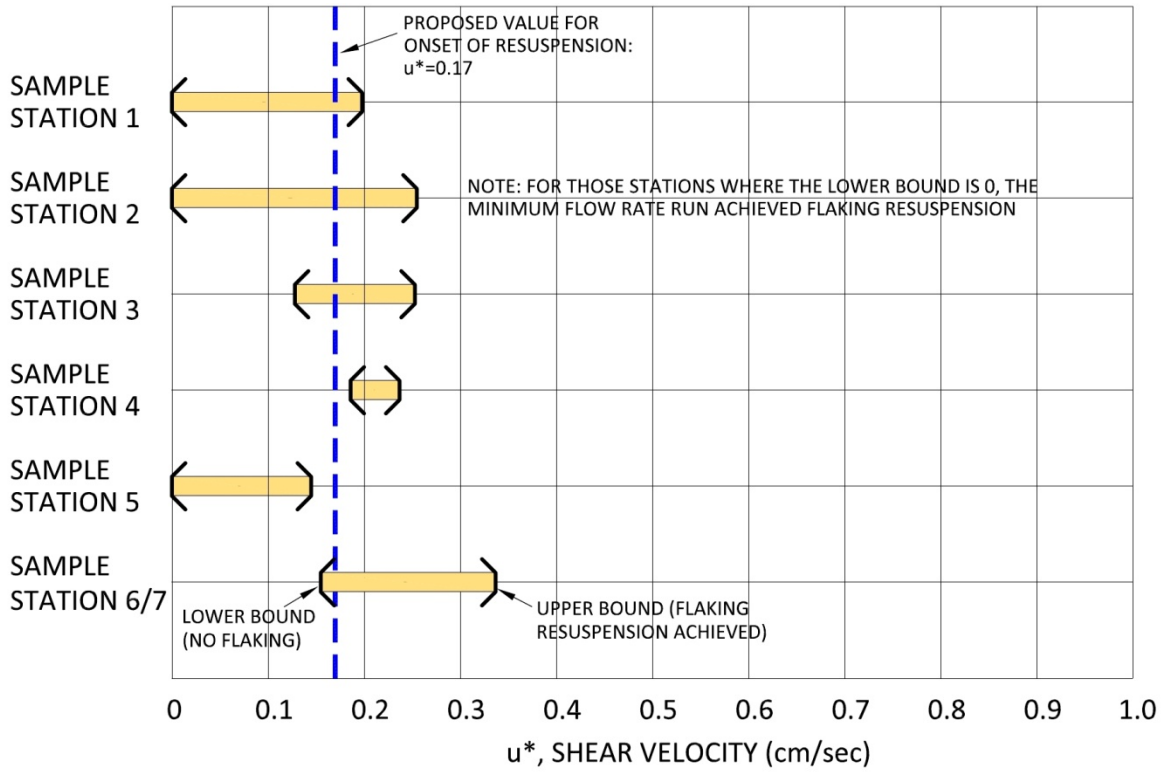

Figure 4-4: Range of Shear Velocity where onset of resuspension occurred

4.4 Suspended Sediment Characterization

We will continue the analysis started in the previous section of finding the relationship:

TSS = f (τ_b, Sediment Texture)

Each sample station represents a specific sediment type; and the relation between TSS and u_* is plotted for each. The shear velocity value of **0.17 cm/sec** established in the previous section is shown on each of the figures as the onset of the flaking phase of resuspension regardless of sediment type or location. Other critical values of shear velocity are also shown with dashed vertical lines and are explained later in Section 4.5.

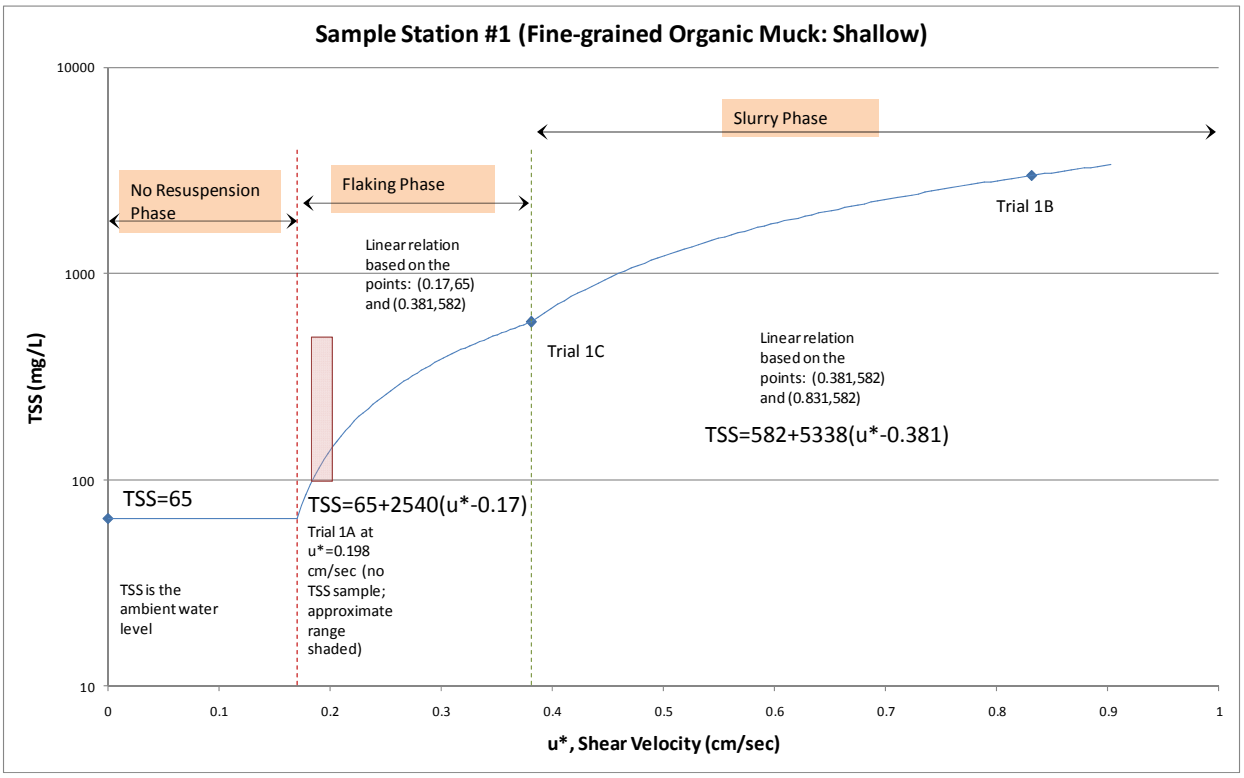

Figure 4-5: Shear Velocity - TSS Relationship for Sample Station #1

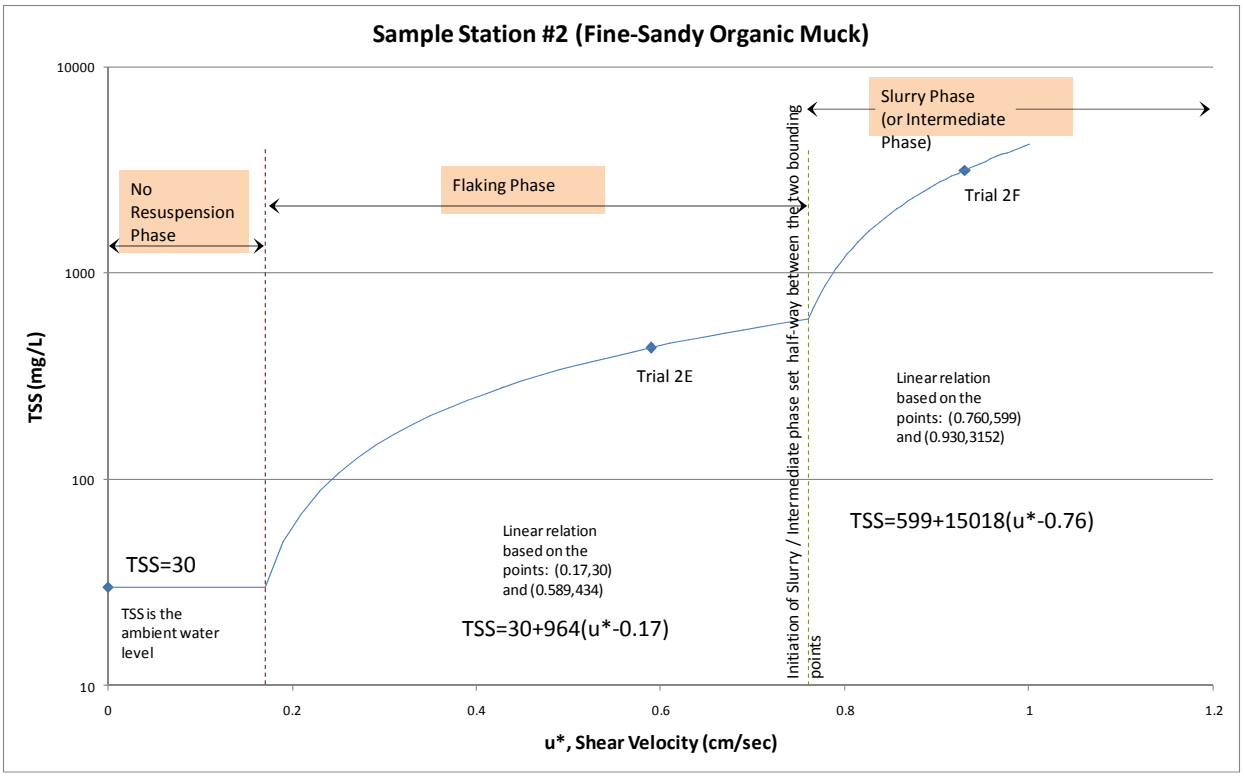

Figure 4-6: Shear Velocity - TSS Relationship for Sample Station #2

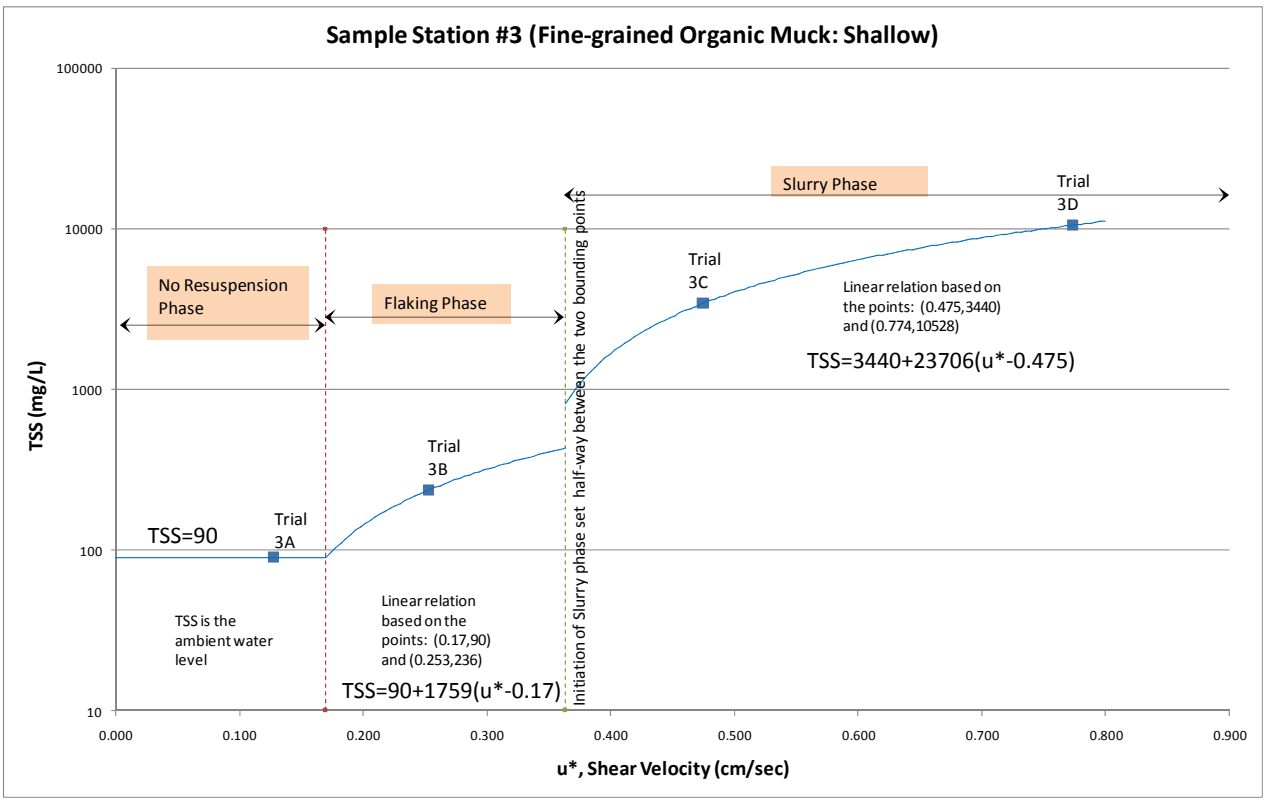

Figure 4-7: Shear Velocity – TSS Relationship for Sample Station #3

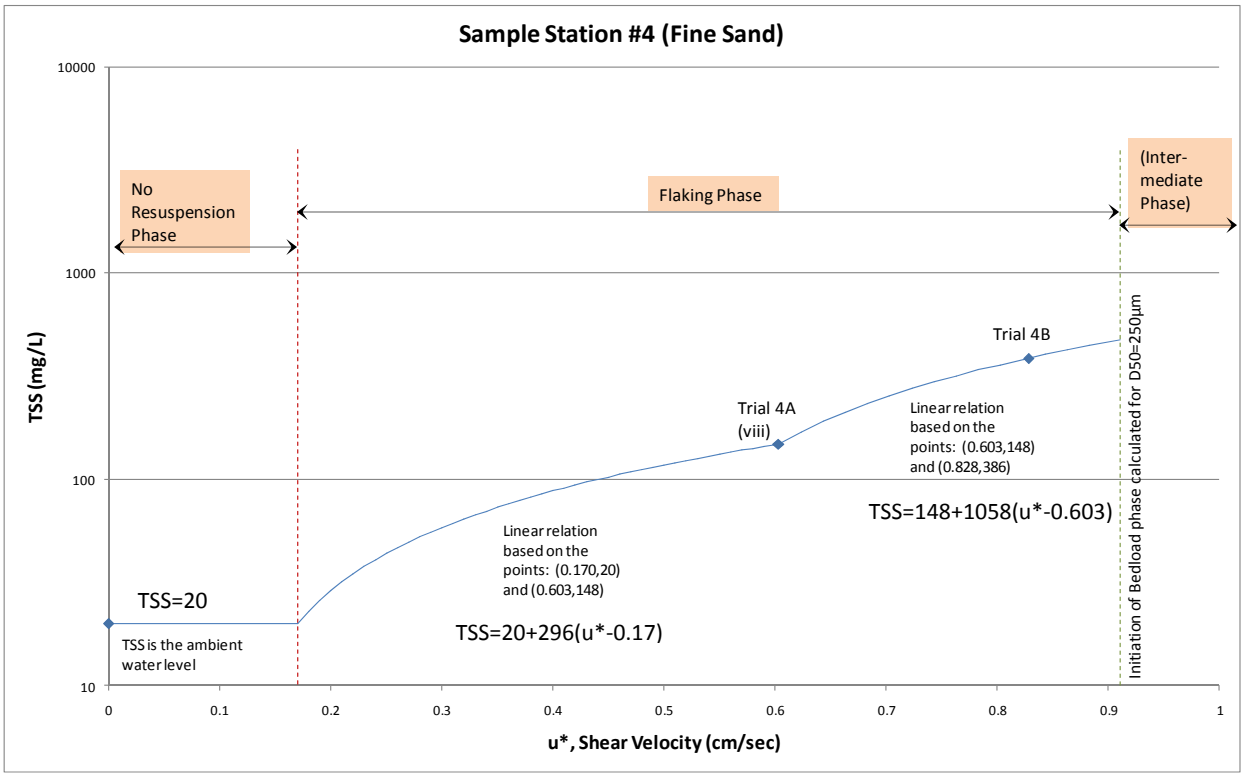

Figure 4-8: Shear Velocity - TSS Relationship for Sample Station #4

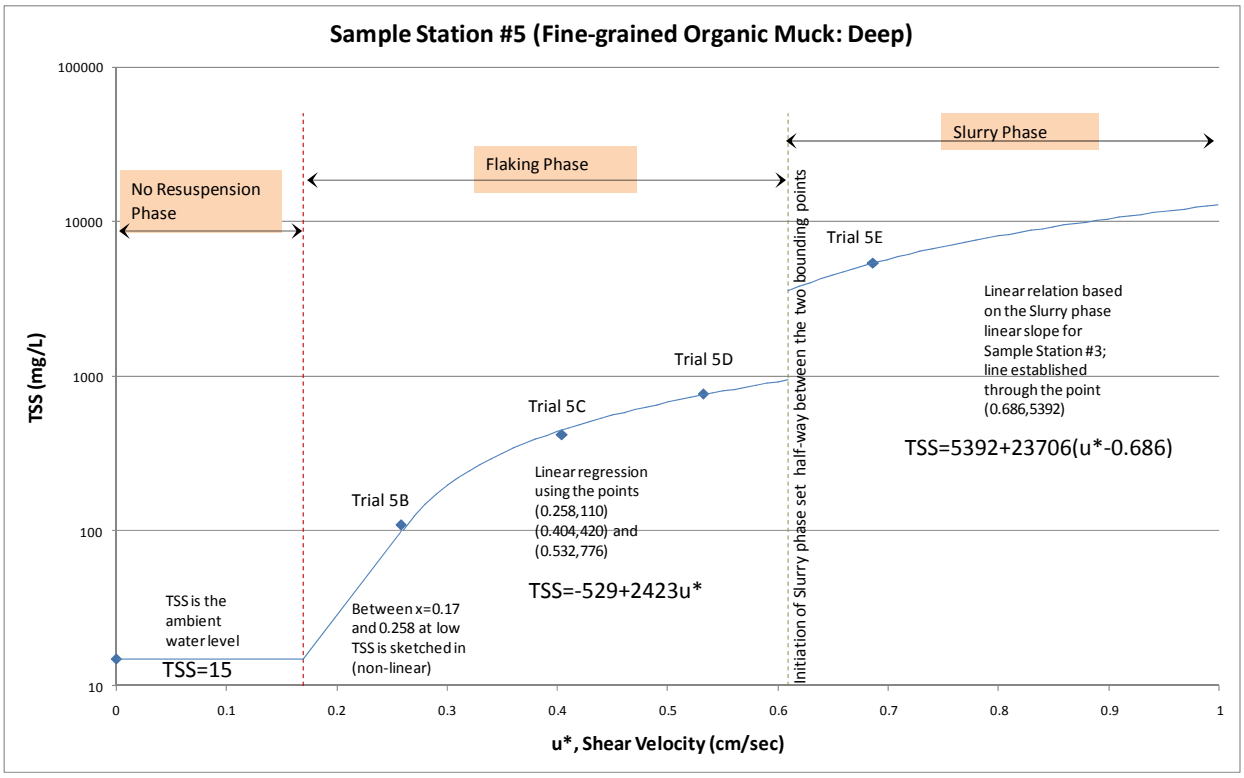

Figure 4-9: Shear Velocity - TSS Relationship for Sample Station #5

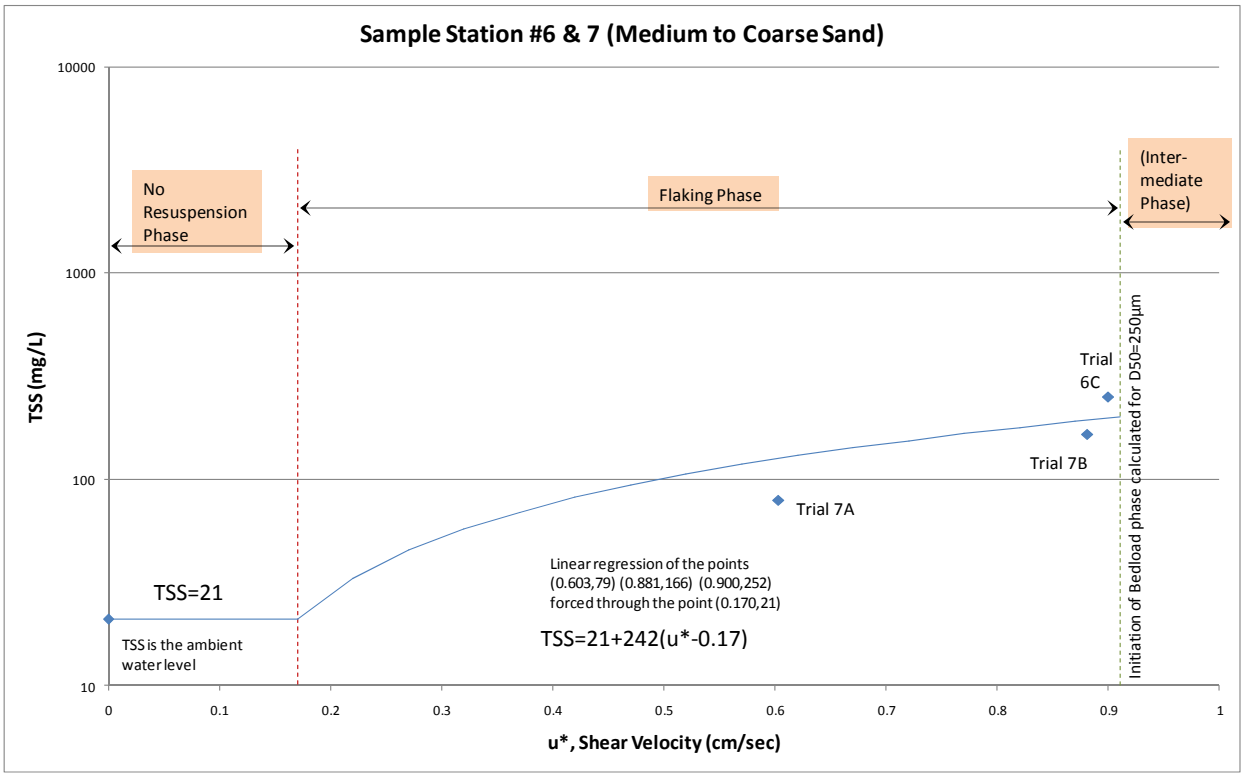

Figure 4-10: Shear Velocity - TSS relationship for Sample Station #6 & 7

Each of the curves was based on a relatively limited number of points. However, they do illustrate the general trend of organic fine-grained sediment entering into the slurry phase with high concentrations of TSS at relatively low levels of bed shear stress; and as the sediment gets coarser (higher percentage of sand), the TSS values still increase with bed shear stress, but at much lower concentrations.

As discussed in Section 2.1, the suspended sediment concentration achieved in the SOD chamber under a given shear stress would disperse into the water column under actual stream flow conditions producing the same shear stress. Because the dispersion is dependent on a whole array of sediment transport and hydrodynamic considerations that are beyond the scope of this study, we cannot produce figures that illustrate TSS concentrations throughout the stream for actual flow events. However, these findings can ultimately be utilized to determine a sediment entrainment rate that is dependent on shear velocity, which can be coupled with a hydrodynamic and sediment transport model to generate TSS concentrations throughout the stream.

4.5 Additional Critical Values of Shear Velocity

In Section 4.3 the critical value of shear velocity for the initiation of flaking was established (**0.17 cm/sec**). In this section, discussion is provided regarding the establishment of additional critical shear velocity values for the initiation of the slurry phase in various sediment types, initiation of sandy material mobilized as bedload, and initiation of sandy material being fully resuspended. The critical shear velocities established have been included on the figures in Section 4.4.

The observations recorded in the field notes in conjunction with the maximum slope of the oxygen drawdown curves led us to conclude that those samples with TSS less than 800 mg/L constituted flaking; and those with TSS exceeding 800 mg/L constituted slurry. The critical shear velocity for initiation of slurry was between the highest shear velocity where flaking still occurred and the lowest shear velocity where the slurry phase was observed.

Sample Stations #1 and #3 were characterized by a fine-grained muck sediment and shallow surface water. At Sample Station #1, Trial 1C was observed to be very close to the threshold between flaking and slurry, at a shear velocity of 0.381 cm/sec. At Sample Station #3, the threshold value lay between the shear velocity for Trial 3B (0.253 cm/sec) and Trial 3C (0.475 cm/sec). The critical shear velocity on Figure 4-5 was established half-way between the shear velocity for Trial 3B and Trial 3C (0.364 cm/sec). This is in the same vicinity as the value of 0.381 cm/sec estimated for Sample Station #1. Therefore we conclude that in the areas with fine-grained organic sediment and shallow water, the critical shear velocity for initiation of slurry is approximately **0.37 cm/sec.**

Sample Station #5 also had fine-grained muck sediment, but was in an area with deeper water than Sample Stations #1 and #3. At Station #5 the water in the sampling system gradually became more opaque as the flow rate was increased, although the oxygen drawdown changed little with each incremental change until Trial 5E was reached at shear velocity 0.686 cm/sec. The increase of shear velocity from 0.532 to 0.686 cm/sec at Trials 5D and 5E was accompanied by a dramatic increase in oxygen drawdown and TSS concentration. Initiation of slurry was clearly between these two trials, and the transition from the flaking phase to the slurry phase appears to be an abrupt transition. This is evidence for the discontinuities in curves between phases. The critical shear velocity was established half-way between the shear velocities of Trials 5D and 5E, at **0.61 cm/sec**.

Sample Station #2 was in an area of fine sandy muck. The sediment sample "2SED" was approximately 10% organic (ie, the volatile fraction of the dried solids was 10% by weight); however, the mineral fraction of the sediment clearly had a higher percentage of sand than the sediment samples collected in the lower part of the stream. The coarser sediment composition altered the resuspension characteristics relative to the organic soils discussed above. Low flow rates were established for Trials 2A through 2D, and these trials were definitively in the flaking category. At Trial 2E, a threshold from light flaking to heavy flaking was recorded and consequently a sample was taken. The shear velocity for the trial was 0.589 cm/sec. It was possible that at that point the sandy portion of the sediment started to be mobilized as bedload and the organic and fine-grained fraction of the sediment began partitioning into suspension. In other words, this may have been the initiation of the bedload (or intermediate) phase described in Section 3.2. Trial 2F was clearly in the slurry category, and the shear velocity was 0.930 cm/sec. Without being able to conclusively determine whether there was an intermediate phase, we simply set the threshold for initiation of the slurry phase half-way between the shear velocity for Trials 5E and 5F, which yields a shear velocity of **0.76 cm/sec**.

At Sample Stations #4, #6, and #7 we concluded that full resuspension was not achieved during the field experiments. These were located in areas whose sediment composition was dominated by sand, with Sample Station #4 consisting of a homogeneous fine-grained sand and Sample Stations #6 and #7 consisting of sand with larger grain size. Although we were not able to determine experimentally the critical shear velocity in the sandy areas, for non-cohesive coarse-grained sediment, accurate theoretical and empirical relations have been formed through extensive studies in the past (Garcia, 2008). Evaluations regarding critical shear velocity for non-cohesive sediment without experimental data can be made with much more confidence relative to the entirely different set of equations used for cohesive soils. Using standard sediment transport relations allows us to establish critical shear velocity values for the coarse-grained reach of the stream.

The method for estimating critical shear velocity for sandy sediment was performed using the modified Shield's diagram and Parker's River Sedimentation Diagram from Garcia (2008). The Shields' diagram is a plot of the relation between the dimensionless Particle Reynold's Number ($\mathcal{R}_{ep}$) and the dimensionless critical bed shear stress (τ_c*). The curves on the Shield's diagram and Parker's River Sedimentation Diagram identify boundaries of the value τ_c*, above which material will be mobilized as either bedload

or full resuspension. Once the value of $\mathbf{R}_{ep}$ is calculated, the critical shear stresses can be determined from the diagrams.

$$\mathbf{R}ep = \frac{D}{\nu}\sqrt{(gRD)} \tag{26}$$

where: D is the particle diameter, typically represented by D_{50} (m)

v is the kinematic viscosity of water, 1.003×10^{-6} (m^2/sec) at 20°C

g is the gravitational acceleration constant, 9.81 (m/sec^2)

R is the submerged specific gravity of sediment grains, calculated as:

$(\rho_s - \rho_{water})/\rho_{water}$, where ρ is the density (kg/m^3)

The value of D_{50} = 0.250 mm = 2.50×10^{-4} m was taken from the USACE particle size distribution for Boring B11.

The value of ρ_s was taken from the USACE geotechnical analysis of specific gravity for boring B11, which was 2.50. Water by definition has specific gravity = 1.00. The calculated value of R is therefore 1.50.

Using these values, the calculated value of $\mathbf{R}_{ep}$ = 15.12.

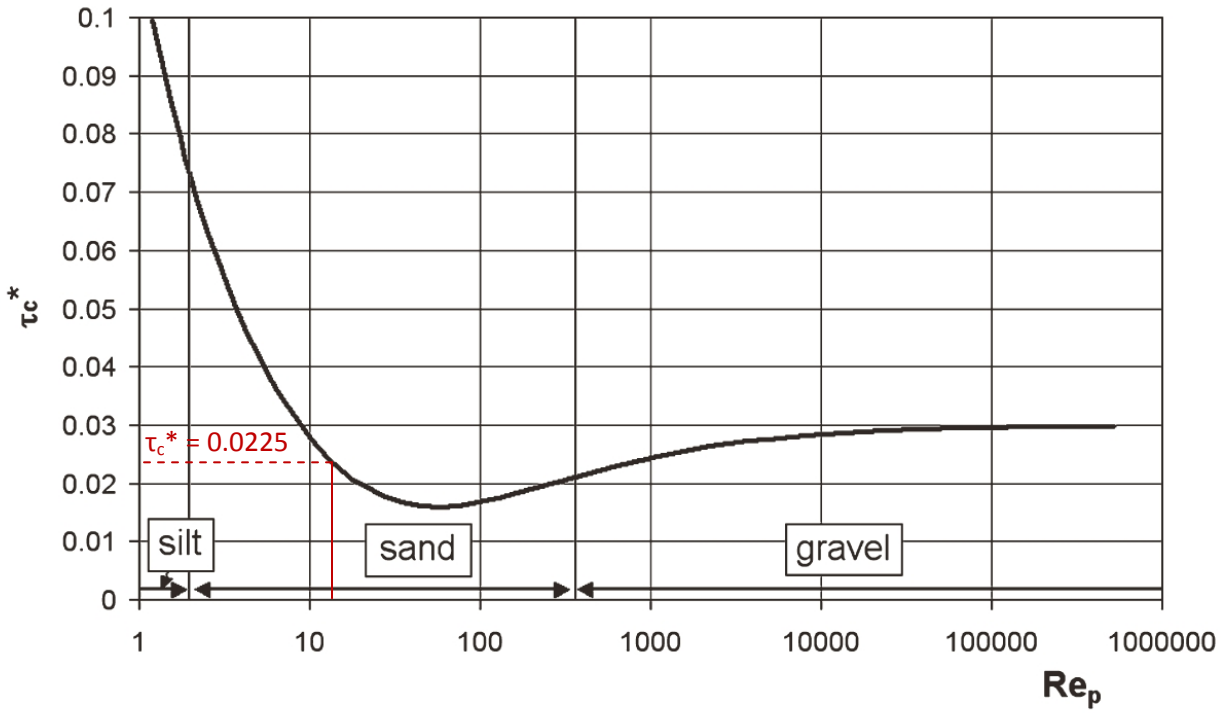

Fig. 2-19. Modified Shields diagram (after Parker 2005).

Figure 4-11: Modified Shields Diagram (from Garcia 2008)

As shown on Figure 4-9, the value for the dimensionless critical bed shear stress (τ_c*) was found to be 0.0225. The next steps involve converting τ_c* to τ_{BC}, the critical bed shear stress; and then using Eq. 21 to convert τ_{BC} to u_*, which defines the critical shear velocity.

The dimensionless τ_c* is defined according to the following equation:

$$\tau_c^* = \frac{\tau_{BC}}{\rho g R D} \tag{27}$$

Where each of the parameters are as defined previously.

Using the value τ_c*=0.0225, the value of τ_{BC} was calculated to be 0.0826 N/m^2.

Converting τ_{BC} to a shear velocity (u_*) per Eq. 21 yields **u_* = 0.0091 m/sec** or **0.91 cm/sec.** This establishes the value of u_* for which sand mobilization is initiated as bedload.

In a similar fashion, we can calculate the value of shear velocity for the transition from bedload (where the coarse material skirts along the bed of the stream) to full resuspension where turbulence conveys material from near the bed into the overlying water column.

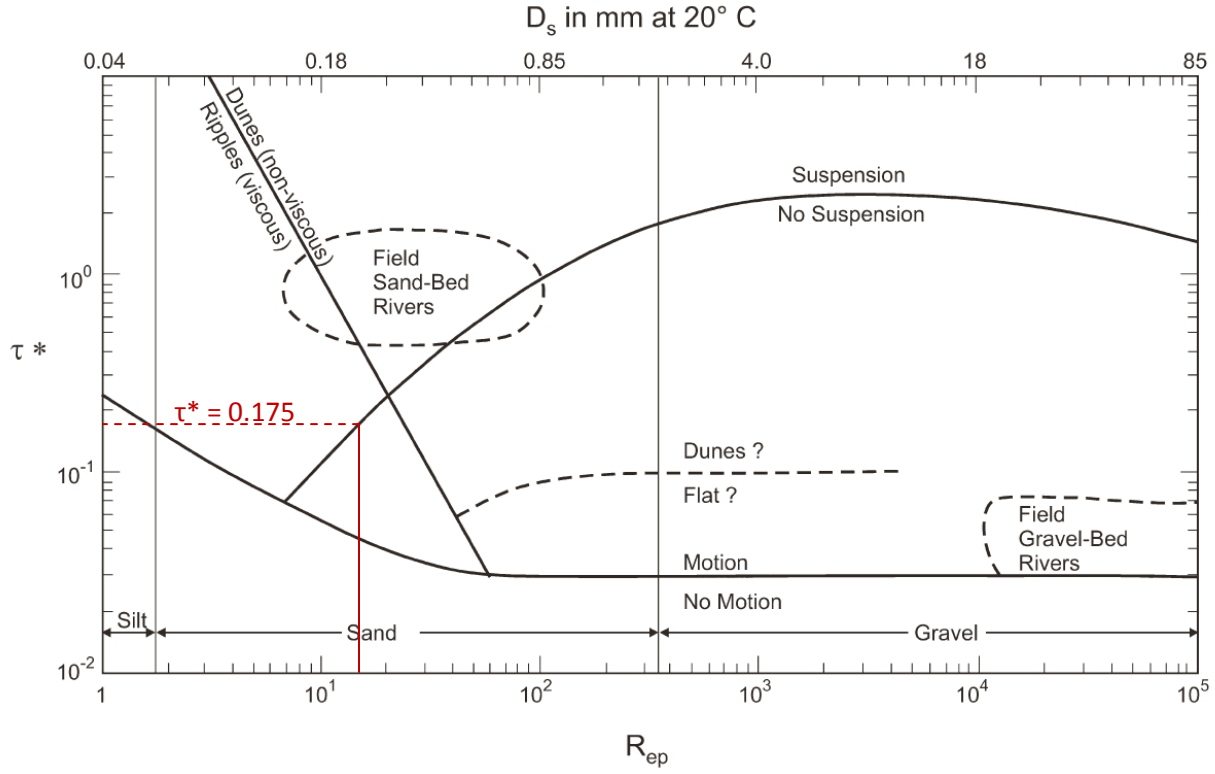

Fig. 2-28. Parker's River Sedimentation Diagram (García 1999).

Figure 4-12: Parker's River Sedimentation Diagram (Garcia, 2008)

As shown on Figure 4-10, the value for the dimensionless bed shear stress (τ^*) was found to be 0.175 for incipient transition between bedload and suspension. Using Eqs. 21 and 27 with the same parameters yields **$u_* = 0.0254$ m/sec** or **2.54 cm/sec**.

All the critical values of shear velocity (u_*) are summarized in Table 4-5.

	Critical Value of Shear Velocity (cm/sec)
Flaking Initiated regardless of sediment type	**0.17**
Fine-grained shallow organic sediment enters full resuspension	**0.37**
Fine-grained deep organic sediment enters full resuspension	**0.61**
Sandy muck enters full resuspension	**0.76**
Sandy sediment is mobilized as bedload; fine-grained and organic fraction is partitioned into the water column	**0.91**
Sandy sediment transitions from bedload to full suspension	**2.54**

Table 4-5: Critical Shear Velocities

4.6 Shear Velocities and Resuspension for Example Flow Simulations

This section provides an example of how the findings of this report can be implemented in other models to simulate resuspension during actual stream flow events. As described previously, modeling the transport and fate of sediment put into suspension is beyond the scope of the current study, although such implementation in the future is practicable.

The hydrodynamics portion of the 2D model STREMR-HySedWq was utilized to model a small number of flow events in Bubbly Creek to determine the resultant shear velocities. Specifications regarding the model were briefly described in Section 2.4.2; a more comprehensive discussion is provided in Motta (2008). Simulations using a 3D model of Bubbly Creek currently under development at VTCHL were also performed to check the STREMR-HySedWq results, and the shear velocity magnitudes were very similar between the two models.

Simulations for Q=2.19 m^3/sec (50.0 million gallons per day (MGD)), Q = 12 m^3/sec (274.0 MGD) and Q = 24 m^3/sec (547.9 MGD) were performed. The following figures illustrate the range of the resultant shear velocities and the associated resuspension phase achieved for each.

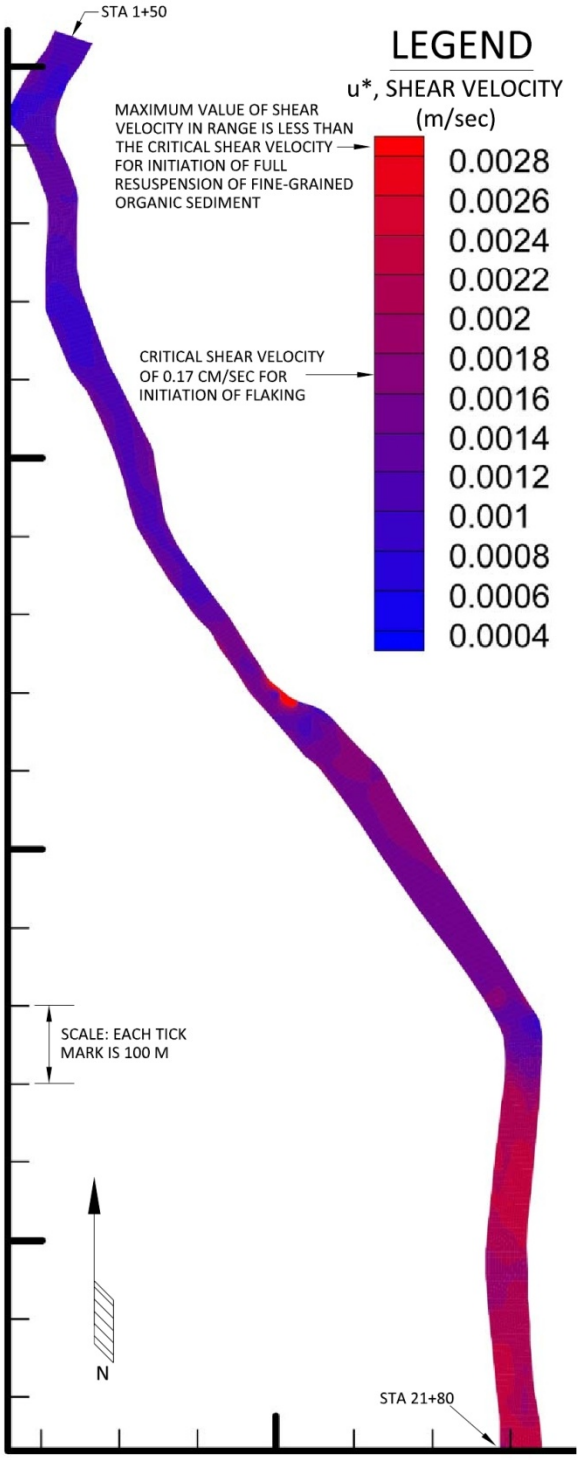

Figure 4-13: Range of Shear Velocities for Q=2.19 m3/sec (50.0 MGD)

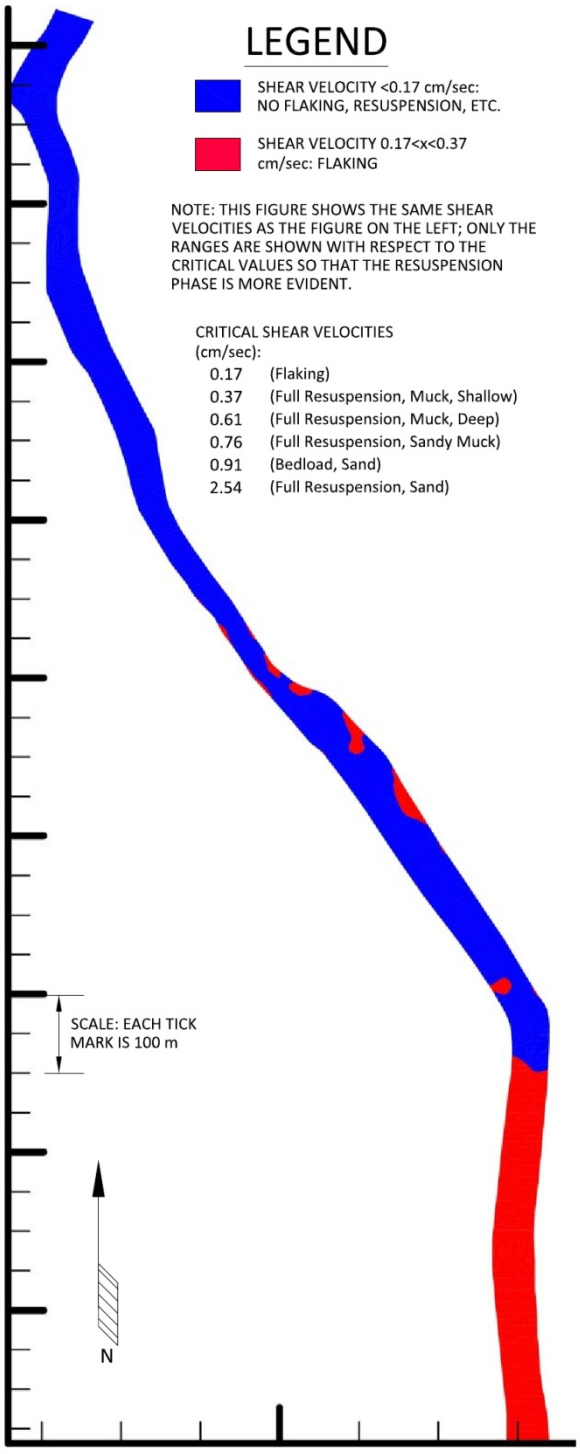

Figure 4-14: Resuspension Phase for Q=2.19 m3/sec (50.0 MGD)

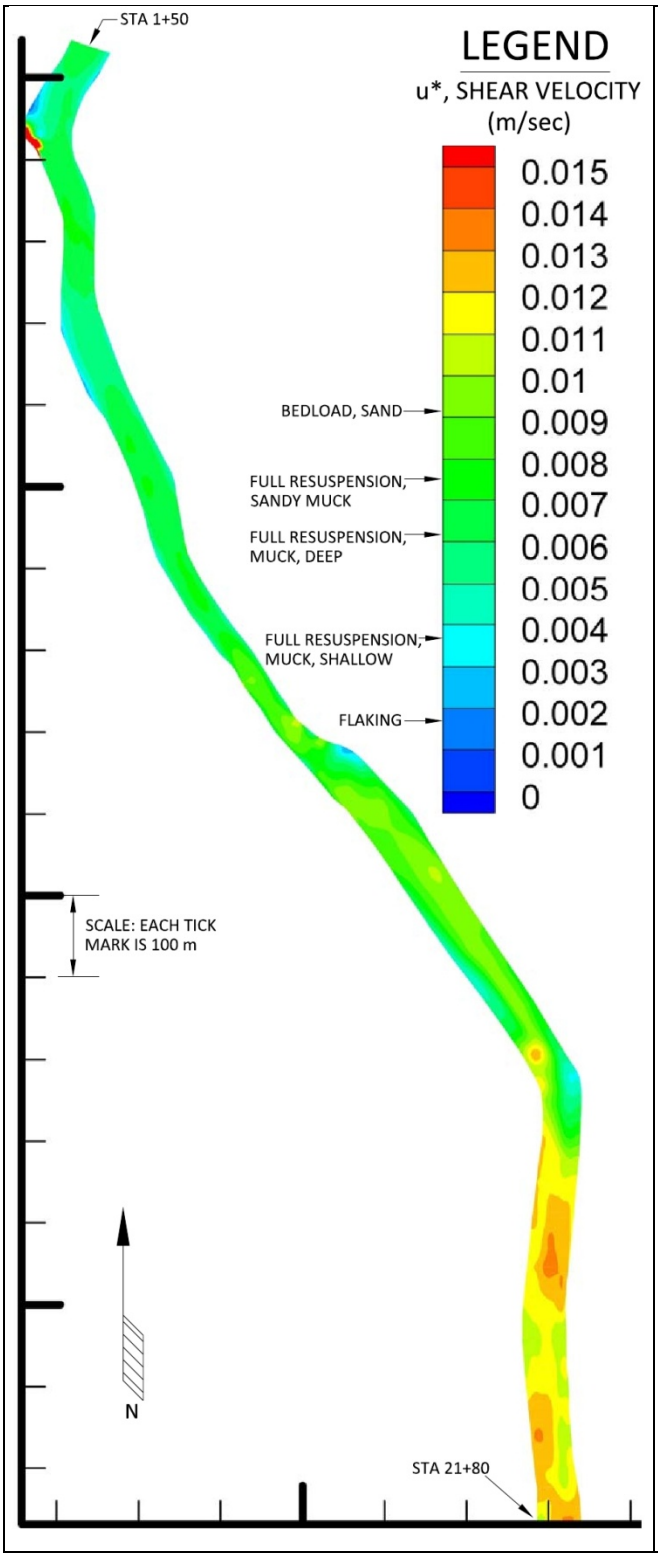

Figure 4-15: Range of Shear Velocities for Q=12 m3/sec (274.0 MGD)

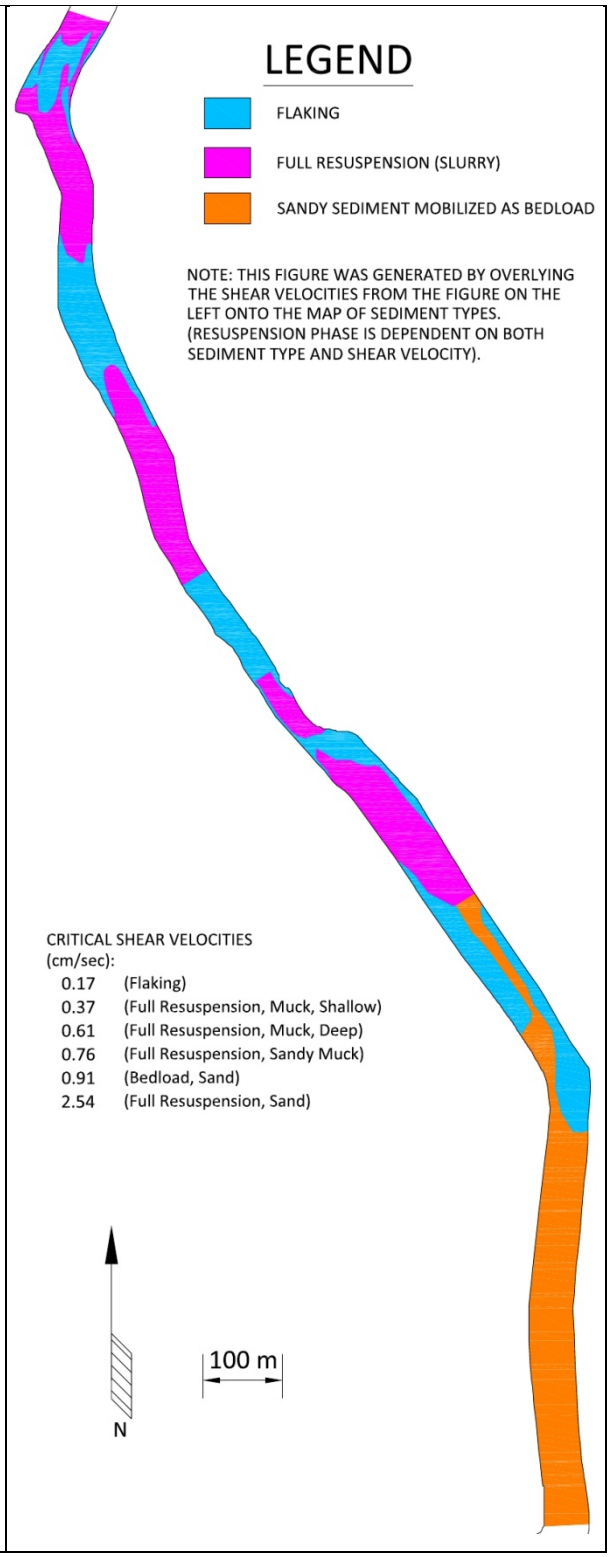

Figure 4-16: Resuspension Phase for Q=12 m3/sec (274.0 MGD)

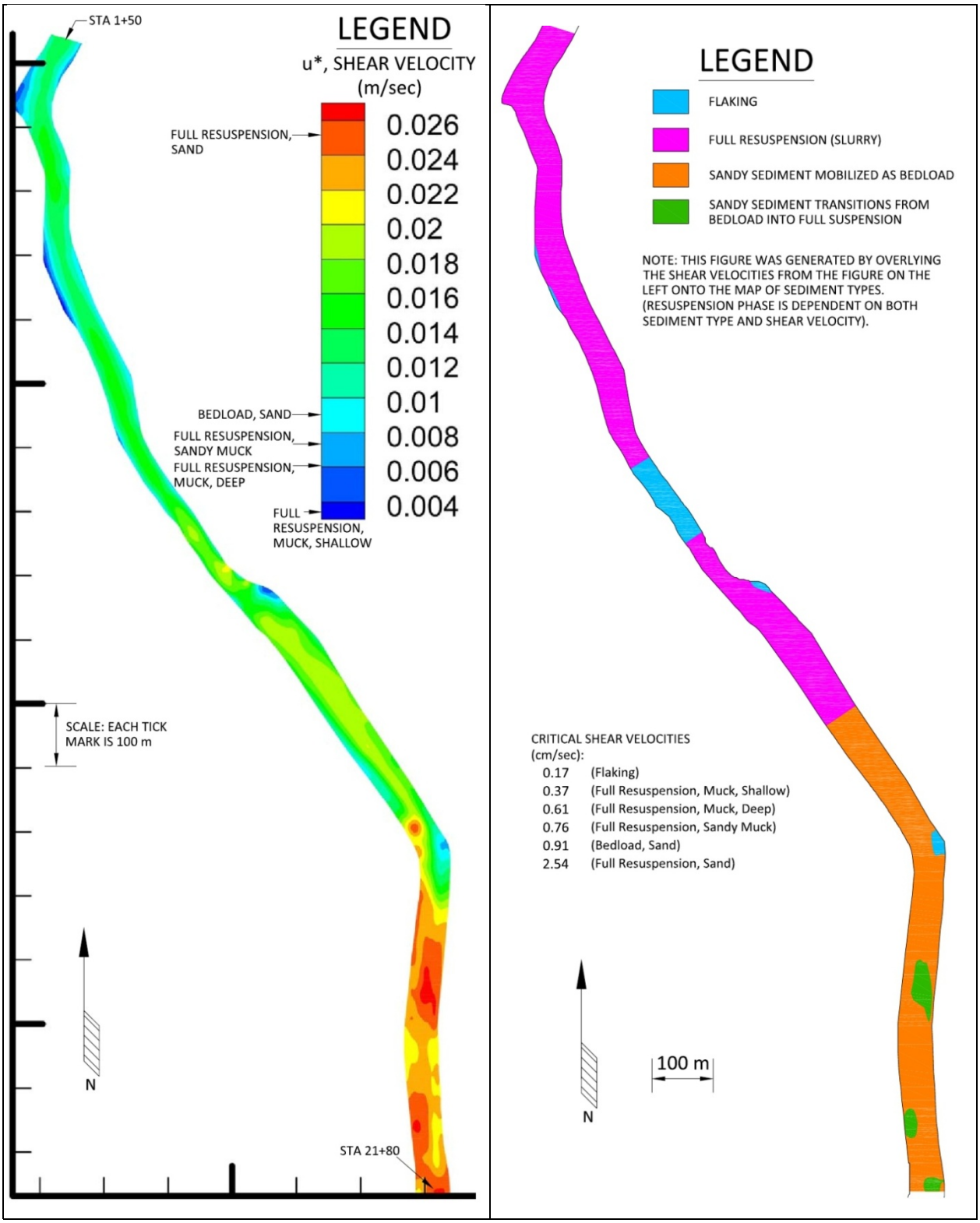

Figure 4-17: Range of Shear Velocities for Q=24 m3/sec (547.9 MGD)

Figure 4-18: Resuspension Phase for Q=24 m3/sec (547.9 MGD)

The above figures reveal that shear velocities (or bed shear stresses) are uniformly higher in the shallow, broad, sandy reach of upper Bubbly Creek. Figures 4-11 and 4-12 show that during the 2.19 m^3/sec (50MGD) event, no sediment in the stream enters the full resuspension phase, although flaking is initiated in the high bed shear area in the upper stream. Figures 4-13 and 4-14 illustrate that during a more substantial 12 m^3/sec (274.0 MGD) flow event, a large portion of the upper sandy streambed is mobilized as bedload, and the lower stream consists of a mosaic of areas that are in the flaking and full resuspension phases. (At this flow rate the entire streambed is in some form of resuspension.) Figures 4-15 and 4-16 show that at a higher 24 m^3/sec (547.9 MGD) flow rate - which begins to approach the average flow rate of 35.1 m^3/sec (801.0 MGD) for a combined sewer overflow (CSO) event generated from RAPS (Motta, 2008) - the entire upper sandy reach is mobilized as bedload, and some of the sand bed begins to transition from bedload into full suspension. Almost the entire portion of the lower stream is in full resuspension. The next section of the report analyzes the resulting oxygen demand associated with resuspension.

4.7 Oxygen Demand Resulting from Sediment Resuspension

As described in Section 2.1, the final step in the establishment of fundamental relationships for sediment oxygen demand is the following:

$SOD_R = f(TSS)$

Due to the whole array of hydrodynamic and sediment transport processes that dictate the dispersion and ultimate fate of sediment that enters suspension, it is not possible to calculate a set value of SOD_R without modeling that is beyond the scope of this study. Furthermore, due to the same factors, it is not realistic to treat SOD_R in an equivalent manner and with the same standard units ($g/m^2/day$) as SOD_{NR}. Oxygen demand for resuspension conditions is dependent on total suspended solids (TSS) concentration, which is based on water volume rather than on sediment area. Because of these issues, the decision was made to treat the problem differently than sediment oxygen demand has been treated in past analyses.

The approach taken in this analysis was to evaluate SOD_R in a fashion similar to first-order BOD kinetics. The exponential oxygen drawdown curves observed during field and laboratory measurements indicated that first-order kinetics may be a realistic means of characterizing the oxygen demand. (It is important to note at the beginning of this discussion that the oxygen sink term established is in a form that specifically accounts for suspended sediment.)

For reference, Eq. 14 from earlier in this report is provided again below. It represents the oxygen sink term associated with BOD. This sink term is one among many in an oxygen mass balance.

$$S_{BOD} = -K_D \Theta_D^{(T-20)} * \left(\frac{C_{DO}}{K_{BOD} + C_{DO}} \right) * C_{BOD} \qquad (14)$$

where,

K_D is the deoxygenation (oxidation) rate coefficient at 20 °C (1/day)

$\Theta_D^{(T-20)}$ is the temperature correction factor, whose standard value is 1.047

C_{DO} is the concentration of dissolved oxygen (mg/L)

C_{BOD} is the concentration of oxidizable material remaining in terms of how much oxygen it will require to oxidize it (mg/L)

K_{BOD} is a half-saturation constant for BOD oxidation (mg/L); Motta (2008) used the value 0.5, derived from a review of previous studies

As evident in Eq. 14 there are four distinct components that need to be addressed to establish a parallel sink term specifically for BOD associated with suspended sediment. These four components are discussed in the subsections that follow in a sequence that facilitates explanation, rather than the sequence the terms are listed in the equation.

4.7.1 Component 1: C_{BOD}

Our modified approach involves replacing the controlling variable C_{BOD} with C_{TSS} (the concentration of total suspended solids, TSS). Theoretically the amount of oxidizable material associated with sediment in suspension ($C_{BOD\ SEDIMENT}$) should be proportional to the TSS; or in other words,

$C_{BOD\ SEDIMENT} \approx \beta^* C_{TSS}$, where β is a coefficient that represents the percentage of the suspended sediment that is oxidizable as BOD at a given time. The coefficient β would vary in time based on the degree to which the material has been oxidized, but that would depend on the time the material has been in suspension. The following analysis represents β when the oxidizable material is effectively unlimited and does not limit the reaction, or $\beta \approx \beta(time=0)$. This is the condition achieved in the experimental trials involving resuspension, which were conducted over a short time period and with very high quantities of oxidizable material. Future work on the subject may address the depletion of $C_{BOD\ SEDIMENT}$ through time, but we reiterate that this analysis represents β at its maximum level when material first enters suspension. We did not attempt to establish a value for $\beta(0)$; but, as will be shown, it is implicitly included in the deoxygenation rate coefficient associated with TSS (referred to as K_{TSS}), given the method of analysis used to establish K_{TSS}.

4.7.2 Component 2: $\Theta_D^{(T-20)}$

This is a standard temperature dependence term, and there was no justification for attempting to modify it. The term has been maintained with its standard value for BOD, $\Theta_D=1.047$.

4.7.3 Component 3: Oxygen Dependent Term, ($C_{DO}/(K_{BOD}+C_{DO})$)

The standard oxygen dependent term is the Monod formulation which establishes a multiplication factor between 0 and 1. The term is approximately equal to 1.0 for unlimited dissolved oxygen (in other words, where oxygen does not limit the reaction); and is equal to 0 when no dissolved oxygen is present. The standard Monod formulation is ($C_{DO}/(K_{BOD} + C_{DO})$); the value for K_{BOD} is dependent on the type of material being oxidized, and the value of 0.5 was used for discharge from Racine Avenue Pumping Station (Motta, 2008). The Monod multiplier using K_{BOD} = 0.5 is illustrated in the following figure.

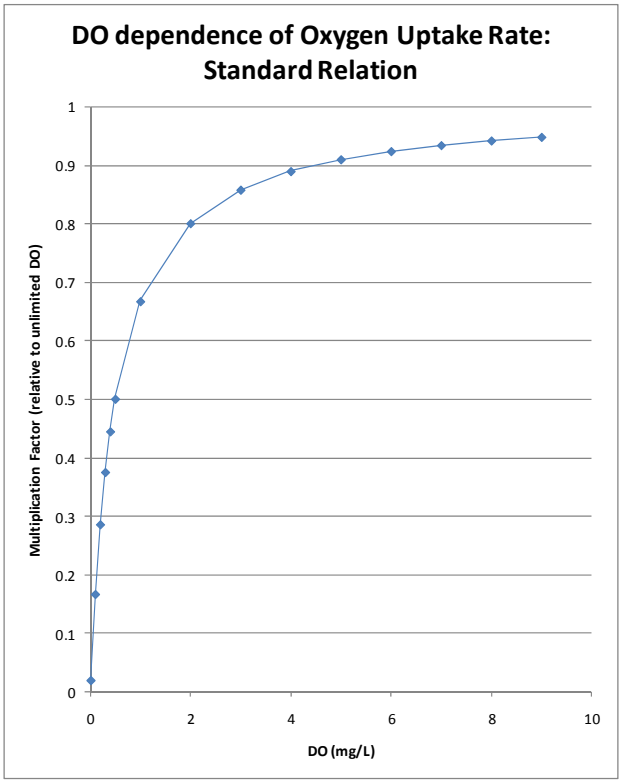

Figure 4-19: Standard Monod relation with Kbod = 0.5

In the current study, it was unknown whether the oxygen-dependent term would take a standard Monod form when applied to organic material associated with suspended sediment; and if it did follow a Monod form, the half-saturation constant for sediment-related BOD needed to be determined.

The method for evaluating the data involved calculating instantaneous slopes of the oxygen drawdown curves at various DO concentrations: 7.0, 6.0, 5.0, 4.0, 3.0, 2.0, 1.5, 1.0, 0.75, 0.50, and

0.25. All the exponential-shaped curves passed through at least six of the given intervals. The instantaneous slopes (ie, the oxygen uptake rates) were calculated by performing a linear regression over a relatively short range that incorporated the DO concentration of concern.

Some additional discussion regarding calculation of the instantaneous slopes is warranted. The intention of the analysis was to establish a sink term specifically for resuspended sediment. Earlier in the report, it was described how SOD_{NR} could be isolated from ambient water BOD (S_{BOD}). It would also be possible to isolate SOD_R from SOD_{NR} and S_{BOD} in the same manner for this portion of the analysis. Both of these latter sink terms would continue to exert oxygen demand during a resuspension event, although at a much lesser magnitude. Modifying Eq. 8 to separate SOD into resuspension and non-resuspension components, the following Eq. 28 takes into account all the known sink terms present during the field experiments under resuspension conditions:

$$\frac{dC}{dt} = SOD_R + (SOD_{NR}) * \frac{A}{V} + S_{BOD} \quad (28)$$

In this equation, dC/dt is graphically represented as the instantaneous slope of the oxygen drawdown curve. As is evident from Tables 4-1 and 4-3, the drawdown associated with SOD_{NR} and S_{BOD} is dominated by SOD_R. (The drawdown associated with SOD_R was typically an order of magnitude larger than SOD_{NR}; and that for SOD_{NR} was typically an order of magnitude larger than S_{BOD}). Because of these differences in magnitude, it would not introduce a great deal of error to consider $dC/dt \approx SOD_R$. Furthermore, since SOD_{NR} was not determined at every station, it would introduce some error to attempt to isolate it at every station. Therefore it is a reasonable assumption to use the formulation:

$$\frac{dC}{dt} \approx SOD_R \quad (29)$$

Returning to the problem of establishing the oxygen-dependent portion of the sink term, it is necessary to create a graph of oxygen uptake rate as a function of dissolved oxygen similar to Figure 4-17. For a given experiment, the instantaneous oxygen uptake rates calculated along a curve need to be compared to each other in terms of a multiplication factor. Unlike the standard Monod relation shown, it was not feasible to do the comparison of the oxygen uptake rate relative to unlimited dissolved oxygen. In fact, there were few experimental trials where the starting DO concentration had high values in the range of 6 to 7 mg/L. Therefore it was necessary to evaluate the oxygen uptake rates relative to the uptake rate at a lower DO concentration. Most of the

exponential-shaped curves passed through, or close to, 2.0 mg/L; and above that concentration, the amount of data was considerably reduced. Therefore for each exponential drawdown curve, the oxygen uptake rates calculated at the various intervals of DO were evaluated relative to the uptake rate calculated for a DO of 2.0 mg/L. (Note that using the standard of 2.0 mg/L required us to use the same standard for determination of the deoxygenation rate coefficient K_{TSS} in the following subsection.) Evaluation of the oxygen uptake rates relative to 2.0 mg/L yielded the following graph:

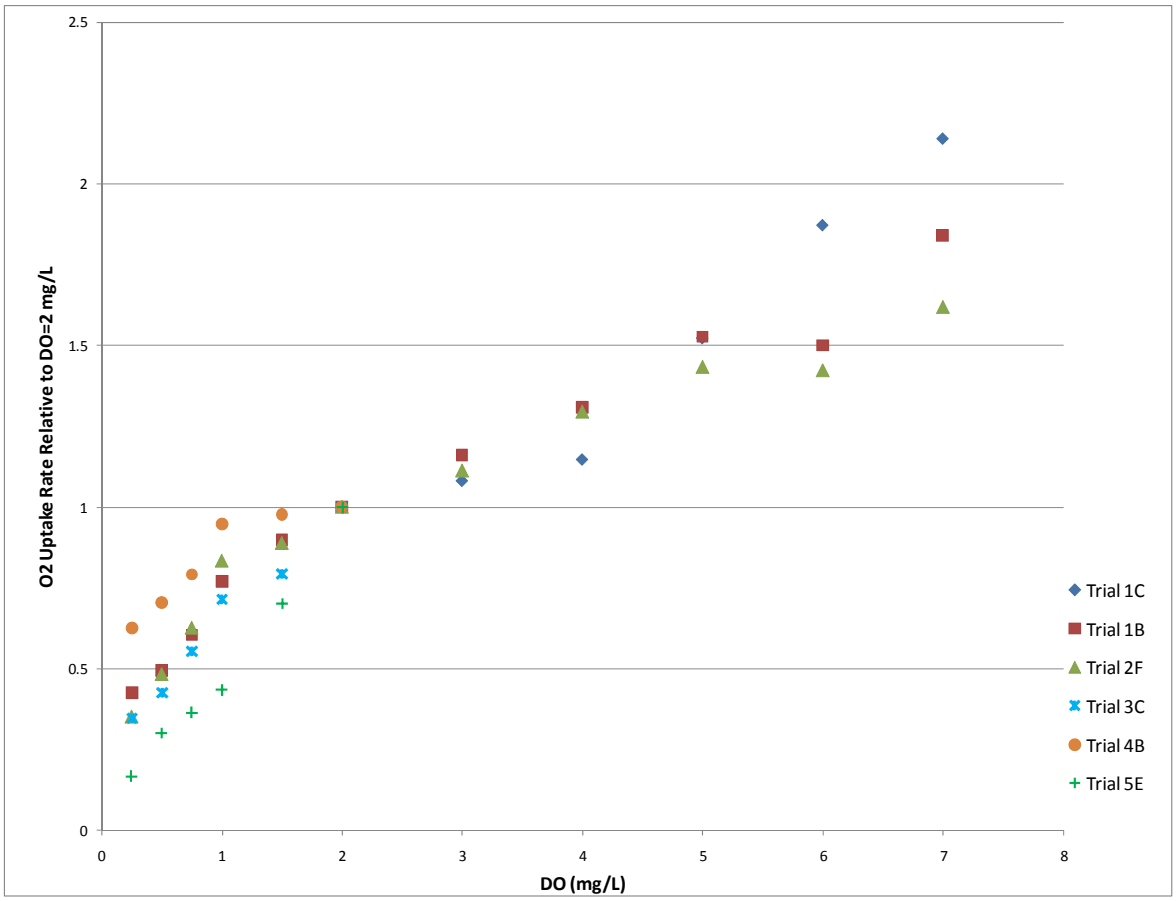

Figure 4-20: Oxygen Uptake Rates as a function of DO

Note that according to the methodology used, since oxygen uptakes were compared relative to DO = 2.0 mg/L, all the data for that value had a multiplication factor of 1. Also note that using the above graph to formulate an oxygen-dependent term, the multiplication factor will not vary from 0 to 1 as in the standard Monod relation, but rather will vary from 0 to some value larger than 1.

Using Figure 4-18, a best-fit analysis was performed by evaluating three different formulations for the oxygen dependent term. The three forms evaluated were as follows:

(1) Monod formulation: $F(C_{DO}) = \frac{C_{DO}}{K_{BOD}+C_{DO}}$

(2) Exponential formulation: $F(C_{DO}) = 1 - e^{(C_{DO}*K_{BOD})}$

(3) Second Order formulation: $F(C_{DO}) = \frac{{C_{DO}}^2}{K_{BOD}+ {C_{DO}}^2}$

The analysis yielded the best match for K_{BOD} for each of the three formulations as indicated by a minimum value of the statistical function RMSE (root mean squared error); and then the three values of RMSE for the three formulations were compared to each other. The results revealed that the Monod formulation was the best fit, with K_{BOD} = 2.44; the RMSE was 0.1655. The best fit curves for each of the three formulations are shown on Figure 4-19 below, with the blue line being the best fit.

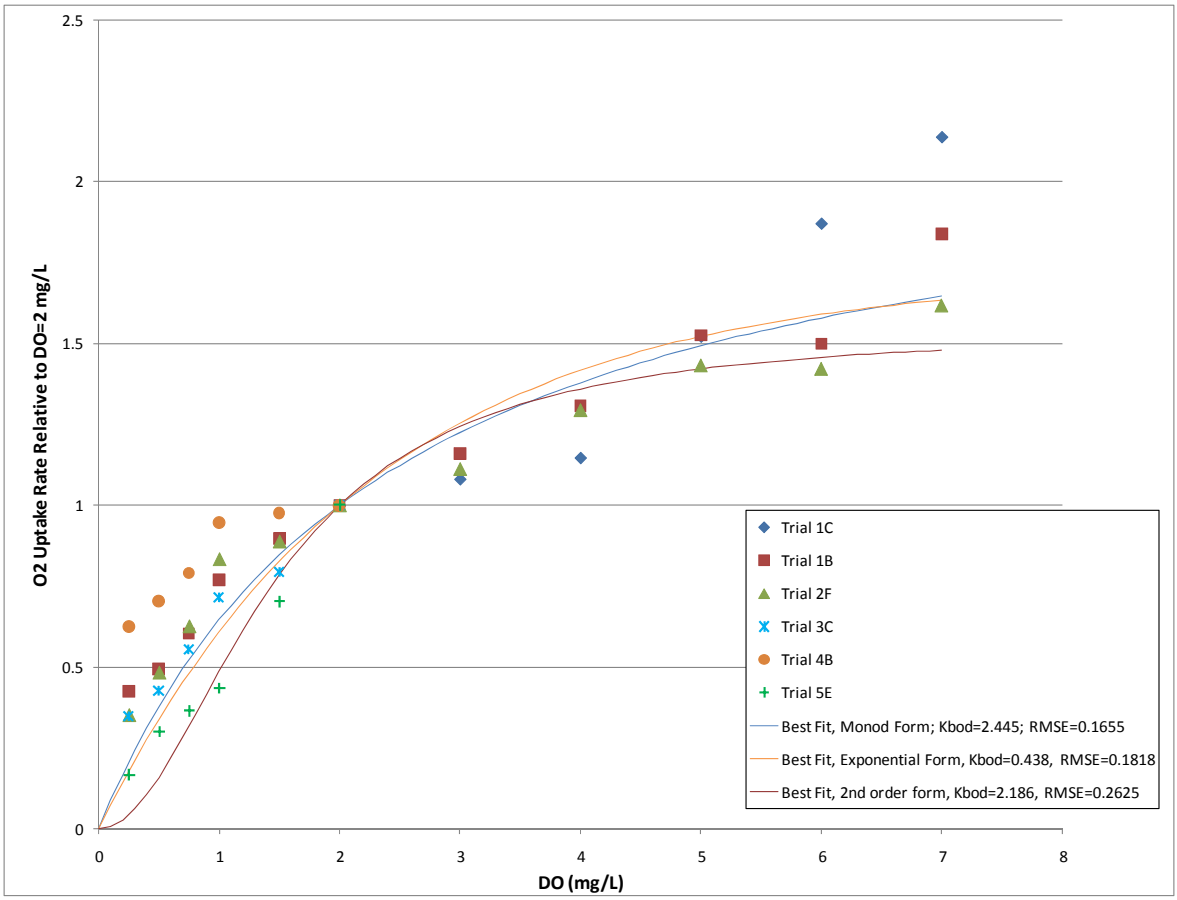

Figure 4-21: Best Fit Curves for Oxygen-Dependence Function

Under the methodology used, the best fit was performed for F(x)/F(2), which is the multiplication factor relative to C_{DO} = 2.0 mg/l. Therefore our final oxygen dependent term will take the form F(x)/F(2) where F(2) is simply a constant equal to (2/(2+2.44)) = 0.450; and (1/F(2))=2.22.

The final form of the oxygen-dependent term used in this analysis is therefore:

$$\left[2.22 * \frac{C_{DO}}{(C_{DO}+2.44)}\right]$$

Some discussion regarding the best-fit curve diverging from several of the points at high concentrations of DO is warranted. A possible explanation for the high oxygen uptake rates at the high values of DO is that those points represent the time immediately following sediment entering suspension. An observation made in the lab may apply to the field experiments at early time stage as well. We observed in the lab a period of very rapid oxidation upon mixing sediment into solution, which was indicated by a short very steep portion of the oxygen drawdown curve, followed by a more gradual typical-shaped exponential decline; see Appendix C. It is possible that when sediment is first put into suspension, a release of dissolved chemical constituents from the pore space of the sediment into the oxygen-rich water is accompanied by rapid chemical oxidation. Once this initial burst of oxidation expends the dissolved constituents, the oxidation of organic material bound onto the sediment particles may proceed in a more gradual manner; the different mechanisms of oxidation may explain why the oxygen uptake rates for the high values do not match well with the remainder of the curve.

4.7.4 Component 4: Deoxygenation Rate Coefficient for Suspended Sediment

The rate coefficient represents the direct relationship between the oxygen uptake rate and the concentration of total suspended solids (TSS). Because this rate coefficient represents a different relation than standard deoxygenation associated with C_{BOD}, a new rate coefficient was introduced, K_{TSS}. This term can be established empirically by plotting TSS versus the oxygen uptake rate for the various experiments and fitting a curve to this data. The oxygen uptake rate plotted on the y-axis is an instantaneous slope of the oxygen drawdown curve.

Because temperature influences this relationship, all oxygen uptake rates were normalized to 20°C. (At 20°C, the temperature correction coefficient yields a value of 1.) The amount of dissolved oxygen present also influences this relationship, as the instantaneous slope of the exponential-shaped oxygen drawdown curves changes due to the dependence on DO, as discussed previously in Section 4.7.3. The method used for the oxygen-dependence term analysis set the coefficient as a multiplier relative to the uptake rate at DO = 2.0 mg/L. Therefore the rate coefficient must be established using the oxygen uptake rate under the same standard, DO = 2.0 mg/L. For a temperature of 20°C, a DO of 2.0 mg/L, and a given TSS concentration, the oxygen uptake rate can be directly obtained from the graph. This is equivalent to graphically forming the relationship, Oxygen Uptake = K_{TSS}*TSS; and if K_{TSS} is a constant, this is a simple linear equation, where K_{TSS} is the slope of the line.

Several approaches were considered for plotting oxygen uptake versus TSS. The first option was to only include those experiments that passed through DO = 2 mg/L. The second option was to include all the experiments involving resuspension, normalizing the oxygen uptake rates to 2 mg/L using the relationship established in Section 4.7.3 for any curves that did not pass through DO = 2 mg/L. The latter approach would provide more comprehensive data for establishing K_{TSS}, but would introduce additional error due to using the normalization. The decision was made to use the more limited data set, whose values of oxygen uptake at DO = 2 mg/L were precisely known.

Figure 4-20 shows oxygen uptake rates calculated at 2.0 mg/L for the various experiments.

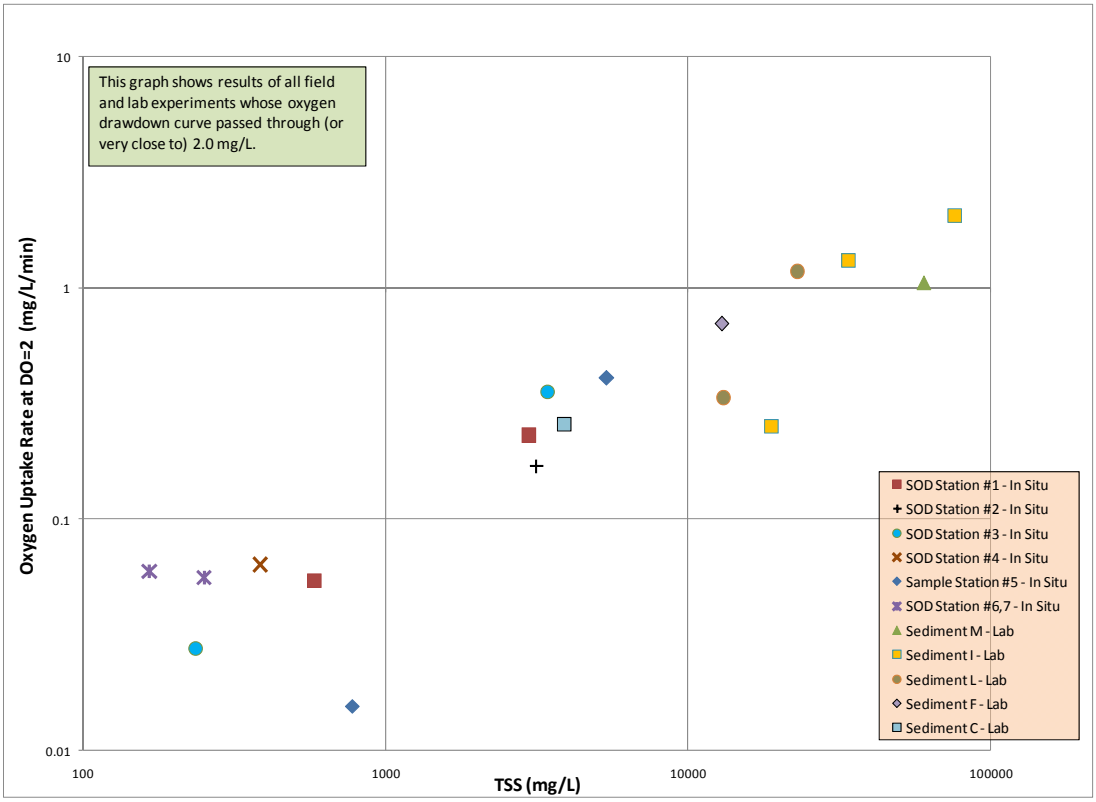

Figure 4-22: TSS versus Oxygen Uptake Rate for Field and Lab Experiments (Log-Log Scale)

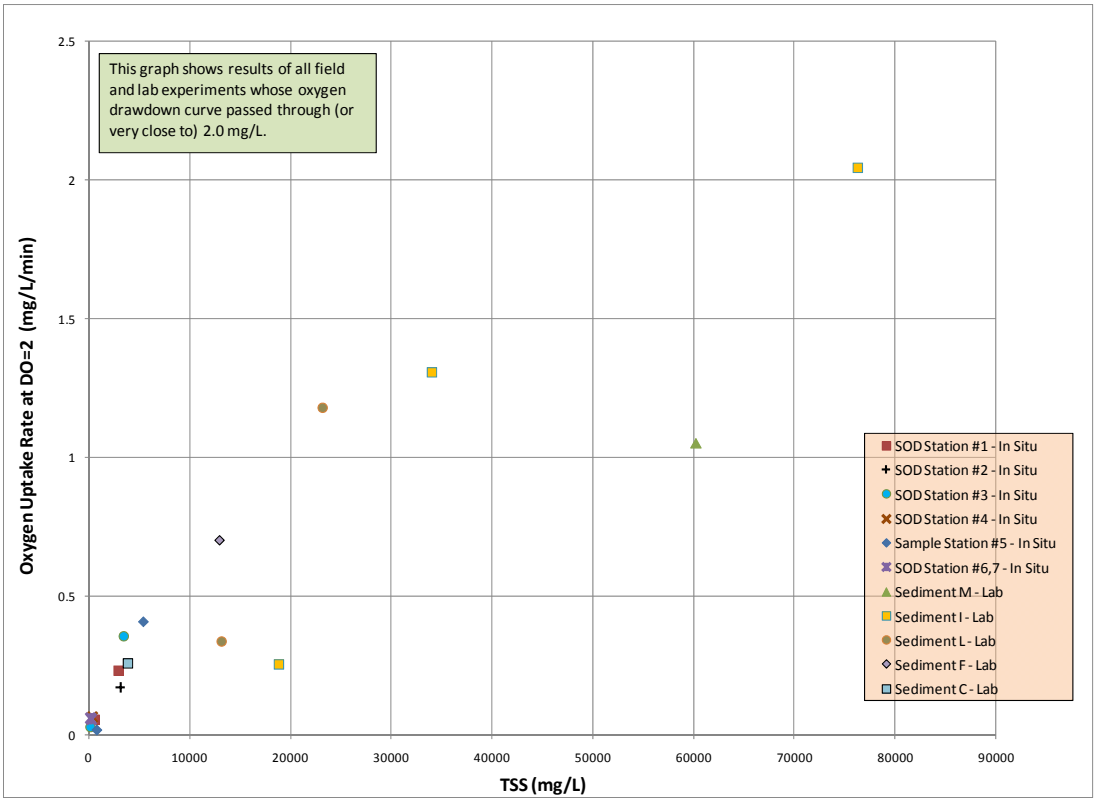

Figure 4-23: TSS Versus Oxygen Uptake Rate for Field and Lab Experiments (Linear Scale)

Figure 4-20 shows the data on a log-log scale so that the full range of data can be more easily observed. It is evident that there is a definite trend of increasing oxygen uptake rate with increasing TSS. However the linear scale graph shown on Figure 4-21 suggests a non-linear shape with decreasing magnitude of slope (ie, the rate at which oxygen uptake increases gets less.) It would be possible to attempt a non-linear curve fit, although the rate coefficient is traditionally considered to be a constant. Since the curves effectively are split into an upper region of lab data and a lower region of field data, the differences in slope may be due to the inherent differences in conditions under which the measurements were made; and therefore a nonlinear curve fit between the two data types may introduce additional error.

We feel the field data is a more reliable predictor of actual conditions; although for TSS concentrations above 5400 mg/L we do not have field oxygen drawdown data. Therefore assuming the oxygen uptake rates continue to increase according to the lower portion of the curve beyond TSS = 5400 mg/L may not be accurate. To model very high concentrations of TSS it may be more reliable to use the laboratory results. Therefore linear regressions for both sets of data are provided separately. The values for the slope of the line, K_{TSS}, are on the same order of magnitude, but the value derived from the field data value is considerably larger.

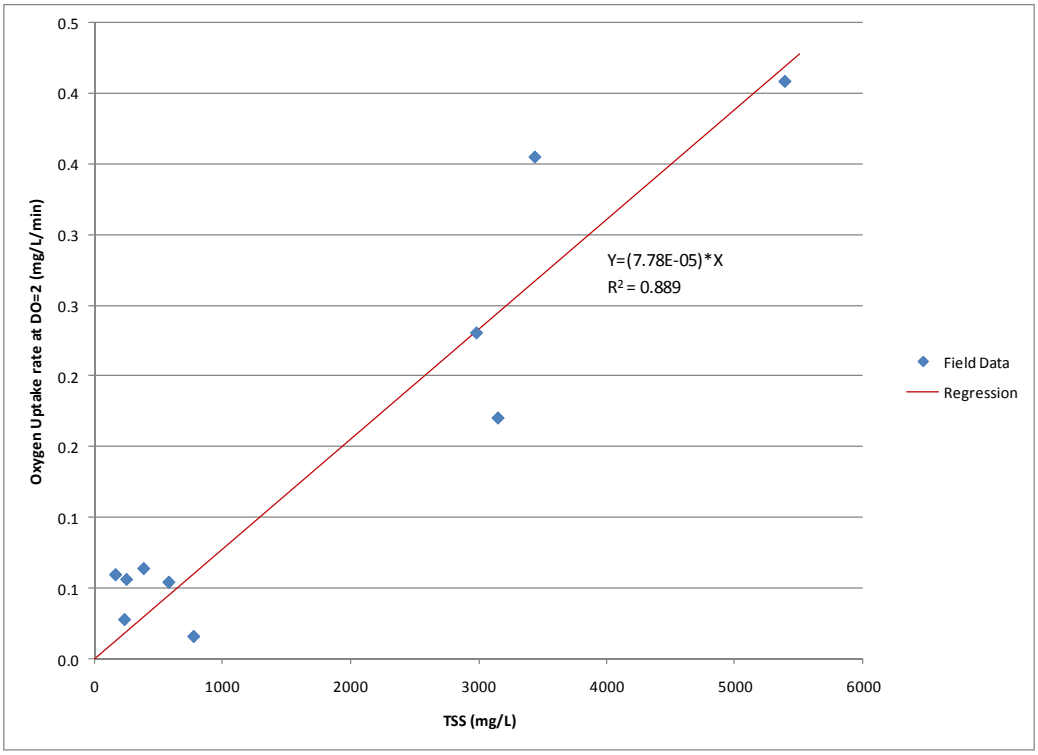

Figure 4-24: Linear Regression on Field Data for Determination of K_{TSS}

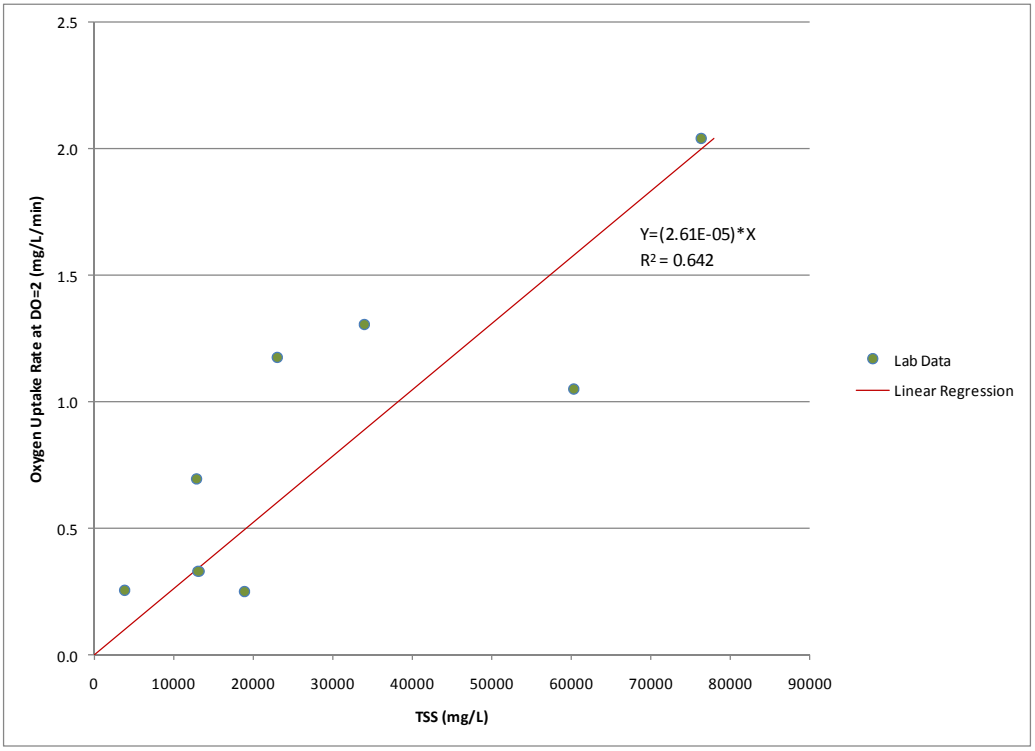

Figure 4-25: Linear Regression on Lab Data for Determination of K_{TSS}

- Therefore the rate constant K_{TSS} is 0.0000778 [mg O_2/mg TSS/min^{-1}] for the field data; or in terms of the traditional units, **0.112 [mg O_2/mg TSS/day^{-1}]**.
- For very high concentrations of TSS, the laboratory data may be more accurate, with K_{TSS} equal to 0.0000261 [mg O_2/mg TSS/min^{-1}]; or **0.038 [mg O_2/mg TSS/day^{-1}]**.

As indicated previously, future studies may find it appropriate to establish the rate coefficient in terms of C_{BOD} rather than TSS so that the kinetics associated with the depletion of BOD can be modeled. Establishing the deoxygenation rate coefficient would then involve multiplying TSS by a coefficient β which would represent the fraction of the TSS that is oxidizable. The graphs shown above would consequently have lower values on the X-axis and steeper slopes; but the sink term would include the multiplier β, yielding the same oxygen sink. Therefore the rate constant shown implicitly includes the value β. We reiterate that this analysis represents conditions when β ≈ β(0).

4.8 The Oxygen Sink Term for Sediment Resuspension

Compiling all the individual components established above into the sink term from Eq. 14 yields the following term that is a function of TSS:

$$S_{O2} = 0.112 \frac{mg\ O_2}{mg\ TSS \bullet day} * 1.047^{(T-20)} * \left[2.22 * \frac{C_{DO}}{(C_{DO}+2.44)}\right] * C_{TSS} \quad (30)$$

This sink term is the same as has previously been referred to as the variable SOD_R; it is in the units (mg/L/day).

The application of this sink term can be applied to the field data to illustrate whether or not it accurately represents conditions observed in the field. For purposes of this illustration, we have assumed that C_{TSS} is constant throughout the experiment; ie, the equilibrium TSS concentration was achieved very shortly after the initiation of scour. We have also assumed that the depletion of BOD associated with the sediment was negligible (as a percentage relative to the start condition), given the very high amount of oxidizable material present and the short time frame of the field experiments.

Therefore, given a concentration of TSS, and an initial concentration of DO, we can step through time such that $C_{DO}(t+1) = C_{DO}(t) - SOD_R(t)*\Delta t$. Because the field data contains time in seconds, the rate constant was consequently divided by 86400 for the simulations. The following graphs show the simulation of oxygen drawdown according to Eq. 30 relative to the actual oxygen drawdown measured in the field. Because the value of K_{TSS}=0.112 [mg O_2/mg TSS/day^{-1}] was derived from a linear regression to attempt to capture a general value, it does not provide the best match to all the data sets. Simulations are provided using K_{TSS}=[mg O_2/mg TSS/day^{-1}]; but where a better fit to the data could be obtained, a separate simulation using a separate value of K_{TSS} is also included. (In reality, K_{TSS} does not likely vary between samples, but rather the relationship between C_{BOD} and TSS; in other words the variation in K_{TSS} is due to variation in the coefficient β which is incorporated into the K_{TSS} term.)

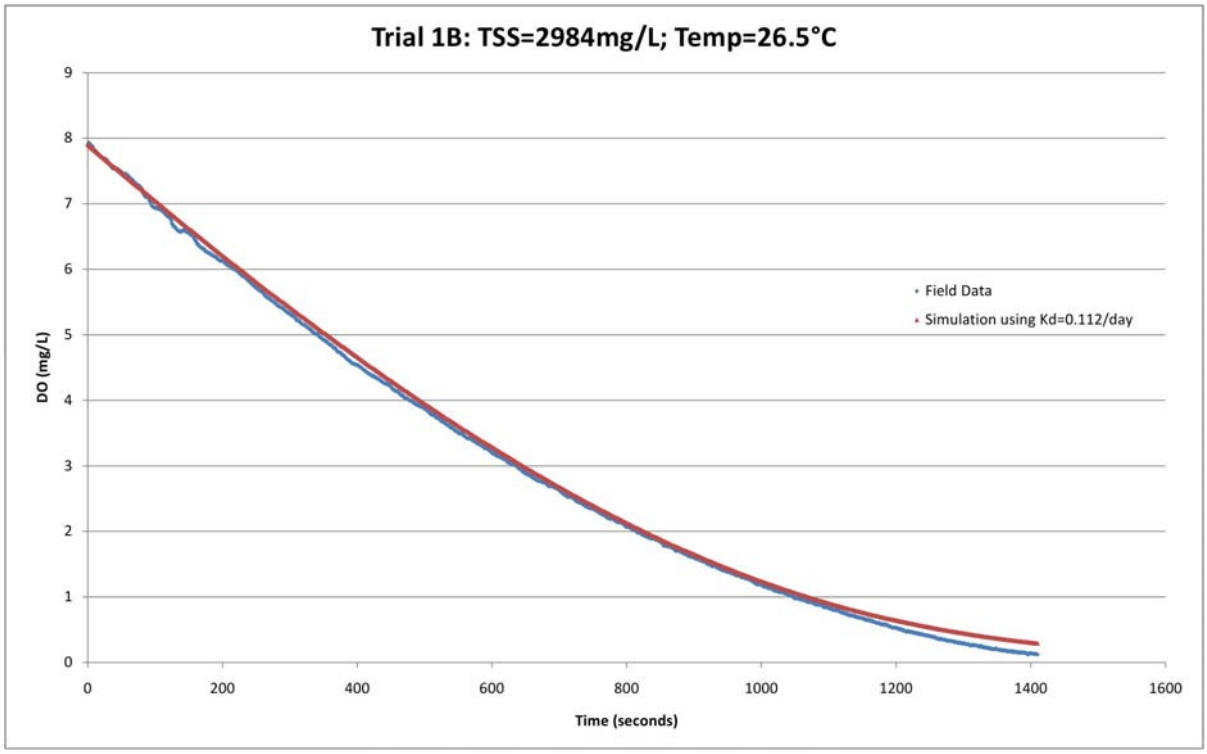

Figure 4-26: Simulation of Sink Term on Trial 1B

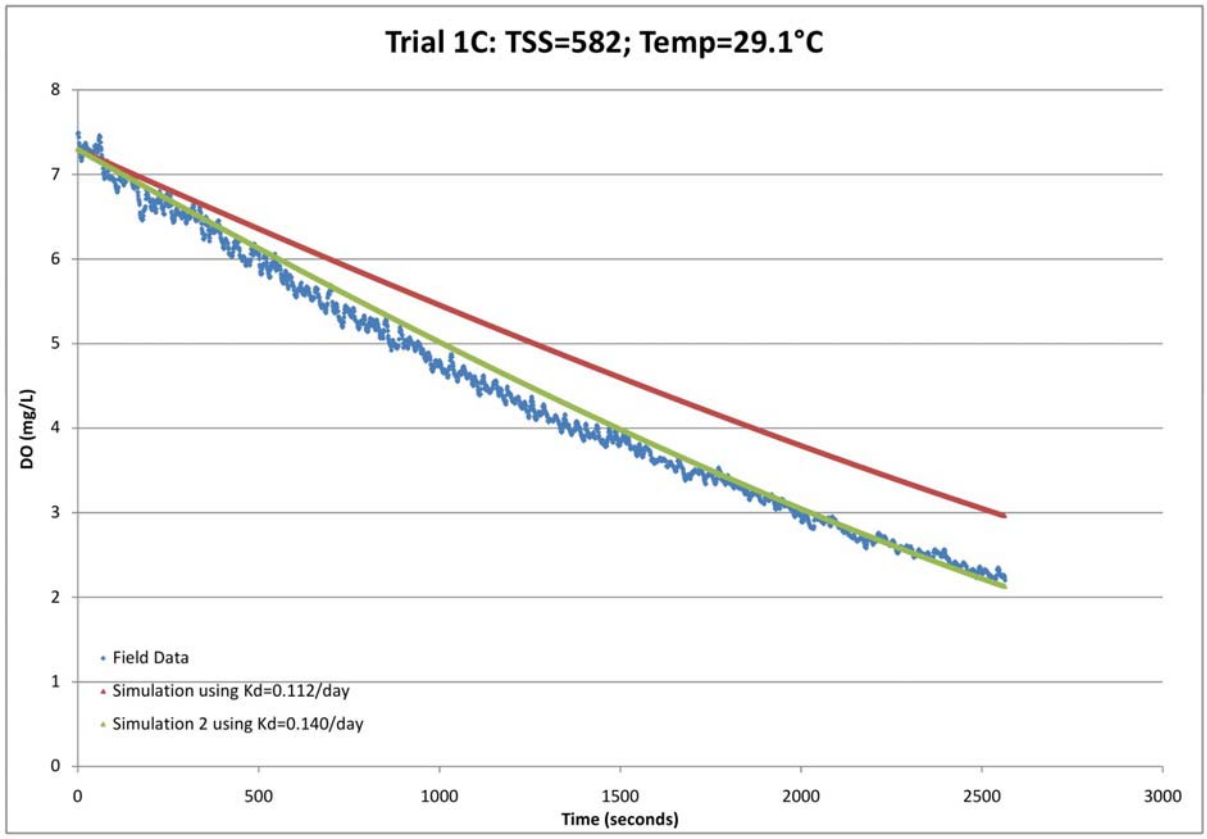

Figure 4-27: Simulation of Sink Term on Trial 1C

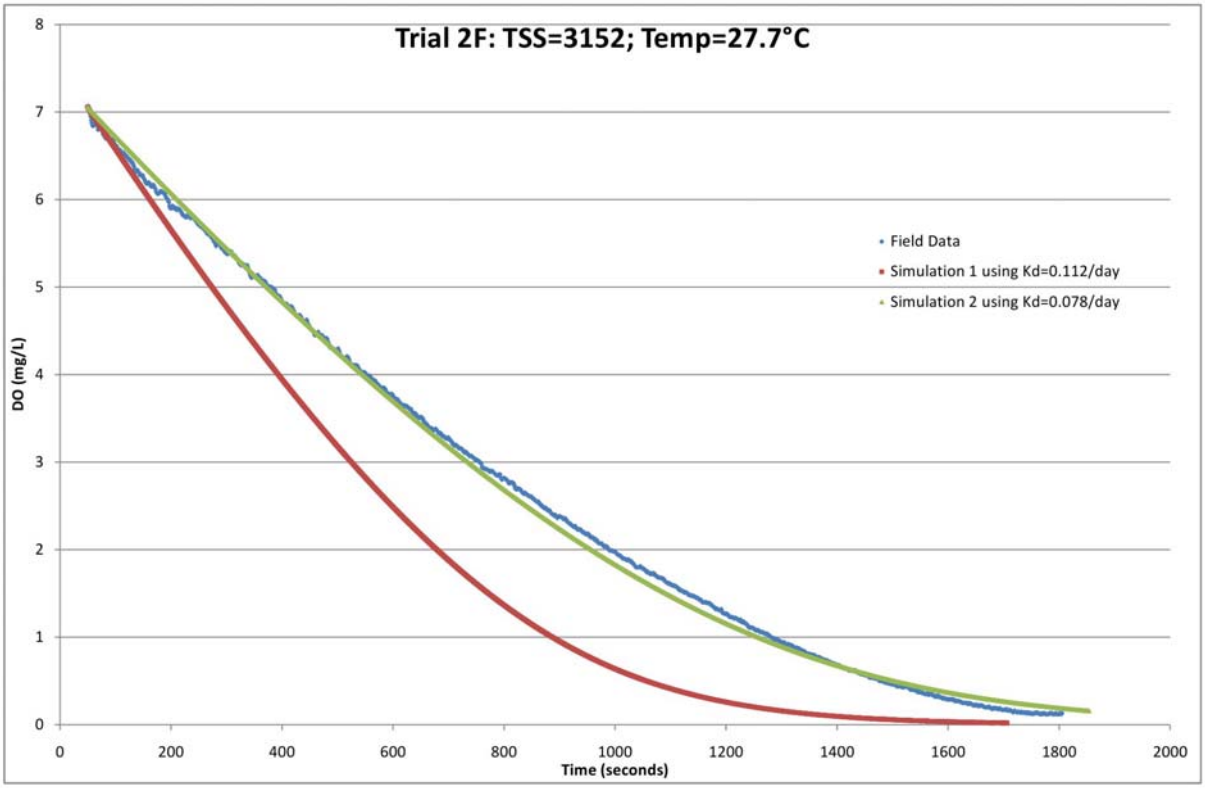

Figure 4-28: Simulation of Sink Term on Trial 2F

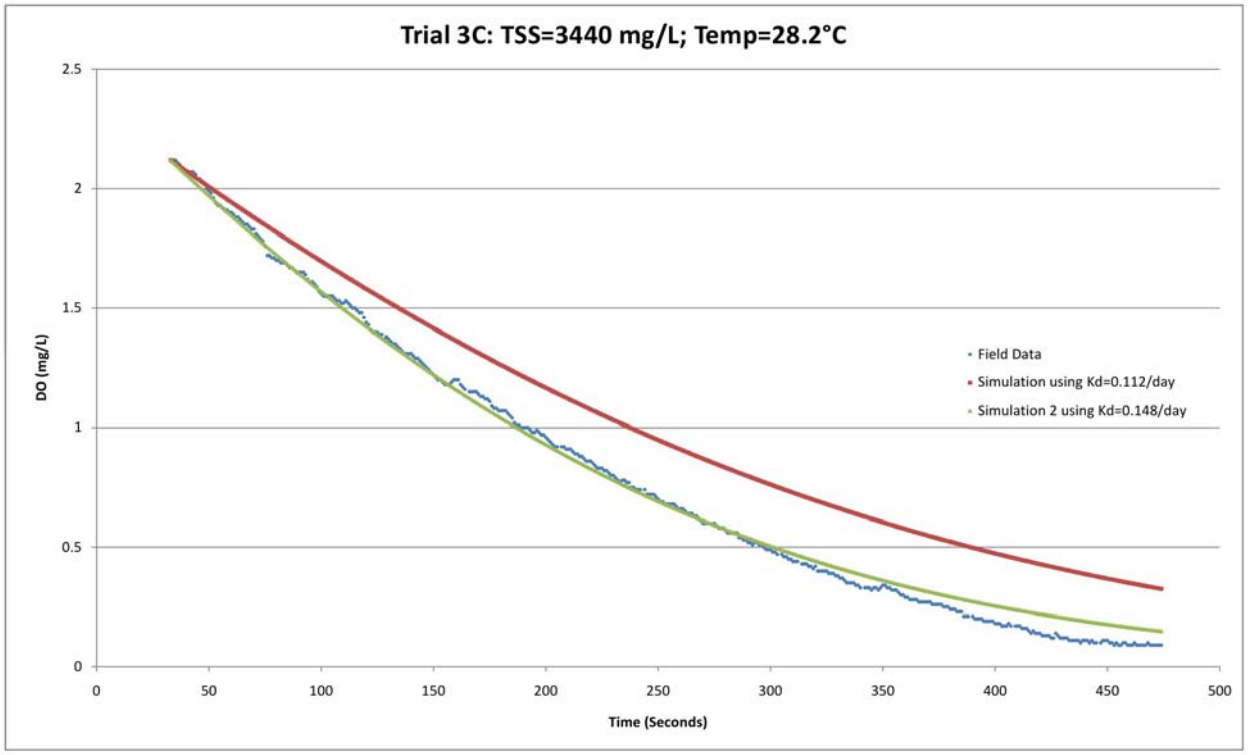

Figure 4-29: Simulation of Sink Term on Trial 3C

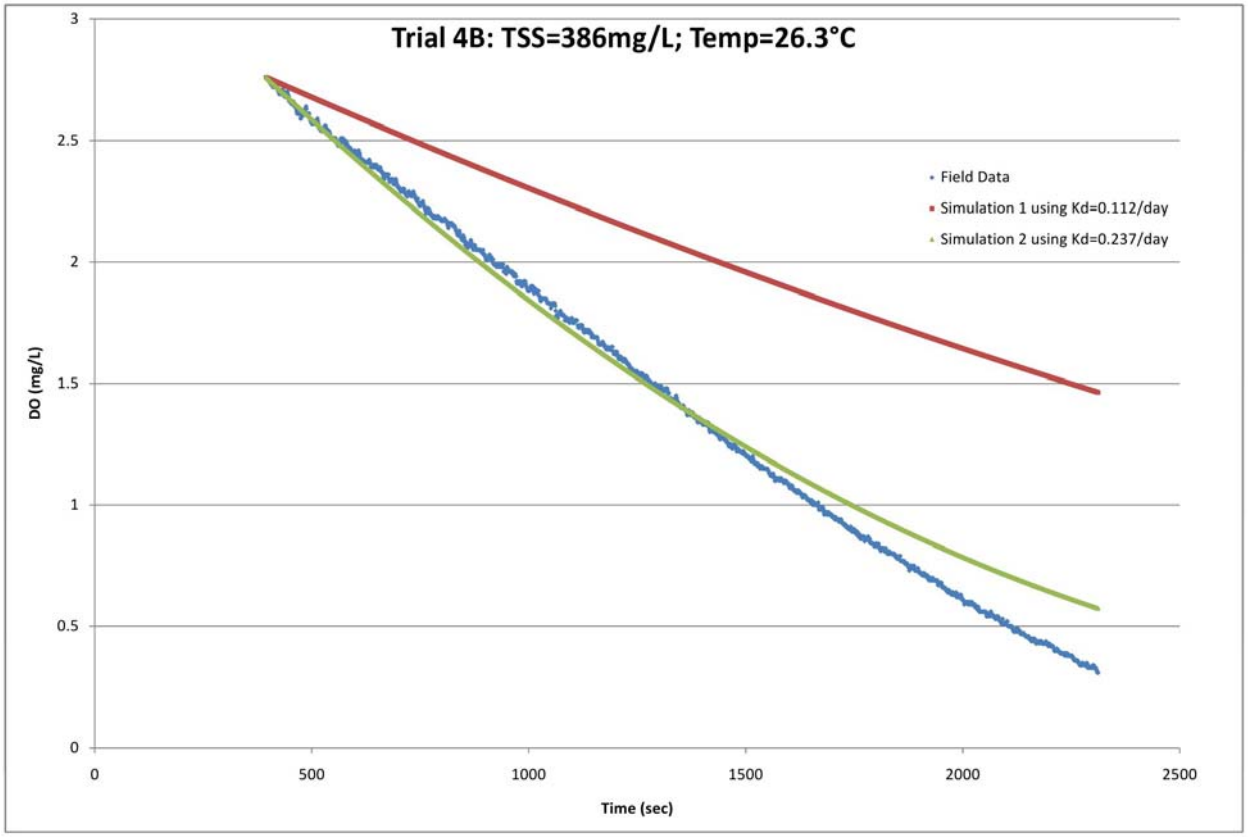

Figure 4-30: Simulation of Sink Term on Trial 4B

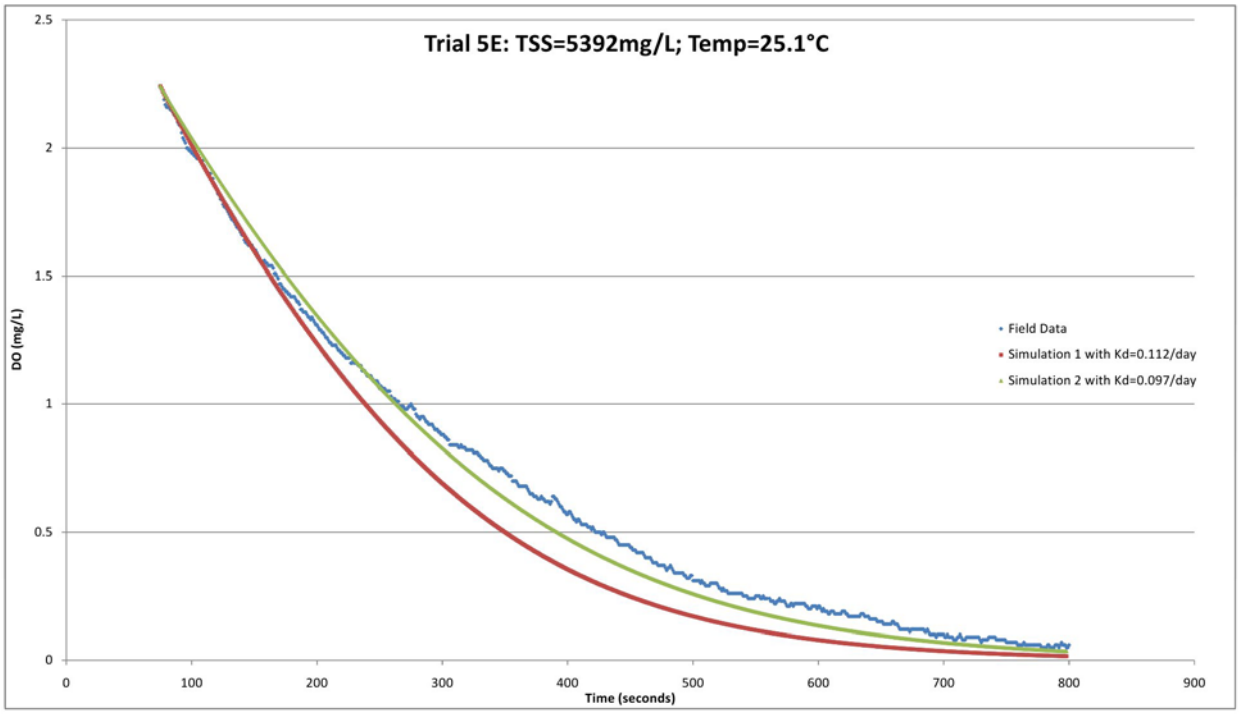

Figure 4-31: Simulation of Sink Term on Trial 5E

4.9 A Simplified Analysis of SOD_R

The analysis provided in Sections 4.7 and 4.8 was determined to be the most accurate way to characterize the dynamic nature of SOD_R. However a simplified approach can be used to characterize the initial, instantaneous oxygen demand associated with the specific resuspension conditions measured in the field. This surrogate of SOD_R must be understood to have limited applicability, but does provide the reader a sense of the magnitude of SOD_R relative to SOD_{NR} under the different phases of resuspension.

Using the same equations from Section 2.2.4 which were used to calculate SOD_{NR}, the surrogate for SOD_R (referred to as Ψ_R) can be calculated from the field-measured oxygen drawdown curves.

$$\Psi_{R\,20} = 501.6\ (S_{DO} - S_{BOD}) * 1.047^{(20\text{-}T)} \qquad (31)$$

where $\Psi_{R\ 20}$ = initial, instantaneous oxygen demand associated with resuspension [$g/m^2/day$]

S_{DO} = dC/dt = Slope of the DO drawdown curve ((mg/L)/minute)

S_{BOD} = Rate of drawdown associated with Biochemical Oxygen Demand present in ambient water (mg/L/day)

T = Temperature in °C

Because the slopes of the drawdown curves under resuspension are not linear, the S_{DO} value must be calculated across a short interval at a given DO level such that all values have the same basis. Since DO = 2.0 mg/L has been used as the standard for the previous resuspension analysis, it has also been used for this simplified analysis. A summary of these calculations for the trials involving resuspension is included in Table 4-6:

Trial ID	Resuspension Phase	Ψ_{20} ($g/m^2/day$)	Associated Water Column O_2 Drawdown (mg/L/day) *
1A	Flaking (Heavy)	25.0	11.4
1B	Slurry	113.8	51.7
1C	Flaking (Heavy)	28.5	13.0
2F	Slurry	83.6	38.0
3B	Flaking	12.1	5.5
3C	Slurry	153.1	69.6
4B	Flaking (Heavy)	29.6	13.5
5A	Flaking	33.4	15.2
5B	Flaking	12.1	5.5
5C	Flaking	19.2	8.7
5D	Flaking	16.2	7.4
5E	Slurry	195.6	88.9
6C	Flaking	28.5	13.0
7A	Flaking	21.6	9.8
7B	Flaking	27.6	12.5

Table 4-6: Initial, Instantaneous Resuspension Oxygen Demand

* The water column oxygen drawdown associated with Ψ_{20} is an approximation, calculated using the average depth of Bubbly Creek (2.2 m) and assuming well-mixed conditions throughout the water column.

Chapter 5: SUMMARY

In this study sediment oxygen demand (SOD) in Bubbly Creek was evaluated as two separate components: SOD_{NR} and SOD_R. SOD_{NR} represents SOD under conditions in which sediment has not been resuspended; it is expressed in the units of $g/m^2/day$, which is the traditional conception of SOD. SOD_R represents SOD under conditions in which sediment has been resuspended due to the shear stress exerted on the bed; it is expressed in the units of mg/L/day and required characterization using non-traditional methods.

Using the U of I Hydrodynamic SOD Sampler, values of $SOD_{NR\ 20}$ were found to vary between 6.7 $g/m^2/day$ and 12.1 $g/m^2/day$ for well-mixed, oxygenated conditions near the bed. (The subscript 20 indicates that the values were normalized to a temperature of 20°C.) Additional characterization of the sediment composition of Bubbly Creek was performed, confirming previous studies that found the sediment transitioned from coarse material (sand) with relatively low organic content at the upper end to fine-grained material (silt/clay) with high organic content at the lower end. These findings were used to evaluate SOD_{NR} in the context of the sediment type. Regarding SOD_{NR}, one of the goals of the study was not achieved; namely, establishing the velocity-dependence of SOD_{NR} for very low-velocity conditions prior to the onset of resuspension. Failure to achieve this goal was due to constraints imposed by field conditions and constrains involving the sampler. Although field measurements were not able to capture this relationship between velocity and SOD_{NR}, a numerical analysis was provided in Section 4.2 that explains how SOD_{NR} would be reduced below the field-measured values when velocity is low.

The majority of the analysis focused on characterizing SOD_R as a function of the bed shear stress (or shear velocity). Several goals were achieved in the characterization of SOD_R, with the first being the quantification of critical shear velocities above which resuspension occurs. The U of I Hydrodynamic SOD Sampler was able to achieve shear velocities (u_*) in the range of 0.13 to 0.93 cm/sec, as determined through CFD (computational fluid dynamics) modeling of the system. Field experiments identified several phases of resuspension, and critical shear velocities were established for each: (1) the "flaking" phase was characterized by a film of organic debris being scoured from the sediment surface at a relatively low shear velocity. The critical shear velocity to initiate flaking was found to be 0.17 cm/sec and did not appear to be dependent on the underlying sediment type. (2) The full resuspension or "slurry" phase involved the main sediment (under the film of organic debris) entering suspension, which

caused a drastic increase in the oxygen drawdown. The critical shear velocity to cause predominantly fine-grained material to enter full resuspension varied between 0.37 and 0.76 cm/sec, depending on the sediment texture and the overlying water depth. For the sediments composed primarily of sand, the maximum shear velocity achieved with the sampler was not sufficient to cause full resuspension; however, critical shear velocities were calculated using standard sediment transport theory available for non-cohesive soils. The critical shear velocity for sandy sediment with D_{50} equal to 0.25 mm was found to be 0.91 cm/sec to initiate sediment mobilization as bedload; and 2.54 cm/sec to initiate sediment entrainment into full suspension. (3) An intermediate or "bedload" phase may have also occurred in those soils with a high sand content, where the bed material was mobilized, but with only the fine-grained and organic fraction entering suspension into the water column. We did not have sufficient data to verify or quantify critical shear velocities associated with this intermediate phase.

Simulations of various flow rates utilizing the hydrodynamic component of the model STREMR-HySedWq allowed mapping of resultant shear velocities, which were evaluated in the context of the critical shear velocities identified. The simulations revealed that a 2.19 m^3/sec (50.0 MGD) low flow rate would be sufficient to induce flaking of organic debris in upper Bubbly Creek. A 12 m^3/sec (274.0 MGD) flow rate would result in the sandy streambed of upper Bubbly Creek being mobilized as bedload; with the remainder of the stream undergoing a mixture of flaking or full resuspension. A 24 m^3/sec (547.9 MGD) flow rate would result in portions of the sandy upper reach transitioning from bedload to full resuspension; and the entire lower portion of Bubbly Creek undergoing full resuspension. The hydrodynamic modeling was intended to provide an illustration of how the experimental results can be applied to actual Bubbly Creek flow events.

Another goal of the study regarding SOD_R was to characterize the magnitude of sediment resuspension as a function of the bed shear stress. Graphical relations were established that illustrated the total suspended solids (TSS) concentration achieved within the SOD chamber for various levels of bed shear stress for the various sediment textures identified in the field. These findings can ultimately be used to establish a sediment entrainment rate. In conjunction with sediment transport modeling, the entrainment rate can be used to model TSS concentrations achieved throughout the water column during an actual flow event.

The final goal regarding SOD_R was to characterize the oxygen demand exerted under a sediment resuspension scenario. Equation 30 was established in a form parallel to first-order biochemical oxygen

demand (BOD) kinetics, which relates instantaneous oxygen demand to the concentrations of TSS, dissolved oxygen (DO), and temperature. It was found to provide a good fit to the oxygen drawdown curves measured in the field. Because application of the equation for SOD_R requires modeling to determine TSS concentrations that will vary over space and time, it was not possible to provide absolute values for SOD_R as was done for SOD_{NR}. However, the sink term for SOD_R is in a form that can easily be incorporated into a hydrodynamic, sediment transport, and water quality model to predict the effect of sediment resuspension on the dissolved oxygen concentrations in Bubbly Creek. Although absolute values of SOD_R cannot be accurately provided without the sediment transport modeling, some general conclusions can be drawn regarding the magnitude of SOD_R relative to SOD_{NR}. The data revealed that the oxygen demand associated with early flaking resuspension was typically 2 times higher than the background oxygen demand associated with SOD_{NR}; it was typically an order of magnitude higher than SOD_{NR} for slurry phase resuspension; and laboratory data indicated it could reach several orders of magnitude higher for a high-concentration slurry. The initial, instantaneous oxygen demand associated with resuspension (a surrogate for SOD_R) at 20°C and ambient dissolved oxygen concentration 2.0 mg/L varied from 12.1 to 33.4 g/m^2/day for flaking phase resuspension; and from 83.6 to 195.6 g/m^2/day for full resuspension within the range of suspended sediment concentrations achieved in the field trials.

We feel the future work that would contribute most to further understanding of SOD in Bubbly Creek would be the following:

(1) In order to characterize velocity dependence of SOD_{NR} at very low flow rates prior to the onset of resuspension, some modifications to the U of I Hydrodynamic Sampler may be warranted. The use of an optical DO probe rather than the Clark-type probe would allow for lower flow operation. Some means of saturating the water in the sampling system with oxygen prior to initiation of sampling would also be a significant improvement to the sampler.

(2) In order to apply the oxygen sink term associated with suspended sediment (Eq. 30), the TSS concentrations must be established throughout the volume of the stream using hydrodynamic and sediment transport modeling. The first step in that process would be establishment of sediment entrainment rates based on the TSS versus shear velocity curves established in Section 4.4 (along with various other soil parameters that would be taken into account).

(3) In Equation 30, C_{TSS} was used as a surrogate for the C_{BOD} associated with the suspended sediment ($C_{BOD\ SS}$). We know that $C_{BOD\ SS}$ is actually only a fraction of the TSS; such that

$C_{BOD\ SS}$ = β(t) * C_{TSS}, where β(t) is a coefficient that defines the fraction of oxidizable material comprising the suspended sediment. If this coefficient remains constant, it can simply be incorporated into the deoxygenation rate coefficient, as was done in Section 4.7; this was valid because under the experimental circumstances, β(t) ≈ β(0). However to evaluate oxygen usage over longer time periods, C_{BOD} will be depleted over time as material is oxidized. Eq. 30 will still be valid, but the coefficient β(t) may need to be separated from the rate coefficient so that variation in time can be taken into account. Future work to establish the kinetics of how β(t) changes through time would be worthwhile.

(4) On the same subject, the data also suggested that β(0) was a function of the amount of material put into suspension (ie, the depth of scour). The percent organic content of the suspended sediment was typically highest for early flaking and declined as additional sediment was put into suspension throughout the slurry phase. This likely has significant influence on best-fit values of K_{TSS} being higher on those trials with low concentrations of TSS (where % organic was very high) relative to those trials with higher concentrations of TSS (where % organic was lower). We feel that establishing the relationship between β(0) and the magnitude of erosion would also be a worthwhile effort. The results could be used to establish relations for "BOD Entrainment" to accompany the sediment entrainment rates.

REFERENCES

Abad, J. D., Bombardelli, F. A., Waratuke, A. R. and García, M. H., (2004). "*Modeling and alternative analysis for SEPA Station No. 3*". In report "SEPA Station No. 3, Siltation Alleviation Study" from Greeley and Hansen LLC to Metropolitan Water Reclamation District of Greater Chicago.

Abad, J.D., Buscaglia, G.C., Garcia, M.H., (2007). 2D stream hydrodynamic, sediment transport and bed morphology model for engineering applications, Hydrologic Processes.

Abad, J.D., Rhoads, B.L., Güneralp, İ, and García, M.H., (2008). "Flow Structure at Different Stages in a Meander-Bend with Bendway Weirs." *Journal of Hydraulic Engineering*, ASCE, 138 (8), 1-12.

Agrawal, Y. C., McCave, I. N., and J. B. Riley. (1991). "Laser Diffraction Size Analysis." *Principles, Methods, and Applications of Particle Size Analysis*, ed. J.P. Syvitski. Cambridge University Press, 119-128.

American Water Works Association, AWWA (2005). *Standard Methods for the Examination of Water and Wastewater, 21st Edition*. American Public Health Association, Washington D.C.

Bernard, B., Grimes, B., Howington, S., Schneider, M., Turner, H., (1992). STREMR Numerical Flow Model, STREMR and ASTREMR PC Packages, Version 2.0.

Bernard, R.S., (1993). STREMR: numerical model for depth-averaged incompressible flow, Technical Report REMR-HY-11, U.S. Army Corps of Engineers.

Briskin, B.J., and Garcia, M.H., (2002). *Application of an Annular Flume to Sediment Oxygen Demand Research: Investigation of Resuspension Effects – McCook Reservoir Studies*. University of Illinois at Urbana-Champaign, Civil Engineering Studies: Hydraulic Engineering Series No. 72.

Butts, Thomas A., (1974). *Measurements of Sediment Oxygen Demand Characteristics of the Upper Illinois Waterway*. Illinois State Water Survey, Urbana, Report of Investigation 76.

CDM Federal Programs Corporation, (2005). *Collection and analysis of sediment samples from the South Fork South Branch, Chicago River, Final Report.* United States Army Corps of Engineers Chicago District.

Collier, D., and Cieniawski, S., (2003). *October 2000 and August 2002 survey of sediment contamination in the Chicago River, Chicago, Illinois*, U.S. Environmental Protection Agency.

Flow Science Inc., (2008). *Flow-3D V 9.2 User's Manual*. Santa Fe, New México.

Garcia, M.H., (2008). "Sediment Transport and Morphodynamics", Chapter 2 ASCE Manual of Practice 110, *Sedimentation Engineering: Processes, Measurements, Modeling and Practice*. Garcia, M.H. (ed). American Society of Civil Engineers. Reston, VA.

Groeneveld, J., Sweeney, C., Mannheim, C., Simonsen, C., Fry, S., and Moen, K., (2007). "Comparison of Intake Pressures in Physical and Numerical Models of the Cabinet Gorge Dam Tunnel", Waterpower XV, Copyright HCI Publications.

Hatton, K.A., Foster, D.L., Traykovski, P., and Smith, H.D., (2007). "Numerical simulations of the flow and sediment transport regimes surrounding a short cylinder." *IEEE J. Ocean. Eng.*, 32(1), 249-259.

Hill, L., (2000). *The Chicago River: A Natural and Unnatural History*. Lake Claremont Press, Chicago, Illinois.

Mackenthun, A.A., and Stefan, H.G., (1998). "Effect of Flow Velocity on Sediment Oxygen Demand: Experiments". *Journal of Environmental Engineering*, Vol. 124, No. 3, 222-229.

Metropolitan Water Reclamation District of Greater Chicago, MWRDGC, (2008). *Ambient water quality monitoring in the Chicago Area Waterway system: a summary of biological, habitat, and sediment quality data between 2001 and 2004*, Research and Development Department, Report no. 08-2.

Metropolitan Water Reclamation District of Greater Chicago, MWRDGC, (2007). Report No. 07-82, Research and Development Department, Environmental Monitoring and Research Division, December.

Motta, D., (2008). *Two-dimensional hydrodynamic, sediment transport and water quality model for Bubbly Creek, Chicago, Illinois*. M.S. Thesis, University of Illinois at Urbana-Champaign, IL.

Motta, D., Abad, J., Liu, X., and Garcia, M.H., (2009). *Two-dimensional BOD and DO water quality model for engineering applications: the case of Bubbly Creek in Chicago, Illinois.* EWRI Conference proceedings, Kansas City, MO.

Parsons, M., (2007). *Sediment Oxygen Demand: Operating Procedure*. Technical Report SESDPROC-507-R1. US Environmental Protection Agency, Region 4, Athens, GA.

Polls, Irwin and Spielman, Charles, (1977). *Sediment Oxygen Demand of Bottom Deposits in Deep Draft Waterways in Cook County*. The Metropolitan Sanitary District of Greater Chicago, Department of Research and Development.

Richardson, J.E., and Panchang, V.G., (1998). "Three-dimensional simulation of scour-inducing flow at bridge piers." *J. Hydraulic Eng*., vol. 124, no. 5, pp. 530–540.

Sequoia Scientific. *LISST-ST Particle Size Analyzer User's Manual*, Version 2.1.

Shepard, D., A two-dimensional function for irregularly spaced data, Proc. ACM Nat. Conf., pg. 517-524, (1968).

Smith, H.D., and Foster, D.L., (2005). "Modeling of flow around a cylinder over a scoured bed." J. Waterway Port Coast. *Ocean Eng*., vol. 131, no. 1, pp. 14–24.

Thomann, R.V., and Mueller, J.A. (1987). *Principles of surface water quality modeling and control*. HarperCollins, New York, NY.

University of Chicago Library (2007, November 26). *Chicago in the 1890s*. Retrieved from http://www.lib.uchicago.edu/e/su/maps/chi1890/.

US Army Corps of Engineers, Chicago District (2007). *BUBBLY CREEK, SOUTH BRANCH OF THE CHICAGO RIVER, ILLINOIS RECONNAISSANCE STUDY: 905(b) ANALYSIS RECONNAISSANCE REPORT*.

Yin, K., Viana, P., Zhao, X., Rockne, K.J. (2007). *Active capping remediation project: Bubbly Creek Turning Basin bore LOG*, Department of Civil and Materials Engineering, Applied Environmental Biotechnology Laboratory, UIC Report.

Yin, K., Viana, P., Zhao, X., Rockne, K.J. (2006). *Active capping remediation project: Bubbly Creek Turning Basin*, Department of Civil and Materials Engineering, Applied Environmental Biotechnology Laboratory, UIC Report.